Nonlinear Propagation of Electromagnetic Beam in Dusty Plasmas

Thesis submitted by

Ruchi Sharma

(2K14/Ph.D/AP/01)

In the fulfilment of the requirement of the degree of

DOCTOR OF PHILOSOPHY
(Department of Applied Physics)

Submitted to

Delhi Technological University

(Formerly Delhi College of Engineering)

Shahbad Daulatpur, Bawana Road, Delhi-110042, India

Supervisor
Prof. (Dr.) Suresh C. Sharma
Department of Applied Physics
Delhi Technological University (DTU)
Delhi-110042

CERTIFICATE

This is to certify that the work embodied in the thesis entitled, "Nonlinear Propagation of Electromagnetic Beam in Dusty Plasmas" being submitted by Ruchi Sharma to the Department of Applied Physics, Delhi Technological University (Formerly Delhi College of Engineering), Delhi for the award of the degree of Doctor of Philosophy is original and has been carried out by her. This work has not been submitted in part or full to any other university or institute for the award of any diploma or degree.

Supervisor
Prof. (Dr.) Suresh C. Sharma
Department of Applied Physics
Delhi Technological University (DTU)
Delhi-110042

ACKNOWLEDGMENT

I have been indebted to many people in the preparation of this thesis and it is indeed a matter of great pleasure for me to acknowledge and thank all those who helped me, in one way or the other, in completing my Doctoral thesis.

First, and foremost, I would like to acknowledge and sincerely express my deep sense of gratitude to Dr. Suresh C. Sharma, Professor. Deptt. of Applied Physics, and Dean (Academic - PG), Delhi Technological University, Delhi, for his extraordinary cooperation, invaluable guidance and supervision. This thesis submission is the result of his painstaking and generous attitude. I wish to thank him for all his humane and able support, advice, encouragement and excellent supervision. I have been greatly benefited from his thorough knowledge and expertise in plasma physics in general and dusty plasma physics in particular. The contribution of his valuable discussions, explanations and original ideas has a great importance to this thesis. I feel very lucky to have such understanding, and I feel honoured to be his student.

I would like to thank HOD, Department of Applied Physics and the members of board of DRC/SRC, DTU, Delhi for their valuable suggestions and useful comments throughout this research work.

I would also extend my special thanks to all my Ph.D fellows and non-teaching staff of Deptt. of Applied Physics for their kind support, constructive discussions, perseverance and encouragement in completing my research work successfully.

On a more personal basis, I would like to thank my father(Sh. Madan Lal Sharma), mother(Smt. Krishana Sharma) and my Siblings for all the good they brought and are still bringing to my life. I also want to thank my husband Narinder Kumar for his love, support and all the happiness he brings in my life.

I sincerely acknowledge the efforts of all those who have directly or indirectly helped me in completing my thesis successfully.

Ruchi Sharma

ABSTRACT

This doctoral thesis focuses on nonlinear propagation of electromagnetic beam in dusty plasmas. In first case, we present a model theoretically to see the results of propagation of Gaussian electromagnetic wave in fully ionized dusty plasma on account of energy loss in thermal conduction. We observed the temporal change in plasma parameters, self-focusing of wave and critical power of self-focusing of wave due to the presence of dust grains.

We have also compared the temporal irradiance of Gaussian and Sine beam in collisional plasma using dust kinetics including neutral atom ionizations, process of reunite the free electrons and ions, phenomena of adsorption on the surface of dust grains and photoemission from the dust grain surface, and binary collisions between dusty plasma constituents.

The study of propagation of electromagnetic wave in non-thermal dusty plasma in exospheric environment considering diffusion limited escape theory, escape mechanism and dust dynamics made it a fascinating field of research for earth-satellite communication system and rocky planets. Modified dielectric permittivity, absorption co-efficient, and refractive index involving dust grains have also been examined.

We have explored the threshold power of self-focusing of amplitude modulated laser beam in dusty plasma and self-trapping of Gaussian beam in complex plasma using dust charge, number density and energy balance of plasma constituents.

LIST OF FIGURES

LIST OF PUBLICATIONS

International Refereed Journals and Conferences

1. **Ruchi Sharma** and Suresh C. Sharma, "*Theoretical model for the effect of dust grains on self-filamentation of a gaussian electromagnetic beam in a fully ionized plasma*,"**Contrib. Plasma Phys**.**59**, 211(2019).

2. **Ruchi Sharma** and Suresh C. Sharma, "*Theoretical analysis for transmission of gaussian and sine time irradiance of electromagnetic beam in collisional dusty plasmas,"* **Contrib. Plasma Phys 60,** 1-4(2020). https://doi.org/10.1002/ctpp.201900175.

3. **Ruchi Sharma** and Suresh C. Sharma, "*Theoretical model for nonlinear propagation of electromagnetic wave in non-thermal exospheric dusty plasmas"*(to be communicated).

4. **Ruchi Sharma** and Suresh C. Sharma, "*Threshold power of amplitude modulated laser beam in complex plasma*," **44th EPS Conference on Plasma Physics,** held at Belfast, P4.311 (2017).

5. **Ruchi Sharma** and Suresh C. Sharma, "*Theoretical model for self-trapping of Gaussian electromagnetic beam in dusty plasma*," **AIP Conference Proceedings, 2136**, 060001(2019).

International Conference Presentations

1. ***"12th International Conference on Plasma Science and Applications (ICPSA-2019),"*** Department of Physics, University of Lucknow (11-14 Nov. 2019).

2. *"**International Conference on Photonics, Metamaterials and Plasmonics (PMP2019),"*** Department of Physics and Material Science and Engineering, Jaypee Institute of Information Technology, Noida (14-16 Feb. 2019).

3. ***"International Conference on Applied Electromagnetic, Sign Processing and Communication (AESPC-2018)***,"at KIIT, Bhubhneshwar (22-24 Oct. 2018).

4. ***"International Conference in Applied Science and Engineering (AASET-2017),"*** School of Basic Science and School of Engineering and Technology, K.R. Manglam, Gurugram (17-18 Aug. 2017).

5. *"**44th International Conference of European Physical Society on Plasma Physics (EPS-2017),"*** held at Belfast, P4.311 (25-30, June 2017).

International Conference Attended

1. ***"TEQIP-III Sponsored One Week FDP on Recent Trends in Material Science and Engineering,"*** Department of Applied Physics, Delhi Technological University, Delhi (17-21 Sep, 2018).

2. ***"International Symposium on Nonlinear Waves in Fluids And Plasmas-BUTIFEST,"*** Department of Physics and Astrophysics, University of Delhi & Department of Physics, IIT, Delhi (1-2 March, 2017).

3. ***"TEQIP-II sponsored one week FDP on Advances in Microelectronics and Plasma Diagnostics,"*** Department of Applied Physics, Delhi Technological University, Delhi (Aug 29- Sep 2, 2016).

TABLE OF CONTENTS

Chapter 1

INTRODUCTION

1.1 Historical Background

In 1929, Tonks and Langumir [1] were the foremost to elaborate the interior of a glowing ionized gas produced via electric discharge in a tube. The term plasma is synonym of neutral gas consist of many interacting charged particles like electrons, ions and neutrals. Star nebulas, auroras are the examples of plasma in which dust is an omniscient ingredient. These microns to nanometer dust particles acquire positive and negative charge on account of interaction with the surrounding plasma and photon flux. In outer space, the particles are generally positively charged particles obtained through photo-ionization. On the other hand, they acquire negative charge due to accretion of electrons. The complex combination of these charged dust particles with electrons, protons and neutrals is called dusty or complex plasma. In space, the bright comet Halley [2] and in the laboratory, the ordinary flame is very familiar examples of dust-plasma interaction. In flame, the thermionic emission of electrons from the dust particles produced plasma at that temperature. Some other examples like, processing plasma used in fabrication of devices such as microchips for computers, amorphous silicon solar cell, ion thrusters used for propagation of satellites, in laboratories for analyzing collective phenomenon and plasma crystals etc. The dust is also formed on the cool edge layer contacted with material wall in thermonuclear fusion plasma. The dust has turned out a safety concern for ITER and future fusion devices. The dust grains may contain a great part of hydrogen atoms which will generate tritium ions [3]. Moreover, the fine dispersed dust particles may be chemically reactive and may spontaneously react with oxygen and water vapours in case of vacuum or coolant leak. Migration of dust particles is also an important feature. On account of thermophoretic forces and repetitive evaporation and condensation, they may deposit at cold area of devices and block spacing and fill gaps caused by engineering reasons. The formation of coulomb crystals in dusty plasmas, exist in astro-plasma system, industrial plasma processing systems, laboratory discharge systems

etc. has attracted millenary in last few decades. These are different from solid state crystals in their interaction energy and lattice spacing. The experimental observation shows that as the coulomb coupling parameter decays with the enhancement of temperature of dust, the dust crystals melt and vaporize to form weakly coupled ideal coulomb plasma [4].

1.2 Phenomenon of dust charging

The charging of dust grains focuses on the phenomenon

(i) Interaction of dust grains with electrons and ions

(ii) Interaction of dust grains with photons

(iii) Interaction of dust grains with plasma particles

When plasma particles like electrons and ions incident on to a dust grain surface, they are either pass through the dust grain material or reflected by dust material. On passage through the dust material, they excite the other electron by losing their energy and generate the secondary electron from dust grain surface and make it positive. Also the photoemission takes place when photons are incident on the dust grain surface and make it positively charged.

Dust particles act as probe when immersed in gaseous plasma and get charged by collecting the electrons and ions on its surface flowing through it. The charge acquired by a dust grain is $dQ/dt = \sum_k I_k$, where k represents the species of plasmas and I_k is the charging current to the dust grain carried by plasma particles k. The net steady state flux towards the dust grain surface becomes zero,

$$\text{i.e.,} \sum_k I_{k0} = 0, \tag{1.1}$$

where charge is connected with surface potential as Q = C ϕ_j , and ϕ_j is the surface potential. Due to lighter mass and high speed of electrons, the dust immersed in plasma acquires the negative charge and some potential in plasma which is -3.6k_BT/e for O plasma and -2.5 k_BT/e for H plasma[5].

In order to evaluate the equilibrium grain charge in isotropic plasma, the orbital motion limited (OML) model is used [6, 7]. Following are the assumptions of OML theory:

(i) Collisions between different plasma constituents like electrons, ions and neutrals are ignored.

(ii) Neutral atoms are produced when a charged particle hitting the grain is either absorbed by the grain or recombine on its surface.

Keeping the energy and angular momentum conservation, the electronic and ionic current reaching the grain surface

$$I_e = -4\pi e a^2 n_e \sqrt{\frac{T_e}{2\pi m_e}} e^{e\phi_0/T_e} \tag{1.2}$$

$$I_i = -4\pi e a^2 n_i \sqrt{\frac{T_i}{2\pi m_i}} \left(1 - \frac{e\phi_0}{T_i}\right) \tag{1.3}$$

where m_e , m_i are the masses, n_e , n_i are the number densities, and T_e , T_i are the temperatures of electrons and ions, respectively and ϕ_0 is the surface electric potential of spherical grain of radius, a. Substituting, these values of currents in equation (1.1), we may obtained the equilibrium surface potential, ϕ_0 .

1.2.1 Other charging processes

There are other dust grains charging mechanism like thermionic emission, field emission, radioactivity, impact ionization etc.

1.2.1.1 Thermionic Emission

When a dust grain is exposed to strong temperature, electrons and ions may be emitted thermionically from the surface of dust grain. The thermionic emission may be induced by thermal infra red, by laser heating, or by hot filament surrounding the dust grain. The thermionic electron emission current I_{th} can be obtained from Richardson equation which, including the increase in work function due to grain electrostatic barrier can be expressed as

$$I_{th} = 4\pi a^2 A_t T_d^2 \exp\left(-\frac{|W_f + e\phi_0|}{k_B T_d}\right), \quad (1.4)$$

where

$A_t = 4\pi e m_e k_B^2 / h^3$ is a constant.

1.2.1.2 Field Emission

The electron field emission from a dust grain surface occurs when its surface electric field occurs upto the order of 10^6 Vcm^{-1}. The corresponding emission flux comes out 10^5 cm^{-2} s^{-1} for a work function of 3.5 eV and corresponding surface potential ϕ_0 is 10^6 V. The dust grain potential is limited by electron (ion) field emission for negatively or positively charged dust grains.

1.2.1.3 Impact Ionization

When a highly energetic ion or neutral atom strikes on a dust grain surface, then either the neutal atom or atoms on a dust grain surface are ionized with subsequent escape of ions and/or electrons. This process of impact ionization becomes more significant for high neutral density and lead to charging of dust grains.

1.3 Grain Charging in Laboratories

In laboratory dusty plasma electron-ion current as shown in equation (1.2) and (1.3) plays a significant role in charging of a dust grain. Since the electrons moves very much faster than the ions, so the negative potential is gained by the electrons, as a consequence electrons are repelled. Hence electron current decreases and ion current increases; the net current at equilibrium is zero as shown in (1.1). Sustituting (1.2) and (1.3) in (1.1), one may obtain surface potential of -2.5 k_BT/e on dust grain surface immersed in H plasma. For a dust grain of radius of 1 μm with k_BT of 3eV, the electronic and ionic charge comes out to be -8.4×10^{-16} C which is almost 5000 times the charge of electrons [8]. This surplus charge than electrons are quite enough that statistical spread and time fluctuation of charge are too small in experiments to use consisitent size and composition of plastic micro particles. Still, the charge to mass ratio is very much smaller than

that of ions. There are various experiments performed by researchers for measuring dust grain charge. For example, the charge on an isolated grain can be measured by them by letting it fall into a Faraday cup or can be derived by decreased electron density on dust grain or speed of plasma waves [9]. Such methods have also proved that the presence of other particle decreased the charge on dust whereas grain's charge varies linearly with its diameter. In non-dusty plasma, usually the charge is not variable, remains fixed on ions but in dusty plasma, charge varies on account of fluctuation in surface potential due to plasma waves. Such alteration can raise the growth rate of particles via collision or coagulation in plasma in the presence of dust particles in pre stellar nebulae and semiconductor manufacturing reactors.

1.4 Plasma Waves

In plasma physics, analytical treatment of waves and instability plays a significanat role. Deliberately inclusion of dust particles to plasma creates a new scope of research to study. Theoretically, the influence of dust has been studied by extending two-fluid treatment with an addition of third component-dust. That is why results in two categories.

First, although the dusty plasma is electrically neutral like plasma but the difference is the significant proportion of negative charge bound to dust grain. The binding is detected by decaying electronic current on dispersing the dust in plasma. This binding influences all kind of plasma wave modes, viz; ion acoustic wave like plasma analogous of sound waves propagate at higher velocity and experience far less damping containing negatively charged dust particles.

Second, due to occurance of charge to mass ratio and large inertia of dust particles give rise to low frequency dust acoustic wave mode in which adjacent dust flux is coupled by electric field associated with the wave rather than by collisions, as they would be in neutral gas.

One attracting feature of these dust waves is that their resemblance can be obtained in the form of compression and rarefaction of scattered light as shown in the figure 1.1 as bright and dark regions that travelles as dust acoustic speed.

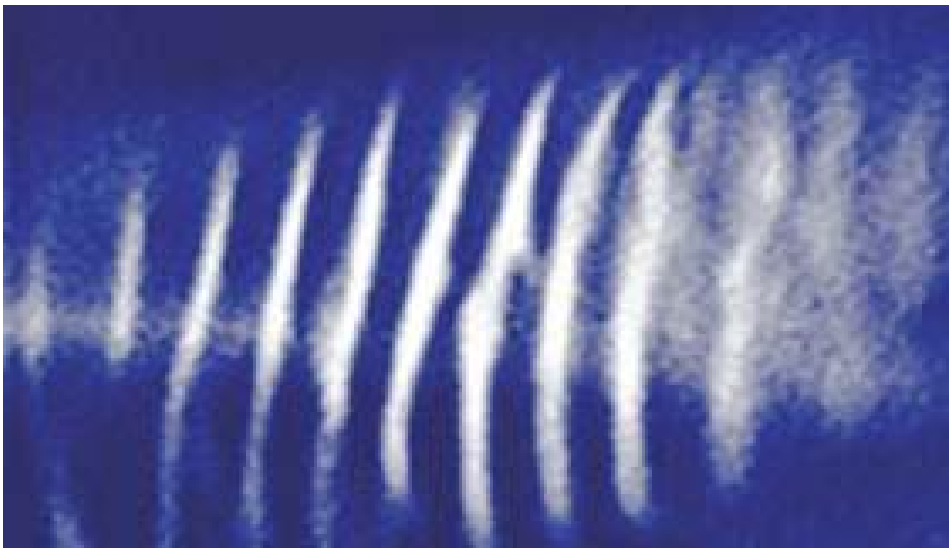

Fig. 1.1 Dust acoustic wave in the form of compression and rarefaction [10]

1.5 Forces

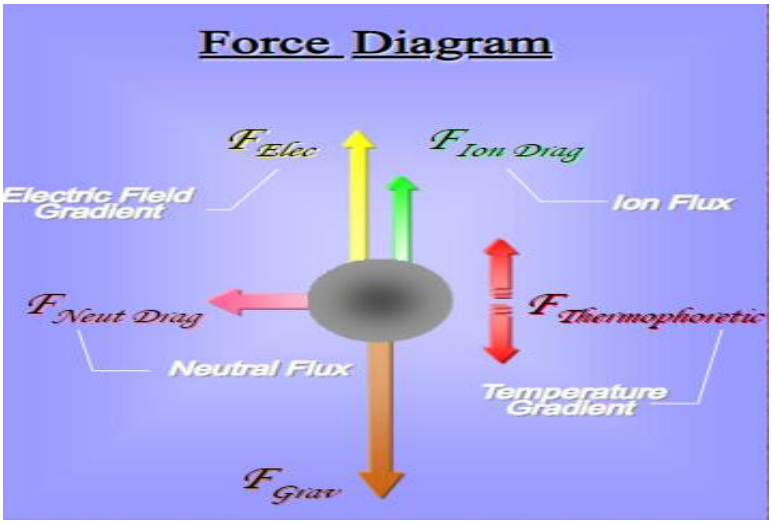

Fig. 1.2 Different forces acting on dust grains floating in plasma [11]

A dust grain floating in plasma is affected by number of forces. In ground experiments, the dominant force is gravity. The mutual electrostatic interaction and by their interaction with the gas molecules and ions are the prominenet forces between the charged dust particles. Thermal gradient produces thermophoretic forces. Ion drag force occurs due to weightlessness condition

which is supposed to have caused the void seen in figure 1.3 by pushing the dust grain out of the centre of plasma chamber's RF discharge.

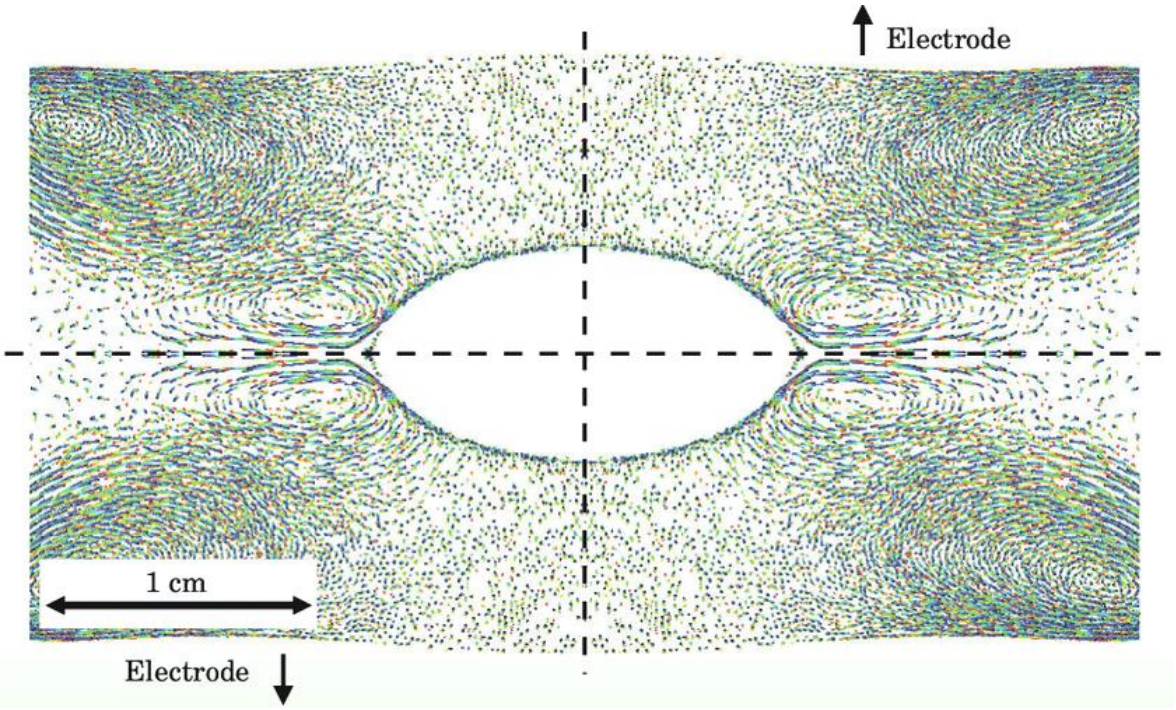

Fig. 1.3 Void due to outward ion drag force on dust grain [12]

1.5.1 Gravity Force

Gravity is the dominant effect in ground based experiment in locating the position of a dust grain. It is significant for the particles greater than 1micrometer. That is why whole volume of discharge is occupied by nanosize particle. For spherical dust grain the force of gravity [13] is given by

$$F_g = m_d g = (4/3)\pi\rho a^3 g, \tag{1.5}$$

where ρ is mass density.

1.5.2 Electric Force

In plasma, unequal space charge distribution is created on account of different mobility of electrons and ions induced an electric field. This induced field exert an electric force on the dust

grain. In the sheath region, the electric field is set up in capacitvely coupled RF discharge which is strong enough to levitate micron size dust particle. Also, the walls of the discharge chamber get negatively charged on account of the ambipolar diffusion and repel the particles. In general, the electric force associated with the particles is given by

$$F_e = Q_d e \,. \tag{1.6}$$

1.5.3 Neutral Drag Force

In plasma, collisions between neutrals and dust grains produce neutral drag force which is therefore, proportional to gas pressure and particle velocity being smaller than thermal velocity of neutrals. Transport of dust particle with respect to neutral in a media depends upon the ratio of mean free path of plasma to the diameter of particles. This ration defines Knudsen number for the momentum transfer $K_n = \lambda_{mfp} / a$. Free molecular range of a particle occurs when $K_n > 1$and continuum range occurs for $K_n < 1$. In this regime, a zero velocity boundary condition exist since gas atoms leaving the surface of a particle interact slowly with those imparting on particle. The presence of zero velocity dramatically increases the drag for transport of particles relative to gas.

Assuming elastic collisions between neutral and dust grain with velocity v_n and v_d, respectively, the neutral drag force can be formulated as

$$F_n = n_n m_n \sigma_{nd} (v_d - v_n) \,. \tag{1.7}$$

In case, relative velocity between dust and neutral is less than neutral thermal velocity, then this expression can be written as

$$F_n = -\frac{4}{3}\pi a^2 n_n m_n \sigma_{nd} (v_d - v_n) \tag{1.8}$$

and in case, relative velocity between dust and neutral is larger than neutral thermal velocity, then this expression can be rewritten as

$$F_n = -\pi a^2 n_n m_n \left| v_d - v_n \right|^2 \,. \tag{1.9}$$

For Knudsen number $K_n << 1$, neutral drag force can be written in the Stokes expression

$$F_n = -6\pi\nu_n a v_d \,, \tag{1.10}$$

where ν_n is neutral gas viscosity.

1.5.4 Ion drag force

Due to the presence of external electric forces and thermal motion of ions and dust particles, momentum is transferred from ions to the dust particles via elastic or inelastic collisions. Ion drag force plays a significant role in positioning of the particle in the discharge, structural arrangement of the particles in the laboratories experiments, voids on ground and microgravity experiments etc. In general, the ion drag force can be approximated as

$$F_i = n_i m_i \int v f_i(v) \sigma_i^{tr}(v) dv \,, \tag{1.11}$$

where $f_i(v)$ is the ion velocity distribution function, σ_i^{tr} is the momentum transfer cross-section for the ion particle collision depending upon the ion velocity through the scattering parameter $\beta = U_0 / m v_i^2 \lambda_D$, where λ_D is effective screening length.

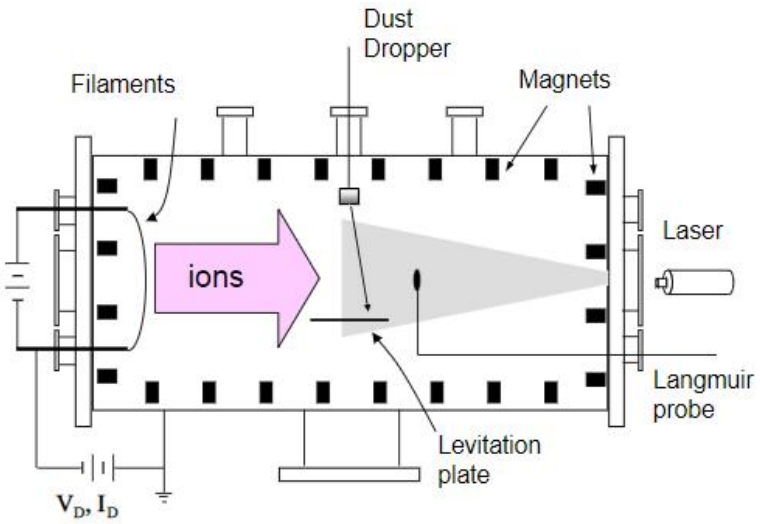

Fig. 1.4 Ion Drag Force: Experimental Measurements

Glass microsphere falling through plasma is deflected by ions which acquire drift due to weak ambipolar electric field in plasma. The ion drag force is determined from the measured deflection angles [12].

1.5.5 Thermophoretic Force

Solid particles suspended in the gas with a temperature gradient will be subjected to a force directed from hot part to cold part. This means that the net momentum transfer occurs from gas to dust particles. The rate of this net momentum transfer is known as thermophoretic force [14, 15]. Its magnitude is directly proportional to the temperature gradient and its direction is opposite to the neutral gas temperature. Then thermophoretic force on a dust particle can be represented as

$$F_{th} = -\frac{8}{3}\frac{a^2}{v_{th}} k_{tr} \nabla T_n \quad , \tag{1.12}$$

where v_{th} is the thermal velocity given by $\left(8kT/\pi m\right)^{1/2}$, k_{tr} is the thermal conductivity, ∇T_n is the temperature gradient. m is the mass of dust particle, k is Boltzmann's constant.

Thermal conductivity for mono atomic gas is given by

$$k_{tr} = 2.4\frac{\eta C}{m} \quad , \tag{1.13}$$

where η is the shear viscosity of the gas, C is the specific heat of the gas. For the viscosity, the expression may be written as

$$\eta = 0.553\frac{\sqrt{mkT}}{\sigma} \quad , \tag{1.14}$$

σ is the atomic cross-section[16,17]. The measured viscosity of Argon at 300K is $\eta = 2.21\times10^{-5}$ Nsm^{-2}, $\sigma = 4.2\times10^{-19}$ m^2. The equations (1.12), (1.13) and (1.14) together give the thermophoretic force on a microparticle

$$F_{th} = -3.33\frac{ka^2}{\sigma}\frac{dT}{dx} \quad . \tag{1.15}$$

Compensating the gravity by thermophoresis in a rf parallel plate plasma results in presence of particles in central plasma so that creation of void can be observed and investigated on ground experiment.

For melamine formaldehyde spherical particle of radius $a = 1.46\mu m$ and density $\rho = 1.51 g/cm^{-3}$ a temperature gradient of 4.65 K/cm is required to compensate the gravity in neon. With precise manipulation, several thermally induced effects can be observed like bubbles, structure, eruption, convection, and particle levitation.

1.5.6 Radiation Pressure Force

In basic dusty plasma experiments, radiation pressure force is exerted on a particle if it is exposed to beam of light. For example, tails of comets always point outward because of the radiation pressure exerted by the sun. The radiation pressure force is significant only for very light particles and intense beam in laboratory experiment. This condition appears atomic physics, colloidal physics, and biological experiments [18].

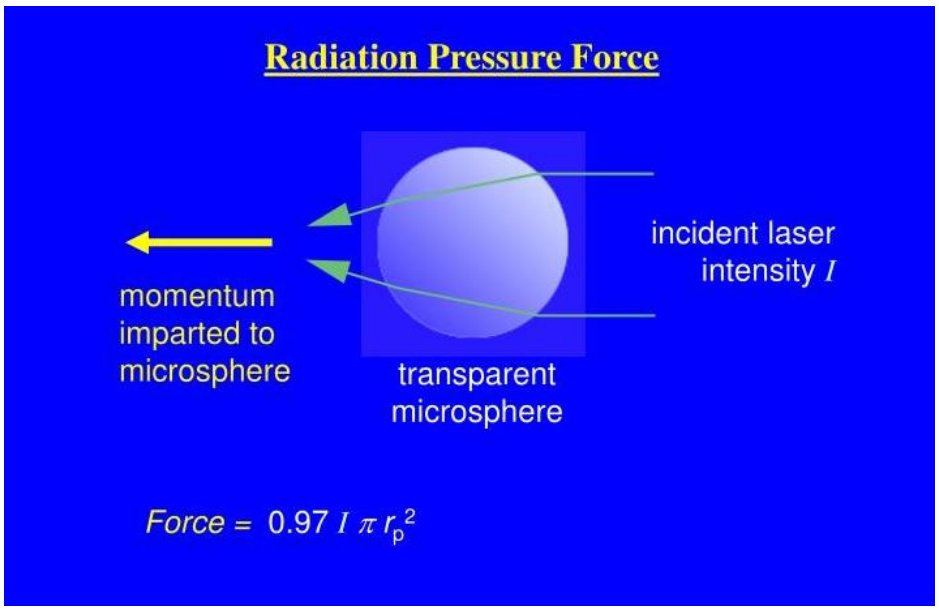

Fig.1.5 Momentum imparted to microsphere [19]

In dusty plasma physics experiments, laser manipulation has been used to induce waves and to cause a suspension of particles to rotate. Laser beam manipulation is much effective than electrical excitation of beam, it can push dust particle without disturbing the surrounding plasma. Using a chopped Ar^+ laser beam transverse shear wave is excited in dusty plasma by Nunomura *et al.* [20].

To measure the radiation pressure force acting on a single melamine formaldehyde microsphere in dusty plasma, a method is developed for computing this force using the trajectory of a single particle accelerated by the radiation pressure force by laser beam that is turned on and off. We record the microsphere trajectory as a time series, and from the time series one can calculate, the displacement, velocity, and acceleration as a function of time. Finally, one can calculate the radiation pressure force and shape of confining potential.

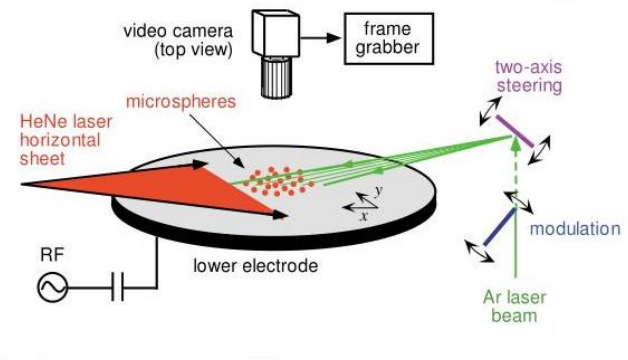

Fig. 1.6 Argon laser pushes particles in the monolayer [19]

Radiation pressure is the momentum per unit area per unit time transferred from photons to a surface. These photons will be reflected, transmitted or absorbed when strikes the particle. All these processes contribute to radiation pressure force. In general, for a laser beam of intensity I_{laser}, the radiation pressure force F_{laser} is

$$F_{laser} = q\frac{n\pi a^2}{c} I_{laser} , \tag{1.16}$$

where n is the refrective index of the material and c is the speed of light. By knowing the value of q, reflection, transmission, and absorption of photons can be calculated. If all the incident photons are absorbed, then q will be 1. If all the particles are reflected then q would be 2 if the particles were a flat disk at normal incidence and less than 2 for any other particle shape. If the microsphere has no significant absorption, only reflection and transmission of light contribute to radiation pressure force, q will depend upon particle refractive index.

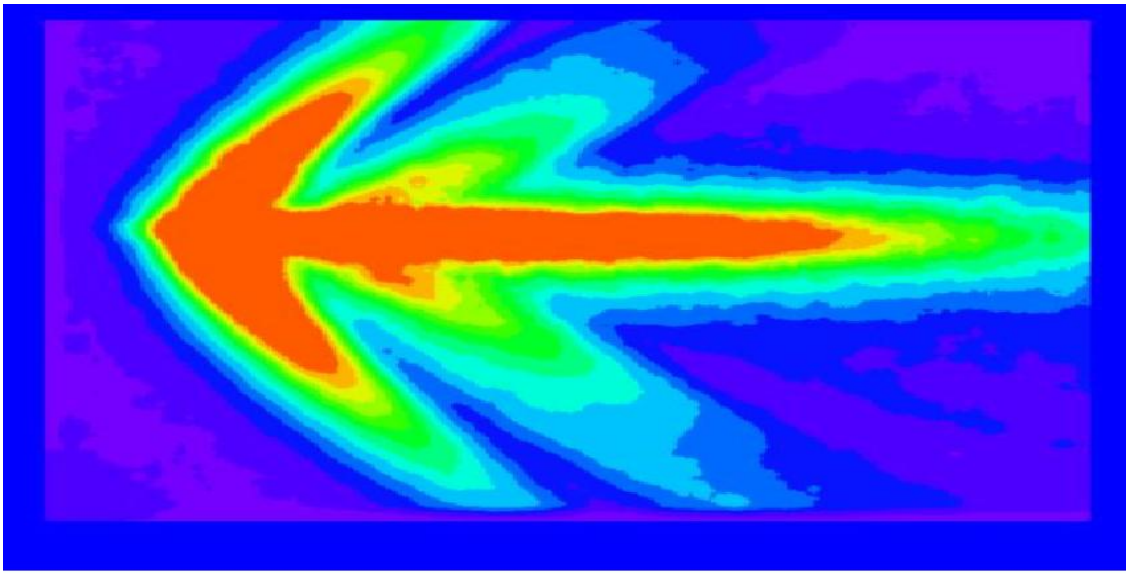

Fig. 1.7 Radiation pressure and gas drag force on a single particle and wave excitation in a dusty plasma [19]

1.6 Ponderomotive Force

Momentum carried by an oscillating electromagnetic wave forces a plasma charged particle for every alternating direction. Due to this force, the charged particle returns to its initial position after each and every oscillation in case of homogeneous field but it will shift towards weak field area in case of inhomogeneous field because of greater force imposed on to the charged particle at the turning point by stronger field [21]. Ponderomotive force plays a significant role in laser energy coupling or in accelerating of particle and in making an enclosed electron bunch. Ponderomotive force also modifies plasma density profiles as a result of which particle velocity

distribution, plasma refractive index, propagation characteristics, self-focusing of beam and laser spot size would be affected.

The equation of motion associated with electric and magnetic field of an electromagnetic wave is

$$m\frac{\partial \vec{v}}{\partial t} + m(\vec{v}.\nabla\vec{v}) = -e\vec{E} - e(\vec{v}\times\vec{B})/c \tag{1.17}$$

The second terms together constitute ponderomotive force for large amplitude wave

$$F_p = m(\vec{v}.\nabla\vec{v}) - e(\vec{v}\times\vec{B})/c \tag{1.18}$$

In the evaluation of F_p, the real part of v and B can be represented as

$$F_p = -m(\overrightarrow{v_r}.\nabla\overrightarrow{v_r}) - e(\overrightarrow{v_r}\times\overrightarrow{B_r})/c \tag{1.19}$$

Using the identity

$$\mathrm{Re}\,\vec{A}.\mathrm{Re}\,\vec{B} = (1/2)\,\mathrm{Re}(\vec{A}.\vec{B} + \vec{A}^*.\vec{B})$$

one can rewrite the ponderomotive force

$$F_p = -(m/2)[(v.\nabla v) + (v^*.\nabla v) - e/c(v\times B + v^*\times B)] \tag{1.20}$$

Electromagnetic wave equation can be represented as

$$E = A(r)\ \exp -i(\omega t - k.z) \tag{1.21}$$

Then

$$v = e\vec{E}/mi\omega \tag{1.22}$$

And time averaged part of ponderomotive force turns out to be

$$F_p = e\nabla\phi_p \tag{1.23}$$

where $\phi_p = -(mc^2/e)(\Upsilon - 1)$

and $\Upsilon = (1 + b^2/2)^{1/2}$ and $b = e|A|/m\omega c$.

1.7 Parametric instability

Parametric instability arises due to coupling of large amplitude of wave with another mode of wave due to the appearance of non-linearity like pressure gradient in plasma. The role of parametric instability is significant in heating of plasma, lower resonance heating etc.

Let the frequency of the wave passing through plasma is ω_0

Frequency of plasma oscillation is ω_1

Then beats appear at frequency ω_0 with the sidebands of frequency $\omega_2 = \omega_0 - \omega_1$ and $\omega_3 = \omega_0 + \omega_1$

Let us assume if the frequency of an another lightly damped plasma mode of oscillation is ω_2 it will now beat with ω_0 with the sidebands at $\omega_1 = \omega_0 - \omega_2$ and $\omega_4 = \omega_0 + \omega_2$.

If ω_2, thus the mode at ω_1 is enhanced and will beat more strongly with ω_0 to give stronger ω_2 mode. So, physically parametric excitation can be assumed as a nonlinear instability of two waves ω_1 and ω_2 by a modulating pump wave ω_0 due to mode coupling interaction. If a pump wave of frequency ω_0 and wave vector k_0 is launched into a collisionless plasma such that its wavelength is very large, its phase velocity may be more than electron thermal speed and the mode will be undamped. If there is low frequency perturbation (ω, k) in plasma such that $\omega << \omega_0$ and $k >> k_0$, it will nonlinearly interact with pump wave leading to generation of side band components at $\omega_\pm \simeq \omega \pm \omega_0$ and $k_\pm \simeq k \pm k_0$ which will have a considerably smaller phase velocity viz, ω/k. The sideband and the pump exert a ponderomotive force on the electrons at frequency and wave vector of the original plasma wave and amplify the plasma wave. This feedback mechanism responsible for simultaneous growth of plasma wave and electromagnetic sideband.

This parametric phenomenon is called as Stimulated Raman Scattering (SRS). In this process, a pump wave photon of energy $h\omega_0$ and momentum hk_0 produces a decay wave plasmons $(h\omega, hk)$ and a sideband photon $(h\omega_s, hk_s)$ and (s = -).

Energy and momentum conservation require that

$$h\omega = h\omega_0 + h\omega_s \tag{1.24}$$

$$hk = hk_0 + hk_s \tag{1.25}$$

These equations also represent the phase matching condition for a three waves resonant interaction. The parametric excitation of upper sideband (ω_+, k_+) is not permissible from energy conservation unless plasma has an additional source of free energy.

1.8 Self-focusing of beam

The nonlinear dependence of the refractive index on the intensity to be of the form

$$n = n_0 + \tfrac{1}{2} n_2 E_0^2 \tag{1.26}$$

where n_0 is the refractive index of medium in the absence of the beam, n_2 is the nonlinear term, E_0 is the amplitude of electric field associated with electromagnetic beam. The nonlinear term appears on account of pressure gradient, temperature gradient, and electrostriction etc. To see the effect of temperature gradient, let us assume a y-axial Gaussian electromagnetic beam propagating along z-direction. The amplitude of electric vector is given by

$$E(x, y, z) = E_0 \cos(kz - \omega t) \tag{1.27}$$

with $E_0 = E_{00} \exp(-r_0^2 / a_0^2)$, where r_0 and a_0 are the cylindrical co-ordinates and beam spot size, respectively. The nonlinear effect supports the convergence of the beam. The equation of refractive index of the medium having the nonlinear effect n_2 is given by

$$n = n_0 + \frac{1}{2} n_2 E_{00}^2 \exp(-2r^2 / a_0^2) \tag{1.28}$$

Expanding the exponential term, we get

$$n = n_0 + \frac{1}{2} n_2 E_{00}^2 - \frac{1}{2} n_0 (r/\beta)^2 , \tag{1.29}$$

where $\beta^2 = \dfrac{n_0 a_0^2}{2 n_2 E_{00}^2}$.

Neglecting the second term, we get

$$n^2 = n_0^2 [1 - (r/\beta)^2]^2 . \tag{1.30}$$

Thus, because of nonlinear effects, the medium will act as a converging lens of focal length approximately given by $f_{nl} = \dfrac{\pi}{2}\beta$.

1.9 Critical power of the beam

The critical power [22] of the beam for self-focusing corresponds to

$$\sqrt{\frac{n_2 E_{00}^2}{n_0}} = \frac{0.61 \lambda_0}{2 a_0 n_0} \tag{1.31}$$

So, critical power P_{cr} is defined as

$$P_{cr} = \pi a_0^2 \frac{c}{n_0} \frac{\varepsilon_0}{8\pi} E_{00}^2 \tag{1.32}$$

$$= \frac{(1.22)^2 \lambda_0^2 c}{128 n_2} \tag{1.33}$$

when power of the beam $P < P_{cr}$, then the beam will converge;

when power of the beam $P = P_{cr}$, then the beam will propagate uniformly without convergence or divergence;

and when power of the beam $P > P_{cr}$, then convergence of the beam will occur.

1.10 Applications of dusty plasmas

Dust grains constitute a major component of matter in the universe. Majority of elements in the interstellar medium (ISM) massive than helium are in the form of dust. Micron/submicron size cosmic dust grains play a major role in physical and dynamical phenomena in the solar system, the ISM, and the interplanetary and planetary world. The awareness of physical, optical and charging characteristics of cosmic dust come up with qualitative information about many topics dealing with the role of dust in spatial world.

1.10.1 Dust in ISM

The phenomena like stellar outflows and supernovae are responsible for the formation of dust in space. Ejected into the ISM, they lead to the formation of diffuse and dense molecular cloud of gas and dust. The gas and dust in the interstellar clouds undergo a variety of complex physical and chemical evolutionary processes leading to the formation of stars and planetary systems, forming a cosmic dust cycles.

1.10.2 Dust in IDM

The interplanetary dust medium (IDM) consists of interplanetary dust cloud (IDC) having the extension from inner solar system to the asteroid belt. Zodiacal light is the visible light scattered by dust particles in the IDC. Particles in the IDC spiral towards the sun with life time of 10^4-10^5 years and are evaporated or driven out by the solar system. The sunlight absorbed and re-radiated in the infra red by the dust dominates the sky in the 3-70 mm spectral region.

1.10.3 Dust in the Lunar Environment

The Apollo astronauts found lunar dust to be unexpectedly high in its adhesive characteristics, sticking to the suits, instruments and lunar rover. The Lunar surveyor spacecraft and the Lunar Ejecta and Meteorite experiment on Apollo 17 indicated the presence of transient dust clouds. A horizon glow over the lunar terminator and high altitude steamers were observed by astronauts on Apollo 17 spacecraft [24].

The lunar dust phenomenon occurs on account of electrostatic charging of dust grain via UV photoelectric emission during day time leading to positively charged dust grains. On the night

side, negatively charged grains are produced by electrons/ions collisions. Secondary electron emission induced by solar wind electrons with sufficiently high energy may produce positively charged grains. Measurement of the optical and physical properties of individual lunar dust grains are required to understand and mitigate the hazardous effect on the lunar dust phenomena.

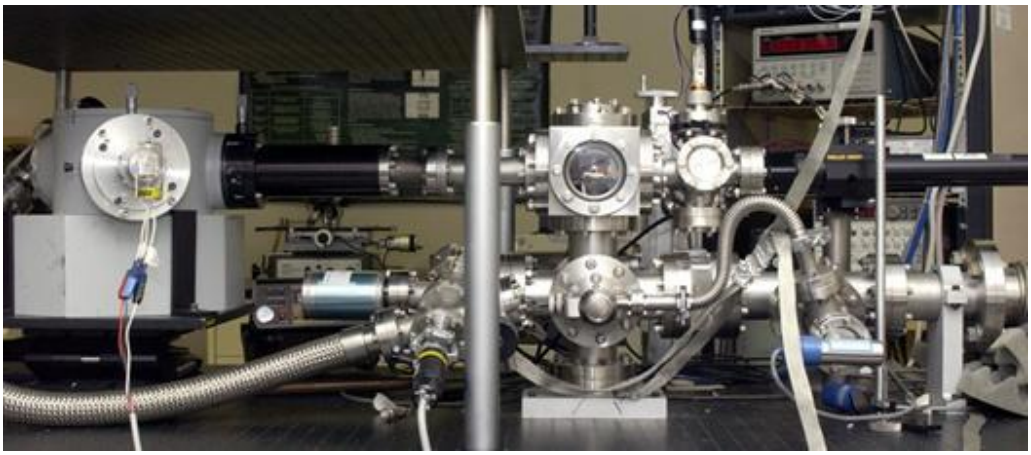

Fig. 1.8 Lab Setup and The EDB [23]

The above photo represents an experimental facility developed at MSFC that is based on electrodynamics balance (EDB) for investigation of the properties of individual micron/submicron size dust particles in simulated space environments. A number of unique experiments have been conducted at this facility to investigate several different properties and processes of astrophysical interest. These studies employed dust grains comprising the analogs of cosmic dust as well as dust grains selected from the sample returns of the Apollo-17 and Luna 24 mission [24].

1.11 Outline of Thesis

The proposed research work is motivated by exciting applications of dust in distinct areas like in planetary atmosphere and planetary rings, radio frequency gas discharge, industrial applications such as in electronic and photonic devices, surface morphology, self-organization etc. Moreover, dusty plasma plays a significant role in studying the nonlinear propagation of electromagnetic wave traversing through the medium, their self-consistent behaviour, modified global and macroscopic properties like evolution of spatial and temporal profile for the electrons

and ions, number densities, plasma potential and electromagnetic field discharge etc. We organize the thesis in the following manner

CHAPTER 1

This chapter introduces the dusty plasmas are characterized by the presence of large-sized dust grains (micron to sub-micron sized) immersed in partially or fully ionized plasma. In addition to electrons, ions, neutrals in "ordinary" plasmas, dusty plasmas contain massive particles of nanometer to micrometer size. Dusty plasma can be produced by dispersing dust grains into plasma (Q- Machine) or by growing dust in plasma made from certain chemically reactive gases such as Silane (SiH_4) and Oxygen (O_2). These are produced by RF and DC glow discharges, in plasma processing reactors, fusion plasma devices, and as fuel combustion products etc. fundamental process involving charging of dust grains mainly depend on the surrounding of dust particles. Various processes like Interaction of dust grains with gaseous plasma particles, energetic particles (electrons and ions), photons, secondary electron emission, thermionic emission, and photoelectric emission are responsible for charging of dust grains in plasma [8]. These dust grains in plasmas acquire a high negative charge in most situations of the order of 10^3e – 10^4e for a 1μm-sized particle and the presence of such highly charged dust grains can significantly influence the global and macroscopic properties of plasma in which they are suspended. Fluctuations of the dust grain charge are found to be a source of modification in number density, energy balance of constituents along with plasma neutrality and also influence the propagation channel of electromagnetic beam traversing through the medium.

CHAPTER 2

This chapter focuses on review of research activities previously performed by various researchers on the topic of dusty plasmas and their importance in various fields like industrial and astrophysics. In this chapter, review of various researchers has been discussed about nonlinear propagation of electromagnetic beam in plasmas and dusty plasmas. In the view of this, we have discussed the effect of dust on nonlinear propagation of electromagnetic beam

including the various processes like ionization of neutrals, electron-ion recombination, electrons-ions accretion on dust particles, photoemission from dust grain surface, collisions between various plasma constituents in the presence of dust, and ohmic heating due to propagation of beam in our present study.

CHAPTER 3

This chapter focuses on the theoretical model for the effect of dust grains on self-filamentation of Gaussian electromagnetic beam prolonging in a fully ionized plasma composed of energy balance of plasma constituents, perturbed electron and ion concentration, and temperature. In this model, neutral atom ionization, reintegration and accumulation of electrons and ions, photoelectric emission of electrons from surface of dust grains, elastic and charging collisions has also been considered. Effective dielectric constant in the presence of dust grains has been constructed. The effect of temporal growth of dust grains on various plasma parameters for the distinct values of dust density has been explored. The variation of the beam width parameter with the normalized channel of prolongation has been observed for distinct dust densities and dust charge states. It is observed that the nonlinearity induced by the effective dielectric constant in the presence of dust grains increases the self-filamentation of the beam, thus enhancing the effective critical power with dust density.

CHAPTER 4

This chapter includes the theoretical investigation of propagation of Gaussian and Sine time irradiance of an electromagnetic beam in collisional dusty plasma. It contains equilibrium of dust charge, particle density and energy balance of plasma ingredients having charge neutrality. Ionization of neutral particles, recombination of free electrons with ions, adsorption and emission of electrons from dust grain surface, and binary collisions between plasma components are also considered in this treatment. Time varying behaviour of modified electron temperature and collision frequency has been illustrated numerically as a function of dust densities. Also, the comparative analyses of variation of beam waist parameter with the dimensionless length of transmission for both the Gaussian and Sine time irradiance are involved in this model as a function of distinguishable time width, collision frequencies, and dust densities

under the condition that the size of dust nebulous is greater than the electrons mean free path for the adsorption on the dust grain surface.

CHAPTER 5

This chapter presents the theoretical model for nonlinear propagation of electromagnetic wave in non-thermal exospheric dusty plasma. A simultaneous solution of escape mechanism of ionic species in exosphere, dust charge kinetics, and electromagnetic wave equations under JWKB approximation has been obtained. We have also considered the process of neutrals, electron-ion recombination, electron adsorption and photoemission of dust grain surface, elastic and charging collisions, and ohmic heating of electrons due to propagation of electromagnetic wave. The dependence of various dusty plasma parameters with square of electric field vectors have been analyzed for an altitude of 1000km based on mid-day, mid-latitude data used by Gurevich. We have also studied the variation of square of electric field vector with the normalized distance of propagation as a function of absorption coefficient, dust density, plasma frequency and collision frequency. It is found that irradiance of electromagnetic wave decreases with dimensionless distance of propagation for different values of dusty plasma parameters. Our results are beneficial for study of earth-satellite orbiting system, solar wind propagation in upper atmosphere, and laboratory experiments.

CHAPTER 6

This chapter covers the theoretical investigation of the effect of dust grains on the threshold power of the amplitude modulated laser beam propagating in complex plasma. In this analysis, momentum and energy balance equations have been solved simultaneously to govern the relation between the beam width parameter and normalizes length of progression of amplitude modified beam advancing in complex plasma. The dependence of beam width parameter on the progression length has been evaluated for different values of dust grain size and dust charge state. Moreover, the dependence of critical power of self-focusing on dust grain size

and dust charge state has also been investigated. It is found that the critical power augments with the increase in dust grain size as well as with the increase of the dust charge state.

CHAPTER 7

This chapter presents the theoretical model for self-trapping of Gaussian electromagnetic beam propagating in dusty plasma. This model comprises of balancing of charge, number density, and energy exchange between plasma components having charge neutrality. Ionization of neutrals, recombination, emission and sticking of electrons to the dust particles, and the collisions between the constituents are considered herein. For numerical appreciation, curves have been drawn for variation of electron density with time and beam waist parameter with the dimensionless length of propagation for different number density and sizes of dust grains.

CHAPTER 8

This thesis provides a broad perspective and opens up future development of the rapidly expanding field to interested researchers normally working in this area. Since our various theoretical results are in line with the experimental outcomes, so the knowledge of our results is very useful in explaining the high-tech applications of dusty plasma systems. We thus expect our results are very helpful in the areas of gas discharge and plasma physics, space and astrophysics, advanced industrial applications of microns and nano-sized particles. Our results are beneficial for study of icy bodies in outer solar system like Moon, Mars, and Venus for which escape mechanism plays a dominant role.

REFERENCES

[1] L.Tonks and I.Langmuir,Phys.Rev.**33**, 195(1929).

[2] D. A. Mendis ed P.K. Shukla, D. A. Mendis, T. Desai (Singapore: World Scientific) pp-3-19.

[3] J. Winter, Plasma Physics and Controlled Fusion **40**, 6 (1998).

[4] J. H. Chu and I L, Phys. Rev. Lett.**72**, 4009(1994).

[5] T G Northrop, Phys. Scripta **45**, 17(1992).

[6] M. S. Barnes, J. H. Keller, J. C. Forster, J. A. O'Neill and D. K. Coultas, Physical Review Letters **68**, 3(1992).

[7] J. E. Allen, Physica Scripta **45**, 497(1992).

[8] P.K.Shukla, and A. A. Mamun, "Introduction to Dusty Plasma Physics", IOP, Bristol(2002).

[9] R.L.Merlino, and J.A. Goree, Physics Today **32**, (2004).

[10] A. Barkan, R. L. Merlino, and N. D'Angelo, Phys. Plasmas **2**, 10(1995).

[11] A. A. Samarian and B. W. James, Physics Letters A **287**, 125(2001).

[12] R.L.Merlino, "Dusty Plasma Physics: Basic Theory and Experiment", The Abdus Salam International Centre for Theoretical Physics Summer College of Plasma Physics, (2007).

[13] https://edoc.ub.uni-muenchen.de/11882/1/Mitic_Slobodan.pdf

[14] K. De Bleecker, A. Bogaerts, and W. Goedheer, Phys. Rev. E **71**, 066405 (2005).

[15] H.Rothermel, T.Hagl, G.E.Morfill, M.H.Thoma, and H.M.Thomas, Phys. Rev.Lett. **89**, 175001 (2002).

[16] R.N. Varney, Phys. Rev. **88**, 362 (1952).

[17] M. Wutz, H.Adam, and W. Walcher, Theorie und Praxis de Vakuumtechnik (Vieweg, Braunschweig 1981).

[18] B. Liu, J. Goree, V. Nosenko, and L. Boufendi, Phys.of Plasmas **10**, 1(2003).

[19] B. Liu, J. Goree, V. Nosenko, and K. Avinash, "Radiation pressure and gas drag forces on a single particle and wave excitation in a dusty plasma," dusty.physics.uiowa.edu.

[20] S. Nunomura, D. Samsonov, and J. Goree, Phys. Rev. Lett. **84**, 5141 (2000).

[21] M. Mahdavi and S. F. Ghazizadeh, The African Rev. of Phys**. 8:0047**, 331(2013).

[22] M.S.Sodha, A.K.Ghatak, V.K.Tripathi, progress in Optics **13**, 169(1976).

[23] J.F.Spann, M.M.Abbas, C.C.Venturini, and R.H. Comfort, Electrodynamic balance for studies of cosmic dust particles, Physica Scripta. **T89**, 147(2001).

[24] M.M. Abbas, D.Tankosic, J.F. Spann, M.J. Dube, and J.A. Gaskin, Measurements of Charging of Apollo 17 Lunar Dust Grains by Electron Impact, STAIF Conference Proceeding, 942(2008).

Chapter 2

LITERATURE REVIEW

In this chapter key attention is paid to literature review which explains the importance of self-focusing. It has become an attractive field of interest in recent years because of the nonlinear interaction of electromagnetic beam in dusty plasmas. Non-linearity appears on ground of nonlinear radial distribution of intensity of beam in dusty plasma and modifies the electron concentration, electron temperature and dielectric constant. Collisional, relativistic and ponderomotive non-linearity have been the leading factors for carrying out research in the field of plasma applications.

The importance of subject is confirmed by various researchers [1-14]. Sharma et al. [15] have analyzed the nonlinear self-modulation of electromagnetic beam in dusty plasma. They measured the nonlinear current density and change in modulation index in the existence of dust grains in plasma and found that the dust grains reduce the self-filamentation of microwaves and decrease its amplitude as compared to dust free plasma. Mishra et al. [16] have considered the prolongation of electromagnetic waves in complex plasma and observed the behavior of the beam for the cases of convergence, oscillatory divergence and steady divergence. Sodha et al. [17] have observed the variation in various parameters of plasma with applied electric field in the existence of dust grains. Verheest and Meuris [18] have developed the nonlinear Schrödinger wave equation and observed the transformation in dust charge due to nonlinear interaction of electromagnetic wave in plasma.

Prasad and Tripathi [19] have reported the self-filamentation characteristics of an electromagnetic beam in weakly ionized plasma in their model. Sambandan et al. [20] have developed a theoretical model for nonlinear propagation of an electromagnetic beam in dusty plasma and found that the electromagnetic beam become self-focused for a power greater than the threshold value. Sodha et al. [21] have developed a theoretical model for the self and cross

filamentation of electromagnetic beam in fully ionized collisional magneto-plasma. They looked upon heating of electrons through plasma due to the beam and energy decay via collisions and thermal conduction. In addition, they observed the self/cross-filamentation of beam for higher and lower values of the magnetic field due to ionic thermal conduction. Sodha et al .[22] have investigated the self-focusing of a laser beam in fully ionized plasma on account of non-linearity appears due to energy loss by thermal conduction. In this case, they have studied the nonlinear dielectric constant for oscillatory and self-focused mode of the beam. They predicted the enhancement of axial intensity for 1010 W laser in a length of 0.6 cm by a factor of 25.

Sodha et al. [23] have investigated the dust particle charging in illuminated open complex plasma. They included neutral atom ionization, ion-electron recombination, electron/ion accretion and electron emission by dust grains, and binary collision between different constituents of complex plasma. They illustrated the parametric study of Cs, LaB6, and CeO2 in the day time ionosphere at an altitude of 150 Km assuming the radius of dust cloud is greater than the mean free path of accretion of dust grains. Sodha et al. [24] have also presented a model for evaluation of dust charge fluctuation in complex plasma considering the cases like photoelectric emission, thermionic emission and no emission of electrons from dust grain surface. Jia et al. [25] have studied the modified dielectric constant for EM wave propagating in fully ionized plasma using the Boltzmann's Distribution law. They considered both the charging and collisional effect of dust grains and studied about the effect of larger dust radii and charge on propagation of EM wave in fully and weakly ionized plasma. Dan et al. [26] have investigated the transmission properties of EM wave propagating in fully ionized plasma with and without dust grains. They considered the FPL and BGK model and compared the result with weakly ionized plasma under matrix method. They observed that the dust radii and density affect the reflection and transmission coefficients of fully ionized dusty plasma slabs. Stoffels et al. [27] have demonstrated the laser particle interaction in an Ar/ CCl_2F_2 RF plasma. In this case, they monitored the white light emitted during this process as a function of time and wavelength, and analyzed with the spectra of black body curves. They obtained a spectral temperature of about 3500K for various dusty plasma states and marked to the decomposition temperature of the particulate material. Li et al. [28] have studied the effect of dust charge and their size on the

propagation of EM waves in dusty plasma using the power law dust size distribution and observed the variation in attenuation coefficient with dust size distribution. Zharova et al. [29] have developed an electrodynamic model for laser particulate interaction in an ionized gas cluster. They studied the self-filamentation of laser radiation using the Schrodinger wave envelope and observed that for laser power exceeding the critical power, wave-field meet with self-compression. Mishra et al. [30] have studied the transportation of complex plasma featured by Mathis, Rumpl, and Nordsieck (MRN) power law grain size distribution with and without electric field. They observed the larger plasma transparency with larger dust grains in dark plasma while the case is reversed in illuminated plasma where the photoemission is predominant. Wang et al. [31] have studied the electromagnetic wave propagation characteristics of inhomogeneous dusty plasma. They developed the models of double exponential and hyperbolic electron number density distribution for dusty plasma and also studied the power transmission and reflection coefficient on the basis of their analytical study. Sodha et al. [32] also analyzed the cases of thermionic emission, photoemission, and emissionless processes to formulate the problem of fluctuation of charge on account of presence of dust grains.

REFERENCES

[1] M. Mikikian, L. Boufendi, A. Bouchoule, H. M. Thomas, G .E. Morfill, A. P. Nefedov,V. E .Fortov, and the PKE–Nefedov team,Formation and behaviour of dust particle clouds in a radio-frequency discharge: results in the laboratory and under microgravity conditions, New Journal of Physics **5**, 19.1(2003).

[2] M.S. Sodha, S. K. Mishra, Shikha Misra, and Sweta Srivastava, Phys. Plasmas **17**, 073705(2010).

[3] V.N.Tsytovich, U. de Angelis, A. V. Ivlev, G. E. Morfill, and S. Khrapak, Nonlinear drag force in dusty plasmas,Phys. Plasmas **12**, 112311(2005).

[4] Y. Hong , C.Yuan , J. Jia , R. Gao , Y. Wang, Z. Zhou , X. Wang , H. Li , and J. Wu, Propagation characteristics of microwaves in dusty plasmas with multi-collisions, Phys.Sci.Technol.**19**, 055301(2017).

[5] J. H. Chu and I. Lin, Direct observation of Coulomb crystals and liquids in strongly coupled rf dusty plasmas, Phys. Rev. Lett. **4009**, 72(1994); H.Thomas, G. E. Morfill,V.Demmel, J. Goree, B. Feuerbacher, and D.Molmann, ibid. Plasma Crystal - Coulomb Crystallization in a DustyPlasma, **652**, 73(1994); H.Thomas and G. E. Morfill,Melting Dynamics of plasma crystal, Nature (London) **806**, 379(1996).

[6] S. V. Vladimirov and K. Ostrikov, Dynamic self-organization phenomena in complex ionized gas systems: new paradigms and technological aspects, Phys. Rep. **393**,175(2004).

[7] G. S. Selwyn, A Phenomenlogical Study of Particulates in Plasma Tools and Processes, Jpn. J. Appl. Phys.**32**, 3068(1993).

[8] Jieshu Jia, Chengxun Yuan, Ruilin Gao, Ying Wang, Yaoze Liu, Junying Gao, Zhongxiang Zhou, Xiudong Sun, Jian Wu and Hui Li, and Shaozhi Pu,Propagation of electromagnetic waves in a weakly ionized dusty plasma, J.Phys.D: Appl.Phys.**48**, 465201(2015).

[9] M. S. Sodha, A. Dixit, S. Srivastava, S. K Mishra, M. P. Verma, and L. Bhasin, Charge distribution of particles in an irradiated dust cloud, Plasma Sources Sci. Technol. **19**, 015006(2010).

[10] M. S. Sodha, S. Misra, and S. K. Mishra, Kinetics of cometary plasma, Plasma Sources Sci. Technol. **19**, 045022(2010).

[11] M. S. Sodha, S. Mishra, S. K. Mishra, and S. Srivastava,Growth of embryonic dust particles in a complex plasma, J. Appl. Phys. **107**, 103307(2010).

[12]M. S. Sodha, S. K. Mishra, and S. Misra, Kinetics of illuminated complex plasmas considering Mie scattering by spherical dust particles with a size distribution, J. Appl. Phys.**109**, 013303(2011).

[13] C.Zafiu, A.Melzer, and A.Piel, Measurement of ion drag force on falling dust particles and its relation to the void formation in complex (dusty) plasma, Phys.Plasmas **10**,1278(2003).

[14]M. S. Sodha, S. Mishra, and S. K. Mishra, Kinetics of complex plasmas having spherical dust particles with a size distribution, Phys.Plasmas **17**, 113705(2003).

[15] Suresh C. Sharma, A.Gahlot, and R.P.Sharma, Effect ofdust on an amplitude modulated electromagnetic beam in a plasma, Phys. Plasmas **15**, 043701(2008).

[16]S. K. Mishra, Shikha Misra, and M. S. Sodha, Self-focusing of a Gaussian electromagnetic beam in a complex plasma, Phys. Plasmas **18**, 043702(2011).

[17] M. S. Sodha, S. K. Mishra, and Shikha Misra, Phys. Plasmas, Nonlinear dependence of complex plasma parameters on applied electric field **18**, 023701(2011).

[18] F. Verheest and P. Meuris, Nonlinear electromagnetic modes in plasmaswith variable dust charges, Phys. Lett. A **210**, 198(1996).

[19] S.Prasad and V.K.Tripathi, Redistribution of charged particles and self-distortion of high - amplitude electromagnetic waves in a plasma, J.Appl.Phys. **44**, 4595(1973).

[20] G. Sambandan, V. K. Tripathi, J. Parashar, and R. Bharuthram,Nonlinear interaction of a high-power electromagnetic beam in a dusty plasma: Two-dimensional effects, Phys. Plasmas **6**, 762(1999).

[21] M.S.Sodha, S.K.Mishra, and S.K.Aggarwal, Self-focusing and cross-focusing of Gaussian electromagnetic beams in fully ionized collisional magnetoplasmas, Phys. Plasmas **14**, 112302(2007).

[22] M.S.Sodha, R.K.Khanna, and V.K.Tripathi, Self-focusing of a laser beam in a strongly ionized plasma, Opto-electronics **5**, 533(1973).

[23] M.S.Sodha, S.Misra, and, S.K.Mishra, Charging of dust particles in an illuminated open complex plasma system, Phys. Plasmas **16**, 123705(2009).

[24] M.S.Sodha, S.K.Mishra, S.Misra, and, S.Srivastava, Fluctuation of charge of particles in a complex plasma system, Phys. Plasmas **17**, 073705(2010).

[25] Jieshu Jia, Chengxun Yuan, Sha Liu, Feng Yue, Ruilin Gao, Ying Wang, Zhong-Xiang Zhou, Jian Wu and Hui Li, Propagation of electromagnetic wave in weak collisional and fully ionized dusty plasma, Phys. Plasmas **23**, 043302(2016).

[26] Li Dan, Li-Xin Guo, and Jiang-Ting Li, Propagation characteristics of electromagnetic waves in dusty plasma with full ionization, Phys. Plasmas **25**, 013707(2018).

[27] E.Stoffels, W.W.Stoffels, D. vender, G.M.W.Kroesen, and F.J de Hoog, Laser Particulate interactions in a dusty RF plasma, IEEE transaction on Plasma Science **22**, 2(1994).

[28] Hui Li, Jian Wu, Zhongxiang Zhou, and Chengxun Yuan, Propagation of Electromagneticwave in dusty plasma and the influence of dust size distribution, Phys.Plasmas **23**, 073702(2016).

[29] N.A.Zharova, A.G.Litvak, and V.A.Mironov, Self-focusing of laser radiation in cluster plasma, JETP Lett. **78**, 619(2003).

[30] S. K. Mishra, and S.Misra, Phys. Plasmas **26**, 023702 (2019).

[31] Hai-bo Wang, Yun-yun Chen, and Chung Huang, Optik-International Journal for Light and Electron optics **196**, 163148(2019).

[32] M. S. Sodha, S. K. Mishra, S. Misra, and S. Srivastava, Phys. Plasmas **17**, 073705 (2010).

Chapter 3

THEORETICAL MODEL FOR THE EFFECT OF DUST GRAINS ON SELF-FILAMENTATION OF GAUSSIAN ELECTROMAGNETIC BEAM IN FULLY IONIZED PLASMA

3.1 Brief outline of the chapter

This work present a theoretical model for dynamics of temporal growth of dust grain in fully ionized complex plasma and expressing the features of non-uniform correspondence of a Gaussian electromagnetic beam with fully ionized complex plasma having electrons, ions and dust grains as the constituents. Diffusion, neutral ionization, recombination of electrons and ions, electrons–ions/dust collisions in plasma, electrons-ions deposition on the dust grain surfaces, thermal conduction are the specific process have been included in this theoretical model. In fully ionized complex plasma, energy loss of electrons via thermal conduction dominates over the collisional effect, so we have to ignore energy loss by collision. The number density of constituents and energy balanced equations have been used to study the non-uniform dependency of different plasma parameters on the dimensionless axial intensity of the beam and also the computation have been made to observe the dependence of dust charge, electrons and ions density, their temperature, effective collision frequency on the time τ for different values of dust density by solving the coupled equations simultaneously. MATHEMATICA and MATLAB softwares have been employed to solve the equations numerically. The variation of the beam width parameter with the normalized channel of propagation has been observed for distinct dust densities and dust charge states. It is observed that the nonlinearity induced by the effective dielectric constant in the presence of dust grains increases the self-filamentation of the beam, thus enhancing the effective critical power with dust density.

3.2 Introduction

Several investigations [1-5] have been carried out on complex plasma because of its exclusive characteristics, especially; self-filamentation has been an attractive field of interest in recent years because of the nonlinear interaction of electromagnetic beam in complex plasmas. Non-linearity appears on ground of nonlinear radial distribution of intensity of beam in complex plasma and modifies the electron concentration, electron temperature and dielectric constant. Collisional, relativistic and ponderomotive nonlinearity have been the leading factors for carrying out research in the field of plasma applications. Collisional non linearity appears due to heating of plasma component on account of dissipation of energy of electromagnetic beam propagating through plasma. Energy gained by the electrons during this process is lost by thermal conduction and electron collisions with ions, dust and neutral particles. In fully ionized plasma, the former mechanism becomes predominant on account of higher degree of ionization as $\delta_0(\rho_0^2/l_m^2) << 1$, where $\delta_0\left(=2m_e/m_i\right)$ is the fraction of energy loss due to collisions, m_e and m_i are the electronic and ionic masses, ρ_0 is the initial width of the beam, l_m is the mean free path of collisions of electrons.

The importance of subject is confirmed by various researchers [6-19]. Sharma *et al*. [20] have analysed the nonlinear self-modulation of electromagnetic beam in dusty plasma. They measured the nonlinear current density and change in modulation index in the existence of dust grains in plasma and found that the dust grains reduce the self-filamentation of microwaves and decrease its amplitude as compared to dust free plasma.

Mishra *et al*. [21] have considered the prolongation of electromagnetic waves in complex plasma and observed the behaviour of the beam for the cases of convergence, oscillatory divergence and steady divergence.

Sodha *et al*. [22] have observed the variation in various parameters of plasma with applied electric field in the existence of dust grains.

Verheest and Meuris [23] have developed the nonlinear Schrödinger wave equation and observed the transformation in dust charge due to nonlinear interaction of electromagnetic wave in plasma.

Prasad and Tripathi [24] have reported the self-filamentation characteristics of an electromagnetic beam in weakly ionized plasma in their model.

Sambandan *et al*. [25] have developed atheoretical model for nonlinear propagation of an electromagnetic beam in dusty plasma and found that the electromagnetic beam become self-focused for a power greater than the threshold value.

Sodha *et al*. [26] have developed a theoretical model for the self and cross filamentationof electromagnetic beam in fully ionized collisional magneto-plasma. They looked upon heating of electrons through plasma due to the beam and energy decay via collisions and thermal conduction. In addition, they observed the self/cross-filamentation of beam for higher and lower values of the magnetic field due to ionic thermal conduction.

Sodha *et al.* [27] have investigated the self-focusing of a laser beam in fully ionized plasma on account of non-linearity appears due to energy loss by thermal conduction. In this case, they have studied the nonlinear dielectric constant for oscillatory and self-focused mode of the beam. They predicted the enhancement of axial intensity for 10^{10} W laser in a length of 0.6 cm by a factor of 25.

Sodha *et al*. [28] have investigated the dust particle charging in illuminated open complex plasma. They included neutral atom ionization, ion-electron recombination, electron/ion accretion and electron emission by dust grains, and binary collision between different constituents of complex plasma. They illustrated the parametric study of Cs, LaB_6, and CeO_2 in the day time ionosphere at an altitude of 150 Km assuming the radius of dust cloud is greater than the mean free path of accretion of dust grains.

Sodha *et al*. [29] have also presented a model for evaluation of dust charge fluctuation in complex plasma considering the cases like photoelectric emission, thermionic emission and no emission of electrons from dust grain surface.

Jia *et al.* [30] have studied the modified dielectric constant for EM wave propagating in fully ionized plasma using the Boltzmann's Distribution law. They considered both the charging and collisional effect of dust grains and studied about the effect of larger dust radii and charge on propagation of EM wave in fully and weakly ionized plasma.

Dan *et al.* [31] have investigated the transmission properties of EM wave propagating in fully ionized plasma with and without dust grains. They considered the FPL and BGK model and compared the result with weakly ionized plasma under matrix method. They observed that the dust radii and density affect the reflection and transmission coefficients of fully ionized dusty plasma slabs.

Stoffels *et al*. [32] have demonstrated the laser particle interaction in Ar / CCl_2F_2 RF plasma. In this case, they monitored the white light emitted during this process as a function of time and wavelength, and analysed with the spectra of black body curves. They obtained a spectral temperature of about 3500K for various dusty plasma states and marked to the decomposition temperature of the particulate material.

Li*et al.* [33] have studied the effect of dust charge and their size on the propagation of EM waves in dusty plasma using the power law dust size distribution and observed the variation in attenuation coefficient with dust size distribution.

Zharova *et al.* [34] have developed an electrodynamic model for laser particulate interaction in an ionized gas cluster. They studied the self-filamentation of laser radiation using the Schrödinger wave envelope and observed that for laser power exceeding the critical power, wave-field meet with self-compression.

In this paper, we have studied the role of dust grains in self-filamentation of highly intense Gaussian electromagnetic beam in fully ionized complex plasmas. Electrons are heated non-linearly when a Gaussian beam passing through complex plasma i.e., bonding of dust particles with the electrons is maximum along axial direction of beam owing to maximal temperature of electrons in the paraxial region. This nonlinear heating causes the variation in electron concentration in the surrounding of axis of the beam even when there is an ambipolar diffusion of plasma. This inhomogeneous distribution of electron density creates a channel which guides the beam to propagate. Energy and momentum acquired by the electrons during the prolongation of electromagnetic beam through the complex plasma is balanced by the loss of energy via collisions and thermal conduction. In fully ionized complex plasma, the latter effect dominates

over the first. In the present analysis of nonlinear interaction of electromagnetic beam in fully ionized complex plasma, following assumptions have been taken into account:

a) Closely packed spherical dust grains,
b) Gaussian profile of amplitude of electromagnetic beam,
c) paraxial ray approximation for the prolongation of Gaussian beam, i.e., all the related parameters are expanded in the surrounding of axis of beam ($\rho = 0$) upto the term ρ^2/ρ_0^2 except the coefficient of thermal conduction, diffusion and mobility that adapt the behaviour of axial temperature of electrons and ions,
d) nonlinear ohmic heating of electrons because of perturbed electron concentration and temperature due to nonlinear irradiance of electromagnetic beam. Ohmic heating of ions may be ignored because of their heavier masses.
e) ionization and reintegration of electrons and ions,
f) elastic and sticking collisions of electrons with constituent particles,
g) accumulation of ions and electrons on dust particle surfaces and photoelectric emission of electrons from the surface of dust grains,
h) steady state number and energy balance of electrons and ions,
i) charge neutrality condition of complex plasma,
j) mobility and diffusion of dust grains are considered as zero on account of their heavy mass,
k) space charge is present due to inhomogeneous electron temperature,
l) steady state balancing of gradient of electron/ion pressure by force due to space charge and,
m) change in electrons and ions concentration is same in steady state due to space charge.

For the photoelectric emission of electrons from the surface of dust particles, density and temperature of electrons should be high enough and the irradiance of light should be low enough to keep the particle negatively charged as in case of Saturn ring. Thus the calculations have been made by processing the data corresponding to metallic dust of high work function of 7.8 eV

(stainless steel) in near space region of atmosphere where photoemission occurs on account of Lyman alpha spectral lines (1215.7 Å) of extreme ultra violet EUV radiations [35].

The remainder manuscript is structured in the subsequent manner: In Sec. 3.3, we formulate the problem using the basic sets of equations. We construct the effective concentration and temperature of electrons and ions using the energy balance to give effective dielectric constant in the existence of dust grains. In Sec.3.4, wave equation has been resolved for the prolongation of Gaussian electromagnetic beam in fully ionized complex plasma in terms of variation of beam width parameter 'f' with the normalized channel of prolongation 'ξ'. In Sec. 3.5, effective critical power of self-filamentation is derived using the initial boundary conditions. Outcomes of the present work are discussed in Sec. 3.6 and finally the conclusion part is given in Sec. 3.7.

3.3 Theoretical Model of Interaction Techniques in Fully Ionized Complex Plasmas

We assume three species plasma to be composed of ions, electrons and dust grains with charge $-Z_d e$ and radius r_d, where Z_d is the dust charge state and e is the electronic charge. The dynamics of fully ionized complex plasma include reintegration of electrons and ions, ionization, neutralization of ions, accumulation of electrons on dust grain surfaces, ohmic heating and thermal conduction.

The following equations explain the dynamics of complex plasma.

Ions and neutral atoms conservation:

$$n_i + n_0 = n_{i0} + n_{00}\,, \tag{3.1}$$

where n_i, n_{i0} and n_0, n_{00} are the densities of ions and neutral atoms with and without dust grains, respectively.

Dust grains charging

The charge on dust grains is controlled by the accumulation of electrons and ions andemission of electrons from dust grain surfaces; thus

$$\frac{dZ_d}{d\tau}=n_{ic}+n_{ph}-\Upsilon n_{ec}, \tag{3.2}$$

where $n_{ic}=\pi r_d^2(8k_BT_i/\pi m_i)^{1/2}n_i\left[1-Z_d\alpha_i\right]$ is the ion accumulation current to dust grain surface and $n_{ec}=\pi r_d^2(8k_BT_e/\pi m_e)^{1/2}n_e\exp\left[Z_d\alpha_e\right]$ is the electron accumulation current to dust grain surface, $n_{ph}\left(=\pi r_d^2 n_p\right)$ is the photocurrent emitting from surface of negatively charged dust grains,where

$$n_p=\chi(\nu)\Lambda(\nu)=(4\pi m_e k_B^2T^2/h^3)\mu(\nu)\Lambda(\nu)\Phi_{ph}(\eta),$$

$\Phi_{ph}(\eta)$ is tabulated integral(Fowler 1936) defined by

$$\Phi_{ph}(\eta)=\int_0^{\exp(\eta)}\frac{\ln(1+\Omega)}{\Omega}d\Omega,$$

$$\eta=(h\nu-\phi_0)/k_BT_d.$$

n_p is rate of photoelectric emission per unit area from a neutral or negatively charged dust surface,

$\chi(\nu)$ is photoelectric efficiency,

$\Lambda(\nu)$ is the number of photons incident per unit area per unit time on a surface normal to the direction of incidence.

h is Planck's constant, ν is frequency of radiation, ϕ_0 is work function of dust, T_d is temperature of dust particle, $\mu(\nu)$ is the probability of absorption of photon by an electron hitting the surface from inside[35].

$\alpha_i=(e^2/r_dk_BT_i)$, $\alpha_e=(e^2/r_dk_BT_e)$, r_d is radius of dust grain, Υ is the coefficient of sticking of electrons on surface of dust grain, k_B is Boltzmann's coefficient, T_i and T_e are the ions and electrons temperature, m_i and m_e are the ionic and electronic masses, respectively.

Dynamics of electron and ions

$$\frac{dn_e}{d\tau} = \beta_i n_0 - \alpha_r n_e n_i - n_d(\Upsilon n_{ec} - n_{ph}) - \nabla\Phi_p \tag{3.3}$$

and

$$\frac{dn_i}{d\tau} = \beta_i n_0 - \alpha_r n_e n_i - n_d n_{ic} - \nabla\Phi_p, \tag{3.4}$$

where β_i is the ionization co-efficient, $\alpha_r = (\alpha_{r0}(300/T_e)^{k'})$ cm^3/s is the reintegration coefficient of ions and electrons, k' and α_{r0} are invariable, n_d is the number density of dust.

Eqs. (3.3) and (3.4) represent the growth rate of electron and ion densities in complex plasma, respectively. The first terms on RHS of Eqs. (3.3) and (3.4) correlate with the rate of gain of electrons and ions densities due to neutral atom ionization. The succeeding two terms in both the equations refer to decaying rate of electrons and ions on account of reintegration, and the net accumulation of electrons and ions on the dust grain surface. The last term $\nabla\Phi_p$ represent density decay due to ambipolar diffusion in both the equations obtained by solving the momentum equations as shown in appendix A.

Neutrality of charge:

Neutrality of charge may be demonstrated by the following equation:

$$Z_d n_d + n_i - n_e = 0. \tag{3.5}$$

Energy balance equations of electrons and ions:

$$\frac{d}{d\tau}\left(\frac{3}{2}n_e k_B T_e\right) = \beta_i n_0 \varepsilon_e - \alpha_r n_e n_i \left(\frac{3}{2}k_B T_e\right) - n_d(\Upsilon n_{ec}\varepsilon_{ec} - n_{ph}\varepsilon_{ph}) + \frac{1}{\rho}\frac{\partial}{\partial\rho}\left(\rho k_{pe}\frac{dT_e}{d\rho}\right) + \frac{n_e e^2 \nu_{eff} U_0^2}{4m_e(\omega_d^2 + \nu_{eff}^2)}, \quad (3.6)$$

and

$$\frac{d}{d\tau}\left(\frac{3}{2}n_i k_B T_i\right) = \beta_i n_0 \varepsilon_i - \alpha_r n_e n_i \left(\frac{3}{2}k_B T_i\right) - n_d n_{ic}\varepsilon_{ic} + \frac{1}{\rho}\frac{\partial}{\partial\rho}\left(\rho k_{pi}\frac{dT_i}{d\rho}\right), \quad (3.7)$$

where ε_e and ε_i refers to the average energy of electrons and ions due to neutral atom ionization,

$\varepsilon_{ec}(=2k_B T_e - Z_d(e^2/r_d))$ and $\varepsilon_{ic}(=(2-Z_d\alpha_i)/(1-Z_d\alpha_i))$ represent the average energy of electrons and ions accumulating on the dust grain surfaces,

$$\varepsilon_{ph} = \left(\frac{k_B T_d}{\Theta(\eta-\xi)}\int_0^\infty 2\xi \ln(1+\exp(\eta-\xi))d\xi\right) - Z_d\alpha_d$$

concerns to the energy of photoemission from the dust grain surfaces,

where $\Theta\left(=Z_d e/r_d\right)$ is the potential of charge dust grains, $\eta\left(=h\nu-\phi_0/k_B T_d\right)$, h is Planck's constant, ϕ_0 is work function of dust grains material, $\alpha_d = (e^2/r_d k_B T_d)$, ξ is the normalized channel of prolongation, and T_d is the dust temperature supposed to be invariable on account of large heat capacity. $k_{ph'}$ is the co-efficient of thermal conductivity of electrons and ions of fully ionized complex plasma given by Spitzer [36]and the subscript h' refers to electrons and ions, respectively.

$$k_{ph'} = \alpha T_{h'}^{5/2},$$

and

$\alpha = 19.6\times10^{-5}/\ln\left\{\frac{3}{2h^3}(k_B^3 T_{h'}^3/\pi n_{h'})^{1/2}\right\}$.

$\nu_{eff}\left(=\nu_{ei}+\nu_{ed}+\nu_{en}+\nu_{sc}\right)$ is the effective collision frequency of electrons,

where $\nu_{ei}=\nu_{ei0}\left(\frac{n_e}{n_{e0}}\right)\left(\frac{T_e}{T_{e0}}\right)^{-\frac{3}{2}}$ is the rate of electron-ion collisions [37], n_{e0} and T_{e0} refer to unperturbed density and temperature of electrons, respectively. $\nu_{ei0}=\left(\frac{5.5n_{e0}}{T_{e0}^{3/2}}\right)\ln\left(\frac{220T_{e0}}{n_{e0}^{1/3}}\right)$ is the unperturbed rate of electron–ion collisions, $\nu_{ed}=\nu_{ed0}\left(\frac{T_e}{T_{e0}}\right)^{-\frac{3}{2}}Z_d^2$ is the rate of electron-dust collisions [22], $\nu_{ed0}=\left(2.9\times10^{-6}\right)n_{d0}T_{e0}^{-3/2}\ln\Lambda_e$ is the rate of unperturbed electron-dust collisions [$\ln\Lambda_e$ (coulomb logarithm)=10-13 for fully ionized plasma] ,

$\nu_{en}=\nu_{en0}\left(\frac{n_0}{n_{00}}\right)\left(\frac{T_e}{T_{e0}}\right)^{\frac{1}{2}}$ is the rate of electron-neutral particles collisions [37], $\nu_{en0}=\left(8.3\times10^5\right)\sigma_0 n_{00}T_{e0}^{1/2}$ is the rate of unperturbed electron-neutral particles collisions, where n_{00} is unperturbed number density for neutral particles, $\sigma_0\left(=6.6\times10^{-15}\left[(T_e/4)-0.1\Big/\left\{1+\left(T_e/4\right)^{1.6}\right\}\right]\right)$ is the cross-section area of collision between electrons and neutral particles averaged over a Maxwellian electron distribution, where T_e is in eV and σ_0 is in cm^2. This indicates that σ_0 increases to a threshold value of electron temperature or energy and then starts decreasing and

$\nu_{sc}=n_d(n_{ec}/n_e)$ is the average count of sticking collisions of electrons with dust grains.

The initial two terms of Eqs. (3.6) and (3.7) correspond to final average energy gain of electrons and ions because of neutral atoms ionization and reintegration of electrons and ions in complex plasma. The succeeding term in both the equations refers to final energy loss of electrons and ions because of their accumulation and photoemission of electrons from the surface of dust grains. The fourth term in both the equations represents final gain in energy density of electrons and ions owing to thermal conduction. The endmost term in Eq. (3.6) corresponds to gain in energy density of the electrons from the field on ground of ohmic heating. Ohmic heating of ions can be neglected because of their heavier mass. The term corresponding to power loss per unit volume due to binary elastic collisions among the components can be neglected in fully ionized complex plasma as

$R' = Loss\ of\ energy\ via\ collisions / Loss\ of\ energy\ via\ thermal\ conduction$.

According to Prasad and Tripathi [24], in fully ionized plasma, $R' << 1$ i.e., the rate of gain in energy owing to electron-ion collisions is less than the work done by the electrons against the thermal forces. The direction of the current flow against the gradient of electron temperature will define the positive or negative sign of latter term.

A comparison term R' shows that later mechanism is more predominant in fully ionized complex plasma because of larger mean free path of the electrons than the Debye length, and hence the former can be neglected.

Estimation of ionization co-efficient (β_i):

The temperature of dust grains and neutral atoms is supposed to be constant due to sufficient energy exchange between them because of their big thermal expanse. Coefficient of Ionization, β_i can be estimated by executing dynamics of electrons in dust independent environment using the initial condition as

$$\beta_i n_{00} - \alpha_r n_{e0} n_{i0} = 0, \tag{3.8}$$

$$\beta_i n_{00} = \alpha_r n_{e0} n_{i0} = \alpha_r n_{e0}^2 . \tag{3.9}$$

Estimation of mean energy of electrons and ions:

Mean energies of electrons and ions appeared on account of ionization can be estimated by applying initial conditions in the energy balance equations for dust free plasma; thus

$$\varepsilon_e = \left(\frac{3}{2} k_B T_{e0}\right), \tag{3.10}$$

and

$$\varepsilon_i = \left(\frac{3}{2} k_B T_{i0}\right). \tag{3.11}$$

Paraxial ray approximation:

Now we consider an electromagnetic beam having its Gaussian irradiance distribution along its wavefront. It is convenient to analyse in cylindrical coordinates system, with the prolongation which may be assumed to be the z – axis (cf. Fig. 3.1).

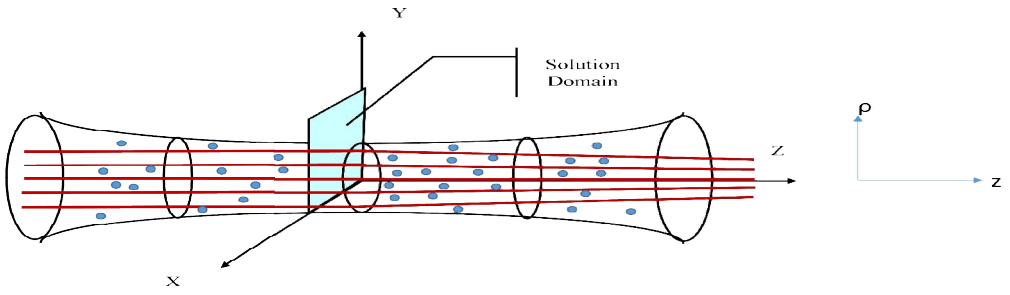

Fig. 3.1 shows the schematic diagram of Gaussian irradiance distribution in complex cylindrical plasma.

The distribution of intensity of the beam at z = 0 is given by

$$U_0^2 = U_{00}^2 e^{\left(-\rho^2/\rho_0^2\right)}, \tag{3.12}$$

where U_0 is the amplitude of electric vector of the Gaussian beam at a distance ρ from axis, U_{00} is the amplitude of the beam along the axis at ρ = 0, ρ_0 is the width of the beam at which

amplitude of the beam is $1/e$ of its value on the axis, and ρ is the radial part of cylindrical co-ordinate system.

For finite value of z, the intensity distribution under the paraxial theory is taken

$$\text{as } U_0^2 = \frac{U_{00}^2}{f^2} e^{\left(-\rho^2/\rho_0^2 f^2\right)}, \tag{3.13}$$

where f is the beam width parameter depends upon the prolongation distance, z,

and $\rho_0 f$ is the beam spot size.

As it is clear from the above expression, almost intensity of beam lies in the vicinity of central axis of beam. Therefore, small angle approximation can be adequately used to analyse the Gaussian beam in paraxial ray approximation [i.e., $\rho/\rho_0 f << 1$]. Related to this concept all the parameters (electron/ion temperature, electron concentration, dielectric function, eikonal function and irradiance profile of the beam) are expended in the surrounding of central axis ($\rho=0$) only upto the term ρ^2/ρ_0^2 as

$$P(\rho,z) = P_a(z) - (\rho^2/\rho_0^2) P_\rho(z), \tag{3.14}$$

where P_a and P_ρ are the components of variables represented by $P(\rho,z)$ along the axis and radius, respectively.

Although the profile of the Gaussian beam remains unaffected during the prolongation of electromagnetic beam in fully ionized complex plasma.

Hence by putting the accordant parameters in dynamic Eqs. (3.2) – (3.4), (3.6) and (3.7) and comparing the coefficient ρ^0 and ρ^2/ρ_0^2 terms, we get,

Charging of dust grains:

$$\frac{dZ_{da}}{d\tau} = n_{ica} + n_{pha} - \Upsilon n_{eca}, \tag{3.2a}$$

and

$$\frac{dZ_{d\rho}}{d\tau} = n_{ic\rho} + n_{ph\rho} - \Upsilon n_{ec\rho} \quad . \tag{3.2b}$$

Dynamics of electron and ions

$$\frac{dn_{ea}}{d\tau} = \beta_{ia} n_0 - \alpha_{ra} n_{ea} n_{ia} - n_d (\Upsilon n_{eca} - n_{pha}) - \frac{(2/\rho_0^2)}{n_{ia} + c_2 n_{ea}} \left[D_{1i} (c_1 n_{ia} n_{e\rho} + c_2 n_{ea} n_{i\rho}) + D_{2i} n_{ea} n_{ia} (c_2 T_{ia}^{-1} T_{i\rho} + c_3 T_{ea}^{-1} T_{e\rho}) \right], \tag{3.3a}$$

and

$$\frac{dn_{e\rho}}{d\tau} = \beta_{i\rho} n_0 - \alpha_{r\rho} n_{ea} n_{ia} - n_d (n_{ec\rho} - n_{pha}) - \frac{(6/\rho_0^2)}{n_{ia} + c_2 n_{ea}} \left[\begin{array}{l} D_{1i} (c_1 + c_2) n_{i\rho} n_{e\rho} - \dfrac{(c_1 n_{ia} n_{e\rho} + c_2 n_{ea} n_{i\rho})(n_{i\rho} + c_2 n_{e\rho})}{n_{ia} + c_2 n_{ea}} \\ + D_{2i} [(n_{ea} n_{i\rho} + n_{ia} n_{e\rho})(c_2 T_{ia}^{-1} T_{i\rho} + c_3 T_{ea}^{-1} T_{e\rho}) \\ - n_{ea} n_{ia} (c_2 T_{ia}^{-2} T_{i'\rho}^2 + c_3 T_{ea}^{-2} T_{e\rho}^2) \\ - \dfrac{n_{na} n_{ia} (c_2 T_{ia}^{-1} T_{i\rho} + c_3 T_{ea}^{-1} T_{e\rho})(n_{i\rho} + c_2 n_{e\rho})}{n_{ia} + c_2 n_{ea}} \end{array} \right]. \tag{3.3b}$$

$$\frac{dn_{ia}}{d\tau} = \beta_{ia} n_0 - \alpha_{ra} n_{ea} n_{ia} - n_d n_{ica} - \frac{(2/\rho_0^2)}{n_{ia} + c_2 n_{ea}} \left[D_{1i} (c_1 n_{ia} n_{e\rho} + c_2 n_{ea} n_{i\rho}) + D_{2i} n_{ea} n_{ia} (c_2 T_{ia}^{-1} T_{i\rho} + c_3 T_{ea}^{-1} T_{e\rho}) \right], \tag{3.4a}$$

and

$$\frac{dn_{i\rho}}{d\tau} = \beta_{i\rho} n_0 - \alpha_{r\rho} n_{ea} n_{ia} - n_d n_{ic\rho} - \frac{(6/\rho_0^2)}{n_{ia} + c_2 n_{ea}} \left[\begin{array}{l} D_{1i}(c_1 + c_2) n_{i\rho} n_{e\rho} - \dfrac{(c_1 n_{ia} n_{e\rho} + c_2 n_{ea} n_{i\rho})(n_{i\rho} + c_2 n_{e\rho})}{n_{i'a} + c_2 n_{e'a}} \\ + D_{2i}[(n_{ea} n_{i\rho} + n_{ia} n_{e\rho})(c_2 T_{ia}^{-1} T_{i\rho} + c_3 T_{ea}^{-1} T_{e\rho}) \\ - n_{ea} n_{ia} (c_2 T_{ia}^{-2} T_{i\rho}^2 + c_3 T_{ea}^{-2} T_{e\rho}^2) \\ - \dfrac{n_{ea} n_{ia} (c_2 T_{ia}^{-1} T_{i\rho} + c_3 T_{ea}^{-1} T_{e\rho})(n_{i\rho} + c_2 n_{e\rho})}{n_{ia} + c_2 n_{ea}} \end{array} \right]. \tag{3.4b}$$

Energy balance equations for electrons and ions:

$$\frac{d}{d\tau}\left(\frac{3}{2} n_{ea} k_B T_{ea}\right) = \beta_{ia} n_0 \varepsilon_e - \alpha_{ra} n_{ea} n_{ia} \left(\frac{3}{2} k_B T_{ea}\right) - n_d (\Upsilon n_{eca} \varepsilon_{eca} - n_{pha} \varepsilon_{pha}) - \frac{4 k_{pe}}{\rho_0^2} T_{e\rho} + \left(\frac{3}{2} k_B T\right) \frac{\beta_0 U_{00}^2}{f^2} n_{ea} \nu_{effa} \delta_{comp} \tag{3.6a1}$$

and

$$\frac{d}{d\tau}\left(\frac{3}{2} k_B (n_{ea} T_{e\rho} + n_{e\rho} T_{ea})\right) = \beta_{i\rho} n_0 \varepsilon_e - \frac{3}{2} k_B \left(\alpha_{r\rho} n_{ea} n_{ia} T_{ea} + \alpha_{ra} (n_{ea} n_{ia} T_{e\rho} + n_{ea} n_{i\rho} T_{ea} + n_{e\rho} n_{ia} T_{ea})\right) - n_d \left(\Upsilon (n_{ec\rho} \varepsilon_{eca} + n_{eca} \varepsilon_{ec\rho}) - (n_{pha} \varepsilon_{php} + n_{php} \varepsilon_{pha})\right) + \left(\frac{3}{2} \delta_{comp} k_B T\right) \frac{\beta_0 U_{00}^2}{f^2} \left(\frac{n_{ea} \nu_{effa}}{f^2} + (n_{e\rho} \nu_{effa} + n_{ea} \nu_{eff\rho})\right) \tag{3.6b1}$$

Substituting $\frac{dn_{ea}}{d\tau}$ and $\frac{dn_{e\rho}}{d\tau}$ from Eqs. 3.3(a) and 3.3(b) into Eqs. 3.6(a1) and 3.6(b1) , we obtain

$$\frac{3}{2}n_{ea}k_B\left(\frac{dT_{ea}}{d\tau}\right)=\left[\begin{array}{l}\beta_{ia}n_0(\varepsilon_e-\frac{3}{2}k_BT_{ea})-n_d\Upsilon n_{eca}(\varepsilon_{eca}-\frac{3}{2}k_BT_{ea})-n_dn_{pha}(\varepsilon_{pha}-\frac{3}{2}k_BT_{ea})\\ +\frac{3}{2}k_BT_{ea}\left(\frac{(2/\rho_0^2)}{n_{ia}+c_2n_{ea}}\right)[D_{2i}(c_1n_{ia}n_{e\rho}+c_2n_{ea}n_{i\rho})\\ \qquad +D_{1i}n_{ea}n_{ia}(c_2T_{ia}^{-1}T_{i\rho}+c_3T_{ea}^{-1}T_{e\rho})]\\ \qquad -\frac{4k_{pe}}{\rho_0^2}T_{e\rho}+(\frac{3}{2}k_BT)\frac{\beta_0U_{00}^2}{f^2}n_{ea}\nu_{effa}\delta_{comp}\end{array}\right], \qquad (3.6a2)$$

where $\beta_0=\frac{e^2}{3m_e\delta_{comp}k_BT\omega^2}$, and $\delta_{comp}\left(=\nu_{sc}/\nu_{eff}\right)$ [Refs.25 and 49] is the mean part of collisional energy loss of electron with the constituents of plasma, and c_1, c_2, c_3, D_{1i}, and D_{2i} are defined in Appendix A and

$$\begin{aligned}\frac{3}{2}n_{ea}k_B\left(\frac{dT_{e\rho}}{d\tau}\right)&=\beta_{ia}n_0[\frac{3}{2}k_BT_{e\rho}-\frac{n_{e\rho}}{n_{ea}}(\varepsilon_e-\frac{3}{2}k_BT_{ea})]+\beta_{i\rho}n_0(\varepsilon_e-\frac{3}{2}k_BT_{e\rho})\\ &\quad -n_d\Upsilon n_{eca}[(\varepsilon_{eca}-\frac{3}{2}k_BT_{ea})+(\varepsilon_{ec\rho}-\frac{3}{2}k_BT_{e\rho})]-n_dn_{ec\rho}(\varepsilon_{eca}-\frac{3}{2}k_BT_{ea})\\ &\quad +\frac{3}{2}k_B(T_{e\rho}+\frac{n_{e\rho}}{n_{ea}}T_{ea})\left(\frac{(2/\rho_0^2)}{n_{ia}+c_2n_{ea}}\right)[D_{2i}(c_1n_{ia}n_{e\rho}+c_2n_{ea}n_{i\rho})+D_{1i}n_{ea}n_{ia}(c_2T_{ia}^{-1}T_{i\rho}+c_3T_{ea}^{-1}T_{e\rho})]\\ &\quad -\frac{3}{2}k_BT_{ea}\frac{(6/\rho_0^2)}{n_{ia}+c_2n_{ea}}\left[\begin{array}{l}D_{2i}(c_1+c_2)n_{i\rho}n_{e\rho}-\frac{(c_1n_{ia}n_{e\rho}+c_2n_{ea}n_{i\rho})(n_{i\rho}+c_2n_{e\rho})}{n_{ia}+c_2n_{ea}}\\ +D_{1i}[(n_{ea}n_{i\rho}+n_{ia}n_{e\rho})(c_2T_{ia}^{-1}T_{i\rho}+c_3T_{ea}^{-1}T_{e\rho})\\ -n_{ea}n_{ia}(c_2T_{ia}^{-2}T_{i\rho}^2+c_3T_{ea}^{-2}T_{e\rho}^2)-\frac{n_{ea}n_{ia}(c_2T_{ia}^{-1}T_{i\rho}+c_3T_{ea}^{-1}T_{e\rho})(n_{i\rho}+c_2n_{e\rho})}{n_{ia}+c_2n_{ea}}\end{array}\right]\\ &\quad -\frac{4k_{pe}}{\rho_0^2}\frac{n_{e\rho}}{n_{ea}}T_{e\rho}+(\frac{3}{2}\delta_{comp}k_BT)\frac{\beta_0U_{00}^2}{f^2}n_{ea}\nu_{effa}+(\frac{3}{2}\delta_{comp}k_BT)\frac{\beta_0U_{00}^2}{f^2}(n_{ea}\nu_{eff\rho})\end{aligned}. \qquad (3.6b2)$$

Similarly,

$$\frac{d}{d\tau}\left(\frac{3}{2}n_{ia}k_BT_{ia}\right)=\beta_{ia}n_0\varepsilon_i-\alpha_{ra}n_{ea}n_{ia}\left(\frac{3}{2}k_BT_{ia}\right)-\Upsilon n_d n_{ica}\varepsilon_{ica}-\frac{4k_{pi}}{\rho_0^2}T_{i\rho}\ , \tag{3.7a1}$$

and

$$\frac{d}{d\tau}\left(\frac{3}{2}k_B(n_{ia}T_{i\rho}+n_{i\rho}T_{ia})\right)=\beta_{i\rho}n_0\varepsilon_i-\frac{3}{2}k_B\left(\alpha_{r\rho}n_{ea}n_{ia}T_{ia}+\alpha_{ra}(n_{ea}n_{ia}T_{i\rho}+n_{ea}n_{i\rho}T_{ia}+n_{e\rho}n_{ia}T_{ia})\right)$$
$$-n_d\left(\Upsilon(n_{ic\rho}\varepsilon_{ica}+n_{ica}\varepsilon_{ic\rho})\right) \tag{3.7b1}$$

Substituting $\frac{dn_{ia}}{d\tau}$ and $\frac{dn_{i\rho}}{d\tau}$ from Eqs. (3.4a) and (3.4b), we obtain

$$\frac{3}{2}n_{ia}k_B\left(\frac{dT_{ia}}{d\tau}\right)=\left[\begin{array}{l}\beta_{ia}n_0(\varepsilon_i-\frac{3}{2}k_BT_{ia})-n_dn_{ica}(\varepsilon_{ica}-\frac{3}{2}k_BT_{ia})+\\ \frac{3}{2}k_BT_{ia}\left(\frac{(2/\rho_0^2)}{n_{ia}+c_2n_{ea}}\right)[D_{1i}(c_1n_{ia}n_{e\rho}+c_2n_{ea}n_{i\rho})+D_{2i}n_{ea}n_{ia}(c_2T_{ia}^{-1}T_{i\rho}+c_3T_{ea}^{-1}T_{e\rho})],\\ -\frac{4k_{pi}}{\rho_0^2}T_{i\rho}\end{array}\right] \tag{3.7a2}$$

and

$$\frac{3}{2}n_{ia}k_B\left(\frac{dT_{i\rho}}{d\tau}\right)=\beta_{ia}n_0[\frac{3}{2}k_BT_{i\rho}-\frac{n_{i\rho}}{n_{ia}}(\varepsilon_{ia}-\frac{3}{2}k_BT_{ia})]+\beta_{i\rho}n_0(\varepsilon_{i\rho}-\frac{3}{2}k_BT_{ia})$$

$$-n_dn_{ica}[\frac{n_{i\rho}}{n_{ia}}(\varepsilon_{ica}-\frac{3}{2}k_BT_{ia})+(\varepsilon_{ic\rho}-\frac{3}{2}k_BT_{i\rho})]-n_dn_{ic\rho}(\varepsilon_{ica}-\frac{3}{2}k_BT_{ir})$$

$$+\frac{3}{2}k_B(T_{i\rho}+\frac{n_{i\rho}}{n_{ia}}T_{ia})(\frac{(2/\rho_0^2)}{n_{ia}+c_2n_{ea}})[D_{2i}(c_1n_{ia}n_{e\rho}+c_2n_{ea}n_{i\rho})+D_{1i}n_{ea}n_{ia}(c_2T_{ia}^{-1}T_{i\rho}+c_3T_{ea}^{-1}T_{e\rho})]$$

$$-\frac{3}{2}k_BT_{ia}\frac{(6/\rho_0^2)}{n_{ia}+c_2n_{ea}}\left[\begin{array}{l}D_{2i}(c_1+c_2)n_{i\rho}n_{e\rho}-\dfrac{(c_1n_{ia}n_{e\rho}+c_2n_{ea}n_{i\rho})(n_{i\rho}+c_2n_{e\rho})}{n_{ia}+c_2n_{ea}}\\ +D_{1i}[(n_{ea}n_{i\rho}+n_{ia}n_{e\rho})(c_2T_{ia}^{-1}T_{i\rho}+c_3T_{ea}^{-1}T_{e\rho})\\ -n_{ea}n_{ia}(c_2T_{ia}^{-2}T_{i\rho}^2+c_3T_{ea}^{-2}T_{e\rho}^2)-\dfrac{n_{ea}n_{ia}(c_2T_{ia}^{-1}T_{i\rho}+c_3T_{ea}^{-1}T_{e\rho})(n_{i\rho}+c_2n_{e\rho})}{n_{ia}+c_2n_{ea}}\end{array}\right] \quad (3.7b2)$$

$$-\frac{4k_{pi}}{\rho_0^2}\frac{n_{i\rho}}{n_{ia}}T_{i\rho}.$$

The stationary solution (i.e., at $t\to\infty$) of the Eqs.(3.2)-(3.7)(a2, b2) jointly gives the dependence of different fully ionized complex plasma parameters on the axial part of radiation by choosing the axial and radial component of relevant set of parameters.

Effective dielectric constant:

Using the above set of parameters, the nonlinear effective dielectric constant may be calculated as

$$\varepsilon_{eff}=1-\left(\frac{\omega_0^2}{\omega_d^2}\right)\frac{\omega_d^2}{(\nu_{eff}^2+\omega_d^2)}\left(\frac{n_e}{n_{e0}}\right)=\varepsilon_a-(\rho^2/\rho_0^2)\varepsilon_\rho. \quad (3.15)$$

Substituting n_e and ν_{eff} corresponding to the Eq. (3.14) and comparing the coefficient of ρ^0 and ρ^2/ρ_0^2 terms, one obtain,

$$\varepsilon_a = 1-\left(\frac{\omega_0^2}{\omega_d^2}\right)\left(1-\frac{\nu_{effa}^2}{\omega_d^2}\right)\left(\frac{n_{ea}}{n_{e0}}\right), \tag{3.15a}$$

and

$$\varepsilon_\rho = \left(\frac{\omega_0^2}{\omega_d^2}\right)\left[\left(1-\frac{\nu_{effa}^2}{\omega_d^2}\right)\left(\frac{n_{e\rho}}{n_{e0}}\right)-\left(\frac{n_{ea}}{n_{e0}}\right)\left(\frac{2\nu_{effa}\nu_{eff\rho}}{\omega_d^2}\right)\right], \tag{3.15b}$$

where ν_{effa} and $\nu_{eff\rho}$ are the axial and radial part of the effective collision frequencies, n_{ea} and $n_{e\rho}$ are axial and radial electron densities, ω_0 and ω_d are the electron plasma frequencies in the absence and existence of dust grains, respectively.

Using the axial and radial parts of electron densities and effective collision frequencies by concurrent solution of Eqs.(3.2)-(3.7)(a2, b2), we get the axial and radial component of effective dielectric constants, ε_a and ε_ρ in terms of $\beta_0 U_{00}^2$.

3.4 Self-Filamentation of Gaussian Electromagnetic (EM) Beam in Fully Ionized Complex Plasma

Consider a uniformly polarized Gaussian EM-beam propagating with the z-axis in a fully ionized complex plasma with its y-axial polarized electric vector; the cylindrical coordinate form of electric field vector U for above defined beam may be expressed as

$$U(z)=\hat{j}\, U_0(\rho,z)e^{i\omega_d t}, \tag{3.16}$$

where $(U_0)_{z=0} = U_{00}e^{\left(-\rho^2/\rho_0^2\right)}$,

and $\hat{j}$ is the y-axial unit vector.

Concerned wave equation is given by

$$\nabla^2 U - \nabla(\nabla \cdot U) + \frac{\varepsilon_{eff}(\rho,z)}{c^2}\frac{\partial^2 U}{\partial t^2} = 0. \tag{3.17}$$

Since the divergence of electric vector of the transverse beam is zero, hence the Eq. (3.17) reduces to

$$\nabla^2 U_0 + (\omega_d^2/c^2)\varepsilon_{eff}(\rho,z)U_0 = 0. \tag{3.18}$$

For a cylindrically symmetric beam (U_0 being independent of θ), so from Eq. (3.18)

we obtain

$$\frac{\partial^2 \vec{U_0}}{\partial z^2} + \frac{1}{\rho}\frac{\partial \vec{U_0}}{\partial \rho} + \frac{\partial^2 \vec{U_0}}{\partial \rho^2} = \frac{\omega_d^2 \varepsilon_{eff}(\rho,z)}{c^2}\vec{U}_0. \tag{3.19}$$

The solution of Eq. (3.19) according to Akhmanov *et al.* [38] can be expressed as

$$U_0(\rho,z) = A_0(\rho,z)e^{-ikz}, \tag{3.20}$$

$$A_0(\rho,z) = A_{00}(\rho,z)e^{-iks(\rho,z)}, \tag{3.21}$$

where $k = (\omega_d/c)\varepsilon_a^{1/2}$,

A_{00} and s are real.

Following Sodha *et al.* [39], substituting U_0 and A_0, respectively from Eqs. (3.20) and (3.21) in Eq. (3.19) and comparing the real and imaginary parts of consequent equations, we obtain

$$2\frac{\partial s}{\partial z} + \left(\frac{\partial s}{\partial \rho}\right)^2 = \frac{1}{\varepsilon_a}\Phi\left(\frac{1}{2}A_0 A_0^*\right) + \frac{1}{k^2 A_{00}}\left\{\frac{\partial^2 A_{00}}{\partial \rho^2} + \frac{1}{\rho}\frac{\partial A_{00}}{\partial \rho}\right\}, \tag{3.22}$$

and

$$\frac{\partial A_{00}^2}{\partial z}+\frac{\partial s}{\partial \rho}\frac{\partial A_{00}^2}{\partial \rho}+A_{00}^2\left(\frac{\partial^2 s}{\partial \rho^2}+\frac{1}{\rho}\frac{\partial s}{\partial \rho}\right)=0, \tag{3.23}$$

where $\Phi\left(\frac{1}{2}A_0A_0^*\right)=(\rho^2/\rho_0^2)\varepsilon_\rho$. (3.23a)

Following earlier analysis [38, 40-41], the solution of A_{00}^2 may be written as

$$A_{00}^2=\frac{U_{00}^2}{f^2}\,e^{-\frac{\rho^2}{\rho_0^2 f^2}}. \tag{3.24}$$

Substituting the expression of Φ and A_{00}^2 from Eq. (3.23a) and Eq. (24), respectivelyin Eq. (3.22), we obtain

$$2\frac{\partial s}{\partial z}+\left(\frac{\partial s}{\partial \rho}\right)^2=\frac{1}{2}\frac{\varepsilon_\rho}{\varepsilon_a}A_{00}^2-\frac{2}{k^2\rho_0^2 f^2}+\frac{\rho^2}{k^2\rho_0^4 f^4}. \tag{3.25}$$

The eikonal function $s(\rho,z)$ in paraxial ray approximation, may be represented as

$$s=\frac{\rho^2}{2}B(z)+\Psi(z), \tag{3.26}$$

where $\Psi(z)$ is any function of z

and $B(z)=\frac{1}{f}\frac{df}{dz}$.

The shape and power of beam is preserved by the solution of A_{00}^2 when the beam propagates.

Employing the expression for $B(z)$ in Eq. (3.26) and comparing the co-efficient of ρ^2/ρ_0^2 of the resulting equation, yields [33] the equation for beam width parameter of the form

$$\frac{d^2f}{dz^2} = \frac{1}{R_d^2}\frac{1}{f^3} - \frac{1}{2\rho_0^2}\frac{\varepsilon_\rho}{\varepsilon_a}\frac{U_{00}^2}{f^3} \tag{3.27}$$

or

$$\frac{d^2f}{d\xi^2} = -\frac{1}{R_{ns}^2}\frac{1}{f^3} + \frac{1}{f^3}, \tag{3.28}$$

where $R_{ns}\left(=\frac{2\varepsilon_a\rho_0^2}{\varepsilon_\rho U_{00}^2}\right)^{1/2}$ is the characteristics length of focusing ,

$\xi = \frac{z}{R_d}$ and $R_d = k\rho_0^2$.

The initial term on the right –hand side in Eq. (3.28) represent the nonlinear self-filamentation term while the last diffraction divergence.

3.5 Effective Critical Power in the Existence of Dust Grains

From Eq. (3.28), the effective critical power P_{cr} (evaluated in Appendix B) of self-filamentation for $R_{ns} = R_d$ (for which $\frac{d^2f}{d\xi^2} = 0$, $f = 1$, for all values of ξ) can be written as

$$P_{cr} = \frac{c^3}{4\omega_d^2}\frac{\varepsilon_a^{1/2}}{\varepsilon_\rho}. \tag{3.29}$$

Thus, an incident electromagnetic plane wave front will travel independent of beam spot size results in linear waveguide prolongation. The effective critical power comes out to be 7.1094×10^{12} (ergs/s) for the given set of parameters.

3.6 Computing Outcomes and Discussion

This work present a theoretical model for dynamics of temporal growth of dust grain in fully ionized complex plasma and expressing the features of non-uniform correspondence of a Gaussian electromagnetic beam with fully ionized complex plasma having electrons, ions and dust grains as the constituents. Diffusion, electrons–ions/dust collisions in plasma, electrons-ions deposition on the dust grain surfaces, thermal conduction are the specific process have been included in this theoretical model. In fully ionized complex plasma, energy loss of electrons via thermal conduction dominates over the collisional effect, so we have to ignore energy loss by collision. The number density of constituents and energy balanced equations have been used to study the non-uniform dependency of different variables on the dimensionless axial intensity of the beam and also the computation have been made to observe the dependence of dust charge, electrons and ions density, their temperature, effective collision frequency on the time τ for different values of dust density by solving the coupled equations simultaneously. MATHEMATICA and MATLAB softwares have been employed to solve the equations numerically. Using these equations ε_a and ε_ρ can be obtained by substituting the appropriate values. From the values of ε_a and ε_ρ, we can gain the beam width parameter depending upon normalized channel of prolongation, $\xi(=z/R_d)$, satisfying the boundary requirements f=1, $\frac{df}{d\xi}=0$ at $\xi = 0$ for different values of beam intensities and dust densities. For the numerical solution of this analytical model, the curve representing the self-filamentation has been obtained by plotting beam width parameter (f) as a function of normalized channel of prolongation of the beam ξ $(=z/R_d)$ for a selected set of variables picturing the region of prolongation for self-filamentation. The set of variables used in the calculations are as follows:

$\alpha_{r0}=5.5\times10^{-7}cm^3/s$, $n_{e0}=n_{i0}=2.45\times10^6cm^{-3}$, $n_0=n_{00}=0.9\times10^{12}cm^{-3}$, $k'=1.1$,

$n_d=10^2cm^{-3}$, $\rho_0=5.5\times10^{-2}cm$, $k_B=1.38\times10^{-16}$ $ergsk^{-1}$, $T_{e0}=1001K$, $m_e=9.1\times10^{-28}g$,

$\nu_{e0}=6.4\times10^3s^{-1}$, $T_{i0}=399K$, $\nu_{i0}=5\times10^2s^{-1}$, $m_d=39\times1.6\times10^{-24}g$, $\omega_d=1.1\times10^8s^{-1}$,

$e = 4.8\times10^{-10}$statcoloumb, $T_d = 300K$, $r_d = 10^{-5}$cm, $\sigma_0 = 1.5\times10^{-16}$cm^2,

$U_{00} = 10^5$ stat volt cm^{-1} 6×10^5 stat volt cm^{-1}.

The variation of electrons normalized number density, $n_{ea}/n_{e\rho}$ has been plotted against time, τ (in sec.) for distinct values of dust grains number density, n_d in fig. 3.2.

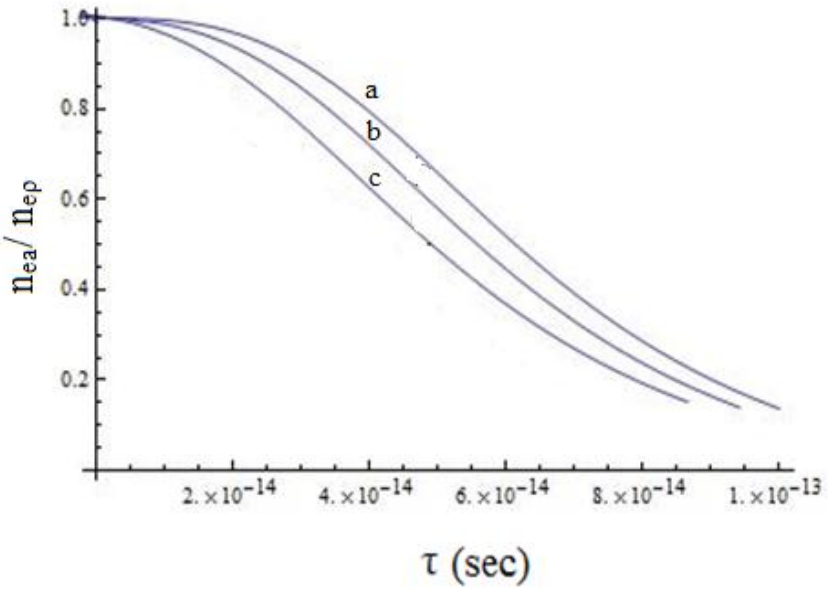

Fig. 3.2 indicates the variation in normalized number density of electrons with the parameter τ *(in sec) for different values of number density of dust grains,* n_d. *The labels a, b andc refer to* $n_d = 2\times10^2, 2\times10^3, 2\times10^4$ *in* cm^{-3}, *respectively.*

This shows that the $n_{ea}/n_{e\rho}$ decreases with time and for larger values of n_d, $n_{ea}/n_{e\rho}$ decay faster because of more and more availability of dust grains for the accumulation of electrons.

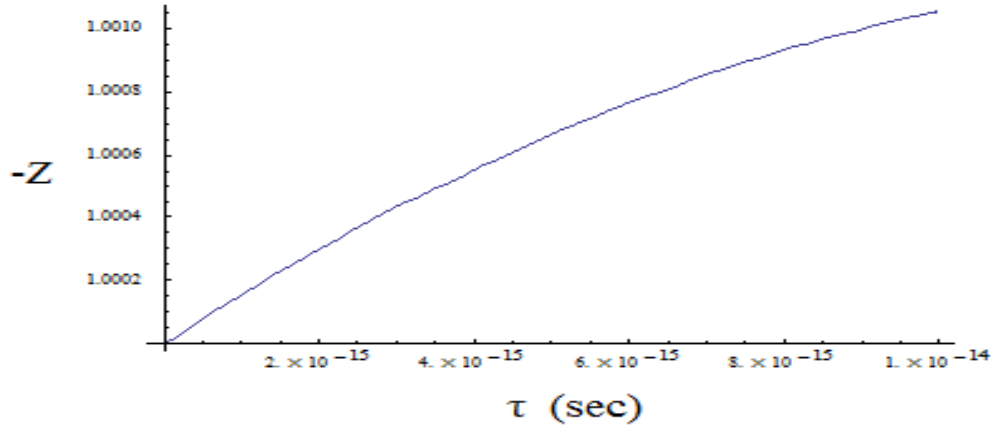

Fig. 3.3 The dependence of negative dust charge state on time τ.

Fig. 3.3 displays the variation of dust charge state with time and indicates that the negative dust charge state decreases with time on account of decaying number density of electrons with enhanced dust density.

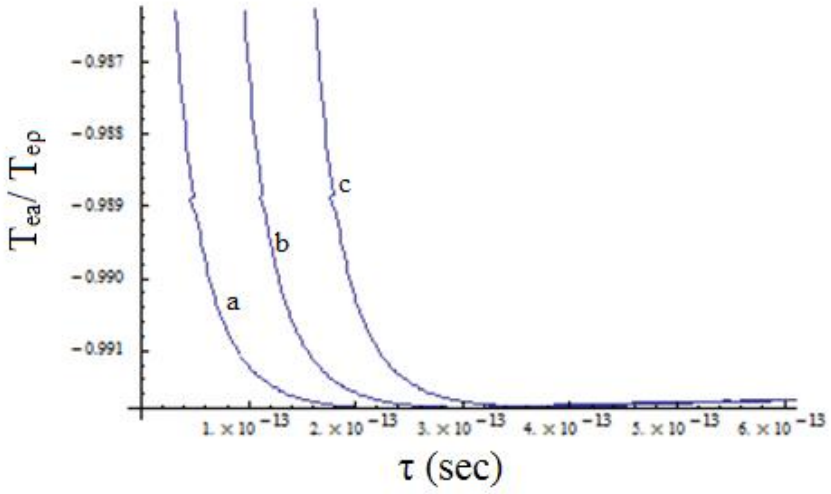

Fig. 3.4 displays the variation in normalized electron temperature with the parameter τ for different values of number density of dust grains, n_d. *The labels a, b and c refer to* $n_d = 2\times10^2$, 2×10^3, 2×10^4 *in* cm^{-3}, *respectively.*

Fig 3.4 presents the dependency of electron temperature on the variable τ (secs.) for the distinct values of dust densities. The figure shows that the temperature of electrons decay faster for greater values of dust density, n_d.These results are in line with the experimental measurements of Couëdel *et.al.*[421and others[43-47].

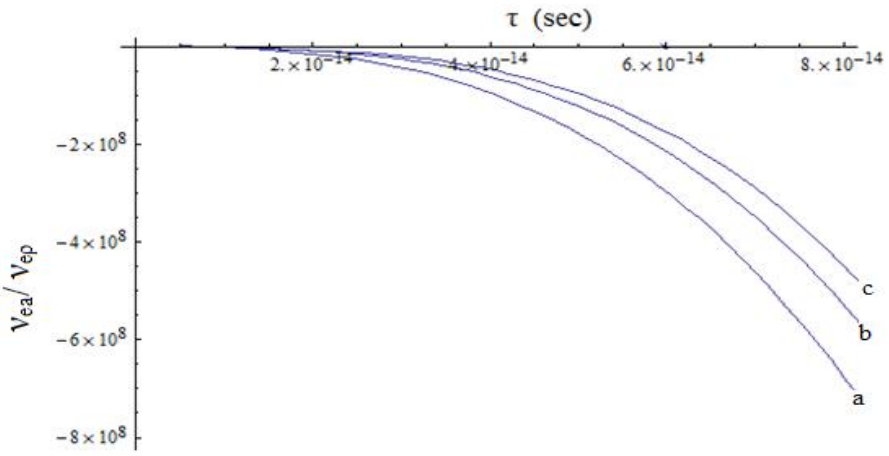

Fig. 3.5 describes the variation of effective collision frequency with time for different values of n_d. *The labels a, b and c refer to* $n_d = 2\times10^2, 2\times10^3, 2\times10^4$ *in* cm^{-3}, *respectively.*

Fig.3.5 describes the variation of effective collision frequency with time. It indicates that the effective collision frequency decreases with time on account of greater accumulation of electrons on dust grains. More the dust density faster will be the mitigation of collision frequency and Fig. 3.6 indicates that the normalized electron density decreases with normalized dielectric constant and hence with the dust density. These outcomes are in good agreement with the conclusion of Schneider *etal.*[48].

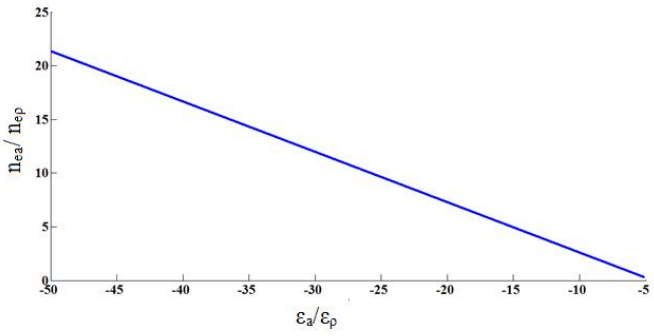

Fig. 3.6 expresses the variation of normalized electron density, n_{ea}/n_{ep} *with normalized effective dielectric constant,* $\varepsilon_a/\varepsilon_\rho$ *for fully ionized plasma in the existence of dust grains.*

Figs. 3.7 and 3.8 indicate the dependence of beam width parameter 'f' on the normalized channel of prolongation for distinct parameters of dust density, n_d and dust charge state, Z_d,respectively. From fig. 3.7, it is observed that the beam width parameter 'f' quickly diminishes with ξ and leads to self-filamentationin the existence of dust grains in fully ionized plasma. It shows that the self-filamentation of Gaussian electromagnetic beam increases in the presence of dust grains which are in contrast with the result obtained by Sodha *et al.* [27] in their earlier analysis for the prolongation of beam in fully ionized plasma without dust. The extent of self-filamentation decreases with dust density on account of reduced nonlinearity due to existence of dust grains whereas the inverse result is obtained in case of dust charge state.

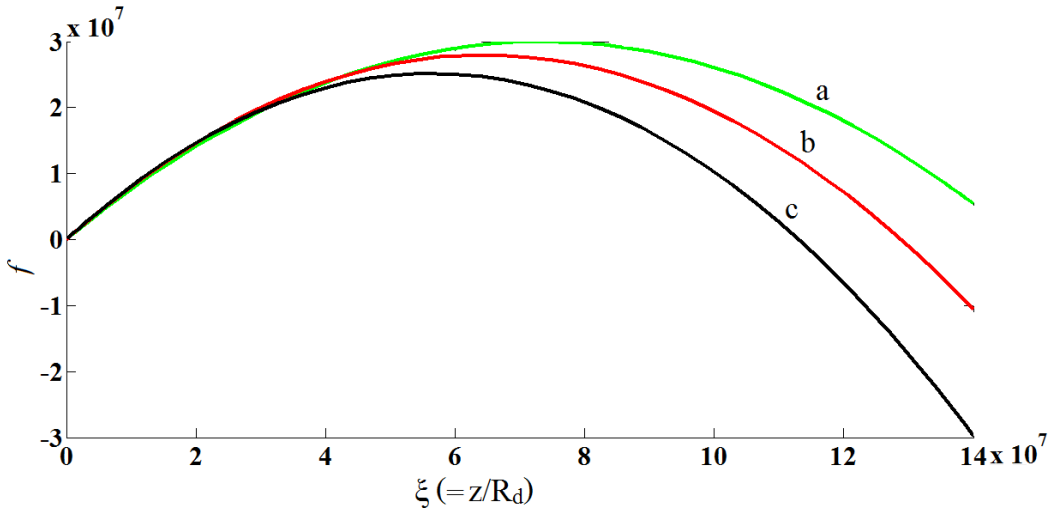

Fig. 3.7 shows the dependence of beam width parameter 'f' on the normalized channel of prolongation ξ (=z/R_d) for the transverse of Gaussian EM beam as a function of the number density of dust grains. The labels a, b and c refer to n_d *=* 2×10^4, 2×10^3, 2×10^2 *in* cm^{-3},*respectively.*

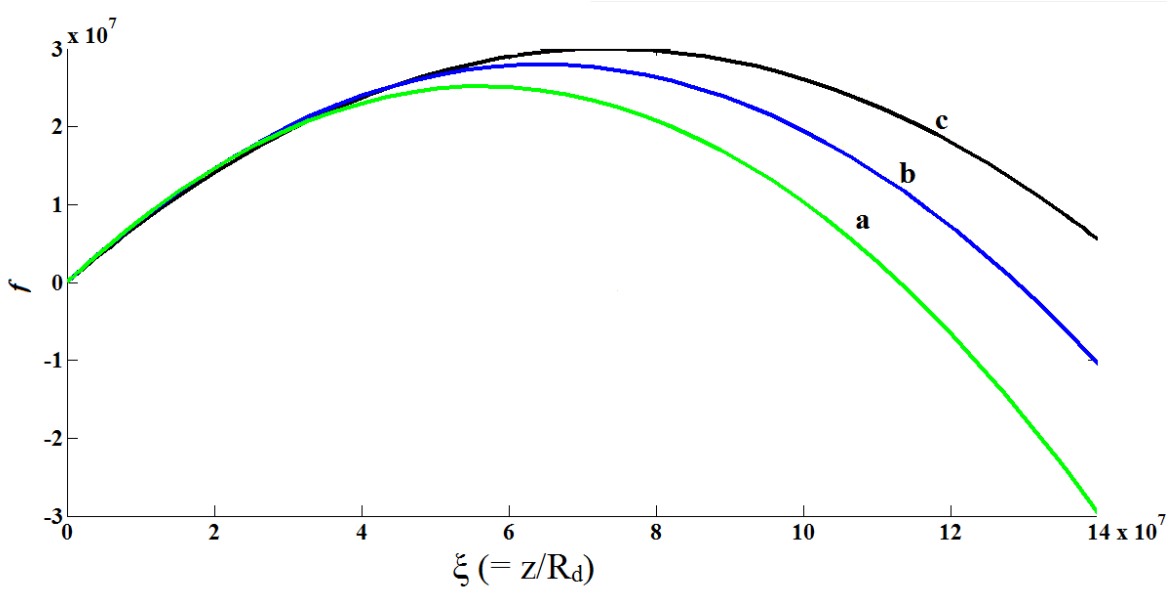

Fig. 3.8 indicates the dependence of 'f' on ξ, for different values of dust charge state Z_d. The other parameters are given in the text. The labels a, b and c refer to $Z_d = -4\times10^3$, -6×10^3, -8×10^3, respectively.

Fig. 3.9 expresses the variation of effective critical power P_{cr} (ergs/s) with normalized electron density, $n_{ea}/n_{e\rho}$ in fully ionized plasma in the existence of dust grains. It indicates that critical power increase with decaying electron density i.e., enhanced dust density. So the power of Gaussian beam must be increased for the beam to be focused for lower values of $n_{ea}/n_{e\rho}$ .From the above discussion, we can conclude that by changing the various dust-plasma parameters, effective nonlinearity can be obtained in plasma. Moreover, effective dielectric constant and self-filamentation behaviour of beam can be estimated by modifying various parameters.

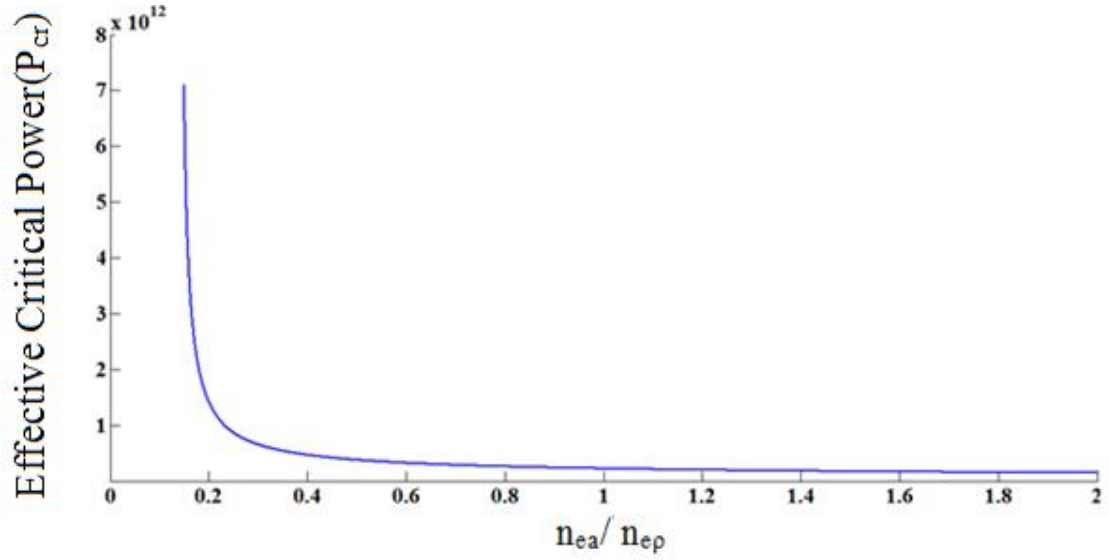

Fig. 3.9 express the variation of effective critical power P_{cr}(ergs/s) with normalized electron density, n_{ea}/n_{ep} in fully ionized plasma in the existence of dust grains.

3.7 Conclusions

This theory investigates the effect of dust grains on self-filamentation of Gaussian EM beam in fully ionized plasma. An analytical model to study the dynamics of fully ionized complex plasma has been established. Under the inclusion of charge neutrality condition, energy balance equations of plasma constituents, perturbed number density of electrons, effective dielectric constant, the effect of growth of dust grains on various plasma parameters have been examined. Moreover, the propagation of Gaussian electromagnetic beam and its critical power in fully ionized plasma in the presence of dust grains have been studied. To analyse the behaviour of beam, paraxial ray approximation has been taken into account and the behaviour of self-filamentation has been described by curves. These outcomes may be useful for space and laboratory plasma experiments as well as for future studies in complex plasma.

APPENDIX A: AMBIPOLAR DIFFUSION AND TRANSPORT COEFFICIENTS

We assume the fully ionized complex plasma made up of the constituent electrons, ions and charged dust grains. The net particle flux or density decay of constituent species is obtained by

$$\Phi_e = - n_e\mu_e U - D_{1e} n_e (\nabla T_e/T_e) - D_{2e}\nabla n_e, \tag{3.30}$$

$$\Phi_i = n_i\mu_i U - D_{1i} n_i (\nabla T_i/T_i) - D_{2i}\nabla n_i, \tag{3.31}$$

$$\Phi_d = - n_d\mu_d U - D_{1d}\nabla n_d, \tag{3.32}$$

where Φ_g , n_g, U , T_g,$D_{1g}(=5k_BT_g/2m_g\nu_{effg})$, $D_{2g}(=k_BT_g/m_g\nu_{effg})$, $\mu_g(=eD_{2g}/k_BT_g)$, are the flux, number density, space charge field, temperature thermal diffusion coefficient,diffusion coefficients and mobility; the subscript g stands for electrons, ions and dust grains, respectively.

The net rate of flow of both the charges per unit area must be balanced in stationary state, so we get

$$\Phi_i = \Phi_e + \Phi_d . \tag{3.33}$$

The dust grains are supposed to be standing still because of their heavy mass and hence their flux comes out to be zero. Thus the Eq. (3.33) gives

$$\Phi_i = \Phi_e . \tag{3.34}$$

Using the Eqs. (3.30), (3.31) and (3.34), eliminating U, net particle flux or density decay comes out to be

$$\Phi_p = - D_{1e} n_e (\nabla T_e/T_e) - D_{2e}\nabla n_e - n_e\mu_e \left(\frac{D_{2i}\nabla n_i - D_{2e}\nabla n_e + D_{1i} n_i (\nabla T_i/T_i) - D_{1e} n_e (\nabla T_e/T_e)}{n_e\mu_e + n_i\mu_i} \right), \tag{3.35}$$

where $c_1=D_{2e}/D_{2i}$, $c_2=\mu_e/\mu_i$ and $c_3=D_{1e}/D_{1i}$.

In this paper, axial parameters of diffusion coefficients and mobility are taken into consideration.

APPENDIX B: EFFECTIVECRITICAL POWER

Consider a uniform waveguide prolongation, a Gaussian beam propagating with a plane wavefront (R=∞) at z =0. If at z = 0, the two terms on the RHS of Eq. (3.28) compensate each other, $\frac{d^2f}{dz^2} = 0$, f = 1(for all values of z). The critical condition for uniform waveguide prolongation is given as

$$R_{ns} = R_d \,, \tag{3.36}$$

$$R_{ns}^2 = R_d^2 \,, \tag{3.37}$$

$$\frac{2\rho_0^2\varepsilon_a}{\varepsilon_\rho U_{00}^2} = k^2\rho_0^4 \,, \tag{3.38}$$

or

$$\frac{2\varepsilon_a}{\varepsilon_\rho k^2\rho_0^2} = U_{00}^2 \,. \tag{3.39}$$

The corresponding critical power is given as

$$P_{cr} = \int_0^\infty \frac{\varepsilon_a}{8\pi} U_{00}^2(\rho,z)\frac{c}{\eta} 2\pi\rho d\rho$$

$$= \frac{c}{8}\varepsilon_a^{1/2}\rho_0^2 U_{00}^2, \tag{3.40}$$

where η is the referactive index of medium .

Substituting U_{00}^2 from (3.39) into (3.40), we obtain

$$P_{cr} = \frac{c\varepsilon_a^{1/2}}{4\varepsilon_\rho k^2}, \tag{3.41}$$

Substituting $k^2 = \varepsilon_a \omega_d^2 / c^2$ in above equation (3.41), we obtain

$$P_{cr} = \frac{c^3 \varepsilon_a^{1/2}}{4\omega_d^2 \varepsilon_\rho}. \tag{3.42}$$

REFERENCES

[1] M.S. Sodha, S. K. Mishra, and S. Misra, *Generation and accretion of electrons in complex plasmas with cylindrical particles,* Phys. Plasmas**16**, 123701(2009).

[2] A. Gahlot, R.Walia, S.C. Sharma, and R. P. Sharma, *Distortion of anamplitude modulated electromagnetic signal with time-dependent dust charging*, J. Plasma Physics **78**, 33(2012).

[3] Z. X. Wang, G. Lu, P. Duan, J.Liu, S.Zheng and Y. Liu, *Effect of thermionic emission on dust-acoustic solitons,*Phys. Scr. **82**, 045501(2010).

[4] I. Denysenko, J. Berndt, E. Kovacevic, I.Stefanovic,V. Selenin, and J.Winter, *The response of a capacitively coupled discharge to the formation of dust particles: Experiments and modelling*,Phys. Plasmas **13**,073507(2006).

[5] M.Kundu, K.Avinash, A.Sen, and R.Ganesh, *On the existence of vapor-liquid phase transition in dusty plasmas,* Phys. Plasmas **21**, 103705(2014).

[6] M. Mikikian, L. Boufendi, A. Bouchoule, H. M. Thomas, G .E. Morfill, A. P. Nefedov, V. E .Fortov, and the PKE–Nefedov team, *Formation and behaviour of dust particle clouds in a radio-frequency discharge: results in the laboratory and under microgravity conditions,* New Journal of Physics **5**, 19.1 (2003).

[7] M.S. Sodha, S. K. Mishra, Shikha Misra, and Sweta Srivastava, *Fluctuation of charge on dust particles in a complex plasma,* Phys. Plasmas **17**, 73705(2003).

[8] V.N.Tsytovich, U. de Angelis, A. V. Ivlev, G. E. Morfill, and S. Khrapak, *Nonlinear drag force in dusty plasmas,* Phys. Plasmas **12**,112311(2005).

[9] Y. Hong , C.Yuan , J. Jia , R. Gao , Y. Wang, Z. Zhou , X. Wang , H. Li , and J. Wu, *Propagation characteristics of microwaves in dusty plasmas with multi-collisions*, Phys.Sci.Technol.**19**,055301(2017).

[10] J. H. Chu and I. Lin, *Direct observation of Coulomb crystals and liquids in strongly coupled rf dusty plasmas*, Phys. Rev. Lett. **72**, 4009(1994); H.Thomas, G. E. Morfill, V.Demmel, J. Goree, B. Feuerbacher, and D.Molmann, ibid. *Plasma Crystal - Coulomb Crystallization in a*

DustyPlasma, **73**,65(1994),; H.Thomas and G. E. Morfill,*Melting Dynamics of plasma crystal*, Nature (London) **379**, 806(1996).

[11] S. V. Vladimirov and K. Ostrikov, *Dynamic self-organization phenomena in complex ionized gas systems: new paradigms and technological spects*, Phys. Rep. **393**,175(1994).

[12] G. S. Selwyn, *A Phenomenlogical Study of Particulates in Plasma Tools and Processes,* Jpn. J. Appl. Phys. **32**, 3068(1993).

[13] Jieshu Jia, Chengxun Yuan, Ruilin Gao, Ying Wang, Yaoze Liu, Junying Gao, Zhongxiang Zhou, Xiudong Sun, Jian Wu and Hui Li, and Shaozhi Pu, *Propagation of electromagnetic waves in a weakly ionized dusty plasma,* J.Phys. D: ppl.Phys.**48**,465201(1993).

[14] M. S. Sodha, A. Dixit, S. Srivastava, S. K Mishra, M. P. Verma, and L. Bhasin, *Charge distribution of particles in an irradiated dust cloud,* Plasma Sources Sci. Technol. **19**,015006(2010).

[15] M. S. Sodha, S. Misra, and S. K. Mishra, *Kinetics of cometary Plasma,*Plasma Sources Sci. Technol. **045022**, 19(2010).

[16] M. S. Sodha, S. Mishra, S. K. Mishra, and S. Srivastava, *Growth of embryonic dust particles in a complex plasma,* J. Appl. Phys. **107**,103307(2010).

[17] M. S. Sodha, S. K. Mishra, and S. Misra, *Kinetics of illuminated complex plasmas considering Mie scattering by spherical dust particles with a size distribution,* J. Appl.Phys.**109**,01330(2011).

[18] C.Zafiu, A.Melzer, and A.Piel, *Measurement of ion drag force on falling dust particles and its relation to the void formation in complex (dusty) plasma*, Phys.Plasmas **10**,1278(2003).

[19] M. S. Sodha, S. Mishra, and S. K. Mishra, *Kinetics of complex plasmas having spherical dust particles with a size distribution,* Phys. Plasmas **17**,113705(2010).

[20] Suresh C. Sharma, A.Gahlot, and R.P.Sharma, *Effect ofdust on an amplitude modulated electromagnetic beam in a plasma,* Phys. Plasmas **15**, 043701(2008).

[21] S. K. Mishra, Shikha Misra, and M. S. Sodha, *Self-focusing of a Gaussian*

electromagnetic beam in a complex plasma, Phys. Plasmas **18**, 043702(2011).

[22] M. S. Sodha, S. K. Mishra, and Shikha Misra, Phys. Plasmas, *Nonlinear dependence of complex plasma parameters on applied electric field* ***8***,023701(2011).

[23] F. Verheest and P. Meuris, *Nonlinear electromagnetic modes in plasmaswith variable dust charges,* Phys. Lett. A **210**, 198(1996).

[24] S.Prasad and V.K.Tripathi, *Redistribution of charged particles and self-distortion of high - amplitude electromagnetic waves in a plasma,* J.Appl.Phys. **44**, 4595(1973).

[25] G. Sambandan, V. K. Tripathi, J. Parashar, and R. Bharuthram, *Nonlinear interaction of a high-power electromagnetic beam in a dusty plasma: Two-dimensional effects,* Phys. Plasmas **6**,762(1999).

[26] M.S.Sodha, S.K.Mishra, and S.K.Aggarwal, *Self-focusing and cross-focusing of Gaussian electromagnetic beams in fully ionized collisional magnetoplasmas,* Phys. Plasmas **14**, 112302(2007).

[27] M.S.Sodha, R.K.Khanna, and V.K.Tripathi, *Self-focusing of a laser beam in a strongly ionized plasma,* Opto-electronics **5**, 533(1973).

[28] M.S.Sodha, S.Misra, and, S.K.Mishra, *Charging of dust particles in an illuminated open complex plasma system,* Phys. Plasmas **16**, 123705(2009).

[29] M.S.Sodha, S.K.Mishra, S.Misra, and, S.Srivastava, *Fluctuation of* charge *of particles in a complex plasma system,* Phys. Plasmas **17**, 073705(2010).

[30] Jieshu Jia, Chengxun Yuan, Sha Liu, Feng Yue, Ruilin Gao, Ying Wang, Zhong-Xiang Zhou, Jian Wu and Hui Li, *Propagation of electromagnetic wave in weak collisional and fully ionized dusty plasma*, Phys. Plasmas **23**,043302(2016).

[31] Li Dan, Li-Xin Guo, and Jiang-Ting Li, *Propagation characteristics of electromagnetic waves in dusty plasma with full ionization*, Phys. Plasmas **25**, 013707(2018).

[32] E.Stoffels, W.W.Stoffels, D. vender, G.M.W.Kroesen, and F.J de Hoog, *Laser Particulate interactions in a dusty RF plasma,* IEEE transaction on Plasma Science **22**, 2(1994).

[33] Hui Li, Jian Wu, Zhongxiang Zhou, and Chengxun Yuan, *Propagation of Electromagneticwave in dusty plasma and the influence of dust size distribution,* Phys.Plasmas **23**, 073702(2016).

[34] N.A.Zharova, A.G.Litvak, and V.A.Mironov, *Self-focusing of laser radiation in cluster plasma,* JETP Lett. **78**, 619(2003).

[35] M.S.Sodha, and A. Dixit, *Photoelectric charging of dust particles: Effect of Spontaneous and light induced field emission of electrons*, Applied Phys. Lett. **95**,101502(2009).

[36] L.Spitzer JR., '*Physics of Fully Ionized Gases*', Inter Science Publishers, John Wiley and Sons, New York (1967).

[37] A.V.Gurevich, *Nonlinear phenomena in the ionosphere* (springer: New York, (1978).

[38] S. A. Akhamanov, A. P. Sukhorukov, and R. V. Khokhlov, *Self-focusing and diffraction of light in a nonlinear medium,* Sov. Phys. Usp. **10**, 619(1968).

[39] M.S.Sodha, R.S. Mittal, S.Kumar, and V.K.Tripathi, *Self-focusing of electromagnetic waves in a magnetoplasma,* Opto-electronics (London) **6**, 167(1974).

[40] M.S.Sodha, A.K.Ghatak, and V.K.Tripathi, *Self-Focusing of Laser Beams in Plasmas and Semiconductors*, Prog.Optics (North Holand and Co.)**13**, 69(1976).

[41] M. S. Sodha, A. K. Ghatak, and V. K. Tripathi, *Self-filamentation of Laser Beams in Dielectrics, Semiconductors and Plasmas* (Tata-McGrawHills, Delhi, (1974)).

[42] L.Couëdel, A.A.Samarian, M.Mikikian, and L.Boufendi, *Influence of plasma diffusion losses on dust charge relaxation in discharge afterglow,*"Fifth International Conference on the Physics of Dusty Plasmas, Ponta Delgada, Azores: Portugal (2008)" DOI:10.1063/1.2996828.

[43] X. Liang, J. Zheng, J. X. Ma, W. D. Liu, J.Xie, G. Zhuang, and C. X. Yu, *Experimental observation of ion-acoustic waves in an inhomogeneous dusty plasma,* Phys. Plasmas **8**, 1459(2001).

[44] A. Douglass, V. Land, L. Matthews, and T. Hydea, *Dust particle charge in plasma with ion flow and electron depletion near plasma boundaries,* Phys. Plasmas **18**, 083706(2011).

[45] A.Barken, N.D'Angelo, and R.L.Merlino, *Laboratory experiments on electrostatic ion cyclotron waves in a dusty plasma,* Planet. Space Sci.**43**, 905(1995).

[46] L. Couëdel, M. Mikikian, A.A. Samarian, and L. Boufendi, Self-*excited void instability during dust particle growth in dusty plasma*, Phys. Plasmas **17**, 083705(2010).

[47]M. Mikikiana, L. Couëdel, M. Cavarroc, Y. Tessier, and L. Boufendi, *Dusty plasmas: synthesis, structure and dynamics of a dust cloud in a plasma,* Eur. Phys. J. Appl. phys**.49**, 13106 (2010).

[48] R. S. Schneider, L. F. Ziebell, *Electrostatic waves in a Maxwellian dusty plasma with variable charge on dust particles,* Brazilian J. of Phys.**36**, 759(2006).

[49] J.D.Huba, *NRL physics Formularly* (Naval Research laboratory Washington,(D.C.)) P.28(1998).

Chapter 4

THEORETICAL ANALYSIS FOR TRANSMISSION OF GAUSSIAN AND SINE TIME IRRADIANCE OF ELECTROMAGNETIC BEAM IN COLLISIONAL DUSTY PLASMAS

4.1 Brief outline of the chapter

In this chapter, an analytical model is evolved to access the transmission kinetics of both Gaussian and Sine time irradiance of electromagnetic wave owing to mutual interactions of dust and other plasma components. It is familiar that the electrons in dusty plasma get heated up because of highly irradiated electromagnetic wave to the stationary state temperature of the order of relaxation time $\tau' = 1/(\delta_{comp}\nu_{ef})$, where δ_{comp} is the fractional loss of energy of electrons due to collisions and ν_{ef} is the effective collision frequency under the influence of dust grains. Consequently, with the increasing electron temperature, electron density attains a steady state value during the relaxation time τ'. For the pulse duration $(t_0) < \tau'$, $n_e/n_{e0} = 1$ and for $t_0 > \tau'$, n_e/n_{e0} attains a steady value. Hence the electron density considered as a function of temperature. In this communication, for $t_0 > \tau'$, the steady state electron density and temperature in dusty plasma is obtained on account of ionization of neutrals, recombination of free electrons with ions, net adsorption on dust grain surface and diffusion due to space charge field and temperature gradient which are ignored in other analytical studies [Refs. 19 and 22]. Power loss due to ohmic heating and collisions between the constituent species has also been taken into account to predict the electron temperature, which causes the nonlinearity. Ohmic heating of ions has been ignored due to their heavier mass. The significance of thermal conduction has been neglected in the present formalism. Time varying behaviour of modified electron temperature and collision frequency has been illustrated numerically as a function of dust densities. Also, the comparative analyses of variation of beam waist parameter with the dimensionless length of transmission for both the Gaussian and Sine time irradiance are involved in this model as a function of distinguishable time width, collision frequencies, and dust densities

under the condition that the size of dust nebulous is greater than the electrons mean free path for the adsorption on the dust grain surface. The observed results are significant for the applications in industry and astrophysics.

4.2 Introduction

Several researches [1-11] have been performed to show the significant effect of dust grains in plasma because of its exciting applications [12-18] in space, industries, and laboratories plasmas. Particularly, the self-focusing behaviour of an electromagnetic beam propagating in dusty plasma becomes an interesting domain of research promoted by the various investigators [19-25]. Mishra *et al.* [26] have studied the transportation of complex plasma featured by Mathis, Rumpl, and Nordsieck (MRN) power law grain size distribution with and without electric field. They observed the larger plasma transparency with larger dust grains in dark plasma while the case is reversed in illuminated plasma where the photoemission is predominant. Sharma and Sharma [27] have discussed the kinetics of non-uniform transmission of a Gaussian electromagnetic beam in strongly ionized dusty plasma considering the elastic and charging collisions with photoemission and electrons adsorption on the boundary of dust grains. Jia *et al.* [28] used the Boltzmann distribution law to study the transportation characteristics of an electromagnetic wave propagating in weakly and strongly ionized dusty plasma. Mishra *et al.* [29] have used the paraxial ray approximation to study the propagation behaviour of a Gaussian irradiance of an electromagnetic beam in dusty plasma under the effect of elastic and inelastic collisions. Wang *et al.* [30] have studied the electromagnetic wave propagation characteristics of inhomogeneous dusty plasma. They developed the models of double exponential and hyperbolic electron number density distribution for dusty plasma and also studied the power transmission and reflection coefficient on the basis of their analytical study. Sodha *et al.* [31] also analysed the cases of thermionic emission, photoemission, and emission less processes to formulate the problem of fluctuation of charge on account of presence of dust grains.

Several investigations on temporal profile of electromagnetic wave propagating in dust free plasma have been carried out by various researchers [32-34] but in this paper; analytical model is evolved to access the transmission kinetics of both Gaussian and Sine time irradiance of electromagnetic wave owing to mutual interactions of dust and other plasma components. It is

familiar that the electrons in dusty plasma get heated up because of highly irradiated electromagnetic wave to the stationary state temperature of the order of relaxation time $\tau' = 1/(\delta_{comp}\nu_{ef})$, where δ_{comp} is the fractional loss of energy of electrons due to collisions and ν_{ef} is the effective collision frequency under the influence of dust grains. Consequently, with the increasing electron temperature, electron density attains a steady state value during the relaxation time τ'. For the pulse duration $(t_0) < \tau'$, $n_e/n_{e0} = 1$ and for $t_0 > \tau'$, n_e/n_{e0} attains a steady value. Hence the electron density considered as a function of temperature. In this communication, for $t_0 > \tau'$, the steady state electron density and temperature in dusty plasma is obtained on account of ionization of neutrals, recombination of free electrons with ions, net adsorption on dust grain surface and diffusion due to space charge field and temperature gradient which are ignored in other analytical studies [Refs. 19 and 22]. Power loss due to ohmic heating and collisions between the constituent species has also been taken into account to predict the electron temperature, which causes the nonlinearity. Ohmic heating of ions has been ignored due to their heavier mass. The significance of thermal conduction has been neglected in the present formalism.

For the computation, metallic dust cloud of stainless steel having work function of 7.8 eV as in ionosphere has been considered so that photoemission can take place for spectrum of Lyman α radiations (1215.7 Å) in extreme UV region.

The left over manuscript is schemed as follows: In Section 4.3, the coupled sets of differential equations of charge neutrality, electron density, and electron temperature are solved considering the paraxial ray approximation to structure the analytical model for formulating the modified dielectric permittivity under the influence of dust grains. Section 4.4 include the solution of propagation of electromagnetic beam for the both Gaussian and Sine time irradiance in dusty plasma following the Akhmanov's *et al*.[38] and its extension by Sodha *et al*.[39] in respect of modification of the beam waist parameter *f* with the dimensionless length of transmission ζ for distinguishable dust parameters. Consequences of the existing model are discussed in Section 4.5, and, in the end, we reach to the conclusions in Section 4.6.

4.3 Analytical Model

Assume dusty plasma to be made up of dust grain spheres with charge $-Z_d e$ and radius r_d, ions, electrons and neutral atoms, where Z_d is the state of charge on dust and e is the charge on an electron. The kinetics of dusty plasma include ambipolar diffusion, neutral ionization, neutralization of the ions, adsorption and photoemission of electrons, collisions between plasma constituents, and Ohmic heating caused by non-uniform irradiance of the beam.

The following equations demonstrate the kinetics of dusty plasma as:

A. *Ambipolar Diffusion Term*

The ambipolar diffusion term due to density decay of constituent species is given by

$$\Pi_e = -n_e\mu_e U - D_{te}n_e(\nabla T_e / T_e) - D_{ne}\nabla n_e, \tag{4.1a}$$

$$\Pi_i = n_i\mu_i U - D_{ti}n_i(\nabla T_i / T_i) - D_{ni}\nabla n_i, \tag{4.1b}$$

$$\Pi_d = -n_d\mu_d U - D_{nd}\nabla n_d, \tag{4.1c}$$

where Π_g , n_g, U , T_g, $D_{tg}(=5k_B T_g / 2m_g \nu_{efg})$, $D_{ng}(=k_B T_g / m_g \nu_{efg})$, $\mu_g(=eD_{ng} / k_B T_g)$, are the flux, number density, space charge field, temperature, thermal diffusion coefficient, diffusion coefficients and mobility; the subscript g stands for electrons, ions and dust grains, respectively.

The net rate of diffusion of both the charges per unit area must be balanced in stationary state, so we get

$$\Pi_i = \Pi_e + \Pi_d . \tag{4.2a}$$

The mobility and diffusion of dust particles are supposed to be zero because of their heavy mass and hence their flux comes out to be zero. Thus the Eq. (4.2a) gives

$$\Pi_i = \Pi_e \tag{4.2b}$$

Using the Eqs. (4.1a), (4.1b) and (4.2b), eliminating U, net particle flux or density decay comes out to be

$$\Pi_p = - D_{te} n_e (\nabla T_e / T_e) - D_{ne} \nabla n_e - n_e \mu_e \left(\frac{D_{ni} \nabla n_i - D_{ne} \nabla n_e + D_{ti} n_i (\nabla T_i / T_i) - D_{te} n_e (\nabla T_e / T_e)}{n_e \mu_e + n_i \mu_i} \right), \quad (4.3a)$$

$$\Pi_p = - \left(\frac{D_{ni} [c_2 n_e \nabla n_i + c_1 n_i \nabla n_e] + D_{ti} n_e n_i [c_2 (\nabla T_i / T_i) + c_3 (\nabla T_e / T_e)]}{n_e c_2 + n_i} \right), \quad (4.3b)$$

where $c_1 = D_{ne} / D_{ni}$, $c_2 = \mu_e / \mu_i$ and $c_3 = D_{te} / D_{ti}$.

In this paper, axial parameters of diffusion coefficients and mobility are taken into consideration.

B. *Charge neutrality*

Neutrality of charge may be forwarded as

$$Z_d n_d + n_i - n_e = 0, \quad (4.4)$$

where dust grains number density is represented by n_d, and n_i and n_e are the ionic and electronic densities under the influence of dust grains, respectively.

C. *Dust charge balance*

The net charge on dust grains is balanced by charge flux through the surfaces of dust grains, thus

$$\frac{dZ_d}{dt} = n_{ph}(Z_d, T_d) + n_{ic}(Z_d, T_i) - \Upsilon n_{ec}(Z_d, T_e), \quad (4.5)$$

where $n_{ph} (= \pi r_d^2 n_p)$ is the rate of photoelectric emission by surfaces of charged dust grains, where

$$n_p = \Lambda(\nu)\chi(\nu) = \Lambda(\nu)(4\pi m_e k_B^2 T_d^2 / h^3)\mu(\nu)\Phi_{ph}(\eta),$$

$\Phi_{ph}(\eta)$ is tabulated integral $\left(\text{Fowler 1936}\right)^{[35]}$ stated as

$$\Phi_{ph}(\eta) = \int_0^{\exp(\eta)} \frac{\ln(1+\Omega)}{\Omega} d\Omega,$$

$$\eta = (h\nu - \phi_0) / k_B T_d.$$

n_p indicates the rate of photon density emitted from surface of neutral or negatively charged dust grains, $\Lambda(\nu)$ represent the photon density incident normally to dust surface, $\chi(\nu)$ is photoelectric efficiency. h represent the Planck's constant, ν indicates the frequency of incident beam, ϕ_0 shows the work function of material of dust grain, T_d represent the temperature of dust grains considered as constant due to large thermal capacity, $\mu(\nu)$ is the the probability of absorption of a photon by an electron striking the surface from inside[36].

$n_{ic} = \pi r_d^2 (8k_B T_i / \pi m_i)^{1/2} n_i \left[1 - Z_d \alpha_i\right]$, and $n_{ec} = \pi r_d^2 (8k_B T_e / \pi m_e)^{1/2} n_e \exp\left[Z_d \alpha_e\right]$ are the ionic and electronic flux charging the dust grain surface respectively[29], $\alpha_e = (e^2 / r_d k_B T_e)$, $\alpha_i = (e^2 / r_d k_B T_i)$, Υ indicates the adsorption coefficient of electrons on surface of dust grains, r_d is the dust grain radius, k_B is the Boltzmann's constant, T_i and T_e are the ions and electrons temperature, m_i and m_e represent the masses of ions and electrons, respectively.

D. *Neutral atoms, electrons and ions number balance*

$$n_i + n_0 = n_{i0} + n_{00} = \mathrm{N}_t, \tag{4.6}$$

where n_0 is neutral particle density under the influence of dust grains, n_{00} , n_{i0} are the densities of neutral atoms and ions in plasma not having dust grains, and N_t is an invariable, respectively.

$$\frac{dn_e}{dt} = (\beta_i n_0 - \alpha_r n_e n_i) - n_d(\Upsilon n_{ec} - n_{ph}) - \nabla \Pi_{\mathrm{p}}, \tag{4.7}$$

and

$$\frac{dn_i}{dt} = (\beta_i n_0 - \alpha_r n_e n_i) - n_d n_{ic} - \nabla \Pi_p, \tag{4.8}$$

where β_i represent the coefficient of ionization, $\alpha_r = (4.5\times10^{-7}(250/T_e)^{-0.7})$ cm^3s^{-1} is the recombination coefficient of electrons with ions corresponding to O^+ present in ionosphere[1] since upto 250 km height, the dominant ionic composition is O^+. Eqs. (4.7) and (4.8) represent the rate of growth of number densities of electrons and ions in plasma under the influence of dust grains, respectively. The initial terms on RHS of Eqs. (4.7) and (4.8) indicate the gain of electrons and ions per unit time per unit volume on account of ionization of neutrals. The succeeding pair of terms in both the equations corresponds to number of neutral atoms formed due to recombination of free electrons into ions, and the net adsorption of electrons and ions on the surface of dust grains.

E. *Electrons and ions energy balance:*

$$\frac{d}{dt}\left(\frac{3}{2}n_e k_B T_e\right) = \beta_i n_0 \varepsilon_e - \alpha_r n_e n_i \left(\frac{3}{2}k_B T_e\right) - n_d(n_{ec}\varepsilon_{ec} - n_{ph}\varepsilon_{ph}) + \frac{n_e e^2 \nu_{ef} U_0^2}{4m_e(\omega_d^2 + \nu_{ef}^2)} - \nu_{em}\delta_{em}\frac{3}{2}n_e k_B(T_e - T_0) + \nu_{ei}\delta_{ei}\frac{3}{2}n_e k_B(T_e - T_i) \tag{4.9}$$

and

$$\frac{d}{dt}\left(\frac{3}{2}n_i k_B T_i\right) = \beta_i n_0 \varepsilon_i - \alpha_r n_e n_i \left(\frac{3}{2}k_B T_i\right) - n_d n_{ic}\varepsilon_{ic} - \nu_{in}\delta_{in}\frac{3}{2}n_i k_B(T_i - T_0) + \nu_{ei}\delta_{ei}\frac{3}{2}n_e k_B(T_e - T_i), \tag{4.10}$$

where ε_e and ε_i are the mean energy of electrons and ions on account of ionization of neutral atoms, $\varepsilon_{ec}(=2k_B T_e - Z_d(e^2/r_d))$ and $\varepsilon_{ic}(=(2-Z_d\alpha_i)/(1-Z_d\alpha_i))$ indicate the average energy of adsorption of electrons and ions on the surface of dust grains,

$\varepsilon_{ph} = \left(\frac{k_B T_d}{\Theta(\eta-\zeta)} \int_0^{\infty} 2\zeta \ \ln(1+\exp(\eta-\zeta))d\zeta \right)$ - $Z_d \alpha_d$ is related to photoemission energy, where $\Theta\ (=Z_d e/r_d)$ is the charged dust grain surface potential, $\alpha_d = (e^2 / r_d k_B T_d)$, $\nu_{ef}\left(=\nu_{ei}+\nu_{ed}+\nu_{en}+\nu_{re}+\nu_{ac}\right)$ is the modified collision frequency owing to ions, dust grains, neutral atoms elastic collisions with electrons and inelastic collisions by virtue of recombination of electrons into ions, and adsorption of electrons on the surface of dust grains, given by $\nu_{ei}[1]=\nu_{ei0}\left(n_i/n_{e0}\right)\left(T_e/T_{e0}\right)^{-3/2}$, $\nu_{ed}[23]=\nu_{ed0}\left(T_e/T_{e0}\right)^{-3/2} Z_d^2$, $\nu_{en}[1]=\nu_{en0}\left(n_0/n_{00}\right)\left(T_e/T_{e0}\right)^{1/2}$, $\nu_{in}=\nu_{in0}\left(n_0/n_{00}\right)\left(T_i+T_d/T_{i0}+T_d\right)^{1/2}$, $\nu_{re}(=\alpha_r n_i)[26]$, $\nu_{ac}=n_d(n_{ec}/n_e)$, where $\nu_{ei0}=\left(5.5 n_{e0}/T_{e0}^{3/2}\right)\ln\left(220 T_{e0}/n_{e0}^{1/3}\right)$, $\nu_{ed0}=\left(2.9\times10^{-6}\right) n_{d0} T_{e0}^{-3/2} \ln\Lambda_e$ [$\ln\Lambda_e$(coulomb logarithm)=10-13], $\nu_{en0}=\left(8.3\times10^{5}\right)\sigma_0 n_{00} T_{e0}^{1/2}$, $\nu_{in0}=(16/3)(2K_B T_d/\pi)^{1/2}\sigma_0 n_{00}(T_{i0}+T_d)^{1/2}$ are the electrons-ions/dust and ion-neutral particles collisions frequencies without dust grains, where n_{e0} is the number density for electrons, T_{e0} is the temperature of electrons without dust grains. $\sigma_0\left(=6.6\times10^{-15}\left[(T_e/4)-0.1\Big/\left\{1+\left(T_e/4\right)^{1.6}\right\}\right]\right)$ is the electrons and neutral particles collisional cross-section area, where σ_0 is in cm^2 and T_e is in eV. The initial pair of terms of Eqs. (4.9) and (4.10) correspond to average energy gain on account of ionization and recombination processes. The third term in both the equations refers to net energy loss due to adsorption process and the succeeding term in Eq. (4.9) belongs to power loss due to process of photoemission from the outer layer of dust grains. The fifth term in Eq. (4.9) corresponds to electrons energy gain from the field due to Ohmic heating effect. Ohmic heating of heavier ions can be ignored. The last term in the two describe the rate of energy loss per unit volume attributed to collisions between dusty plasma components. The term regarding thermal conduction can be ignored on account of predominant collisional effect.

F. *Evaluation of ionization coefficient and average energy of electrons and ions*

By executing kinetics of electrons density and energy balance equations in dust free plasma ionization coefficient and average energies of electrons and ions can be evaluated as

$$\beta_i n_{00} = \alpha_r n_{e0} n_{i0} = \alpha_r n_{e0}^2 . \tag{4.11}$$

$$\varepsilon_e = \frac{d}{dt}\left(\frac{3}{2}k_B T_{e0}\right) + (\alpha_{r0} n_{e0})^{-1}[\nu_{en}\delta_{en}\frac{3}{2}k_B(T_{e0} - T_0) + \nu_{ei0}\delta_{ei}\frac{3}{2}k_B(T_{e0} - T_{i0})], \tag{4.12a}$$

and

$$\varepsilon_i = \frac{d}{dt}\left(\frac{3}{2}k_B T_{i0}\right) + (\alpha_{r0} n_{e0})^{-1}[\nu_{in}\delta_{in}\frac{3}{2}k_B(T_{i0} - T_0) + \nu_{ei0}\delta_{ei}\frac{3}{2}k_B(T_{e0} - T_{i0})]. \tag{4.12b}$$

G. *Paraxial approximation approach*

Let us suppose that the electromagnetic beams with Gaussian and Sine time irradiance spreading along their wave front. Cylindrical coordinates system is suitable to study for their propagation, which may be considered along the z – axis. Propagation of Gaussian irradiance is shown in fig. 4.1.

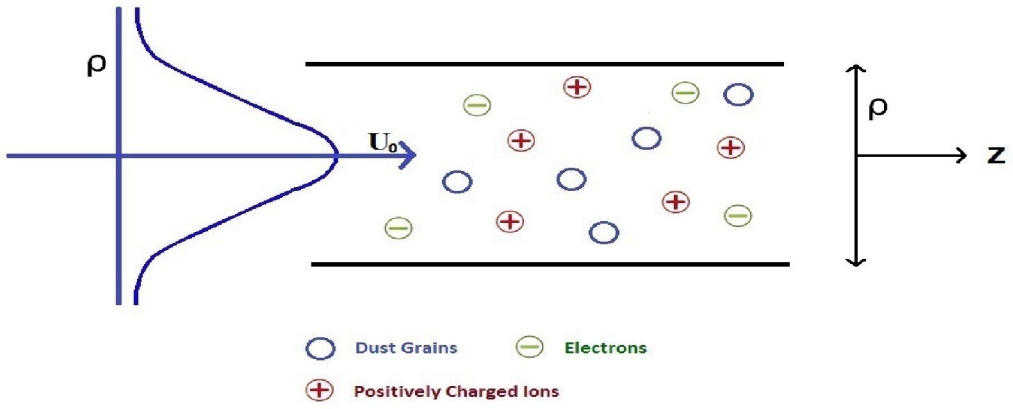

Fig.4.1 Scheme of irradiance of Gaussian electromagnetic beam in dusty plasma.

The spatial irradiance of the beam along z = 0 is described by

$$U^2 = U_0^2(t)e^{\left(-\rho^2/\rho_0^2\right)}, \tag{4.13}$$

where U^2 is the electric field intensity of the Gaussian beam at a length ρ from axis, U_0^2 is the axial intensity at $\rho = 0$, where ρ is the radial coordinate of cylindrical system. Major analysis of the theory assume the time irradiance of Gaussian function of the form

$$U_0^2(t) = U_{00}^2 F'(t/t_0), \text{ where } t_0 \text{ is the beam time width,} \tag{4.13a}$$

$$F'(t/t_0) = \begin{cases} Sin(\pi - t/t_0) & [0 < t/t_0 < \pi] \text{ for Sine beam,} \\ 0, \text{or else} \end{cases} \tag{4.13b}$$

$$F'(t/t_0) = \exp(-t^2/t_0^2) \qquad [-\infty < t/t_0 < \infty] \text{ for Gaussian beam} \tag{4.13c}$$

For a defined value of z, the irradiance in paraxial approximation is represented as

$$U_0^2 = \frac{U_{00}^2(z,t)}{f^2(z,t)} e^{\left(-\rho^2/\rho_0^2 f^2(z,t)\right)} F'(t/t_0), \tag{4.14}$$

where $f(z,t)$ is the beam waist parameter depends upon the length of transmission, z and time t, and $\rho_0 f$ represent the spot of the beam.

From above, it is suggested that the major intensity of beam survive along its principal axis. Therefore, Gaussian beam can be analysed by paraxial approximation approach i.e., $\rho/\rho_0 f$ <<1. So, all the applicable variables are expanded along the principal part (ρ=0) only up to the quadratic expression ρ^2/ρ_0^2 as

$$P(\rho,z,t) = P_a(z,t) - (\rho^2/\rho_0^2)P_\rho(z,t), \tag{4.15}$$

where P_a and P_ρ are the parts of all the accordant parameters characterized by P(ρ,z), along axis and radius, respectively. Although the spatial irradiance of the Gaussian beams do not modify during its propagation in dusty plasma. Hence by introducing the accordant parameters and the

dimensionless variable $t/t_0 = \tau$ in kinetic Eqs. (4.5), (4.7)-(4.10) and comparing the coefficients of ρ^0 and ρ^2/ρ_0^2 terms, we can write the above equations as

H. *Dust charge balance*

$$\frac{dZ_{da}}{d\tau} = t_0[n_{ica}(Z_d,T_i)+n_{pha}(Z_d,T) - \Upsilon n_{eca}(Z_d,T_e)] \tag{4.5a}$$

and

$$\frac{dZ_{d\rho}}{d\tau} = t_0[n_{ic\rho}(Z_d,T_i)+n_{ph\rho}(Z_d,T) - \Upsilon n_{ec\rho}(Z_d,T_e)]. \tag{4.5b}$$

H. *Electrons and ions number balance*

$$\frac{dn_{ea}}{d\tau} = t_0[\beta_{ia}n_0 - \alpha_{ra}n_{ea}n_{ia} - n_d(\Upsilon n_{eca} - n_{pha})]$$
$$-\frac{(2/\rho_0^2)\,t_0}{n_{ia}+c_2n_{ea}}\left[D_{1i}(c_1n_{ia}n_{e\rho}+c_2n_{ea}n_{i\rho})+D_{2i}n_{ea}n_{ia}(c_2T_{ia}^{-1}\,T_{i\rho}+c_3T_{ea}^{-1}\,T_{e\rho})\right] \tag{4.6a}$$

and

$$\frac{dn_{e\rho}}{d\tau} = t_0[\beta_{i\rho}n_0 - \alpha_{r\rho}n_{ea}n_{ia} - n_d(\Upsilon n_{ec\rho} - n_{pha})]$$

$$-\frac{(6/\rho_0^2)t_0}{n_{ia}+c_2n_{ea}}\left[\begin{array}{l} D_{1i}(c_1+c_2)n_{i\rho}n_{e\rho} - \dfrac{(c_1n_{ia}n_{e\rho}+c_2n_{ea}n_{i\rho})(n_{i\rho}+c_2n_{e\rho})}{n_{ia}+c_2n_{ea}} \\ +D_{2i}[(n_{ea}n_{i\rho}+n_{ia}n_{e\rho})(c_2T_{ia}^{-1}\,T_{i\rho}+c_3T_{ea}^{-1}\,T_{e\rho}) \\ -\,n_{ea}n_{ia}(c_2T_{ia}^{-2}\,T_{i'\rho}^{2}+c_3T_{ea}^{-2}\,T_{e\rho}^{2}) \\ -\dfrac{n_{na}n_{ia}(c_2T_{ia}^{-1}\,T_{i\rho}+c_3T_{ea}^{-1}\,T_{e\rho})(n_{i\rho}+c_2n_{e\rho})}{n_{ia}+c_2n_{ea}} \end{array}\right]. \quad (4.6b)$$

$$\frac{dn_{ia}}{d\tau} = t_0[\beta_{ia}n_0 - \alpha_{ra}n_{ea}n_{ia} - n_dn_{ica}]$$
$$-\frac{(2/\rho_0^2)}{n_{ia}+c_2n_{ea}}\left[D_{1i}(c_1n_{ia}n_{e\rho}+c_2n_{ea}n_{i\rho}) + D_{2i}n_{ea}n_{ia}(c_2T_{ia}^{-1}\,T_{i\rho}+c_3T_{ea}^{-1}\,T_{e\rho})\right] \quad (4.7a)$$

and

$$\frac{dn_{i\rho}}{d\tau} = t_0[\beta_{i\rho}n_0 - \alpha_{r\rho}n_{ea}n_{ia} - n_dn_{ic\rho}]$$

$$-\frac{(6/\rho_0^2)\,t_0}{n_{ia}+c_2n_{ea}}\left[\begin{array}{l} D_{1i}(c_1+c_2)n_{i\rho}n_{e\rho} - \dfrac{(c_1n_{ia}n_{e\rho}+c_2n_{ea}n_{i\rho})(n_{i\rho}+c_2n_{e\rho})}{n_{i'a}+c_2n_{e'a}} \\ +D_{2i}[(n_{ea}n_{i\rho}+n_{ia}n_{e\rho})(c_2T_{ia}^{-1}\,T_{i\rho}+c_3T_{ea}^{-1}\,T_{e\rho}) \\ -n_{ea}n_{ia}(c_2T_{ia}^{-2}\,T_{i\rho}^{2}+c_3T_{ea}^{-2}\,T_{e\rho}^{2}) \\ -\dfrac{n_{ea}n_{ia}(c_2T_{ia}^{-1}\,T_{i\rho}+c_3T_{ea}^{-1}\,T_{e\rho})(n_{i\rho}+c_2n_{e\rho})}{n_{ia}+c_2n_{ea}} \end{array}\right]. \quad (4.7b)$$

I. *Electrons and ions energy balance:*

$$\frac{d}{d\tau}\left(\frac{3}{2}n_{ea}k_BT_{ea}\right) = t_0[\beta_{ia}n_0\varepsilon_e - \alpha_{ra}n_{ea}n_{ia}\left(\frac{3}{2}k_BT_{ea}\right) - n_d(\Upsilon n_{eca}\varepsilon_{eca} - n_{pha}\varepsilon_{pha})]$$
$$-\delta_{en}\nu_{ena}t_0\frac{3}{2}n_{ea}k_B(T_{ea}-T_0) + \delta_{ei}\nu_{eia}t_0\frac{3}{2}n_{ea}k_B(T_{ea}-T_{ia})$$
$$+\delta_{comp}\nu_{efa}t_0\left(\frac{3}{2}k_BT_0\right)\frac{\beta_0U_{00}^2}{f^2}n_{ea} \quad (4.9a)$$

and

$$\frac{d}{d\tau}\left(\frac{3}{2}k_B(n_{ea}T_{e\rho}+n_{e\rho}T_{ea})\right) = t_0\left[\begin{array}{l}\beta_{i\rho}n_0\varepsilon_e - \frac{3}{2}k_B\left(\alpha_{r\rho}n_{ea}n_{ia}T_{ea}+\alpha_{ra}(n_{ea}n_{ia}T_{e\rho}+n_{ea}n_{i\rho}T_{ea}+n_{e\rho}n_{ia}T_{ea})\right)\\ -n_d\left(\Upsilon(n_{ec\rho}\,\varepsilon_{eca}+n_{eca}\,\varepsilon_{ec\rho})-(n_{pha}\,\varepsilon_{ph\rho}+n_{ph\rho}\,\varepsilon_{pha})\right)\end{array}\right]$$
$$-\frac{3}{2}k_B\delta_{en}t_0[(n_{e\rho}\nu_{ena}+n_{ea}\nu_{en\rho})(T_{ea}-T_0)+n_{ea}\nu_{ena}T_{e\rho}]$$
$$-\frac{3}{2}k_B\delta_{ei}t_0[(n_{e\rho}\nu_{eia}+n_{ea}\nu_{ei\rho})(T_{ea}-T_{ia})+n_{ea}\nu_{eia}(T_{e\rho}-T_{i\rho})]$$
$$+(\frac{3}{2}\delta_{comp}\,t_0k_B\,T)\frac{\beta_0U_{00}^2}{f^2}\left(\frac{n_{ea}\,\nu_{efa}}{f^2}+(n_{e\rho}\,\nu_{efa}+n_{ea}\,\nu_{ef\rho})\right) \qquad (4.9b)$$

where $\beta_0=\dfrac{e^2}{3m_e\delta_{comp}k_BT\omega^2}$ and $\delta_{comp}\left(=\nu_{ac}/\nu_{ef}\right)$ [Refs. 22 and 37] is the fractional loss of collisional energy of electron with the dusty plasma components,

$$\frac{d}{d\tau}\left(\frac{3}{2}n_{ia}k_BT_{ia}\right) = t_0[\beta_{ia}n_0\varepsilon_i-\alpha_{ra}n_{ea}n_{ia}\left(\frac{3}{2}k_BT_{ia}\right)-\Upsilon n_dn_{ica}\varepsilon_{ica}]$$
$$-[\delta_{in}\nu_{ina}t_0\frac{3}{2}n_{ia}k_B(T_{ia}-T_0)+\delta_{ei}\nu_{eia}t_0\frac{3}{2}n_{ea}k_B(T_{ea}-T_{ia})] \qquad (4.10a)$$

and

$$\frac{d}{d\tau}\left(\frac{3}{2}k_B(n_{ia}T_{i\rho}+n_{i\rho}T_{ia})\right)=t_0\left[\begin{array}{l}\beta_{i\rho}n_0\varepsilon_i-\frac{3}{2}k_B\left(\alpha_{r\rho}n_{ea}n_{ia}T_{ia}+\alpha_{ra}(n_{ea}n_{ia}T_{i\rho}+n_{ea}n_{i\rho}T_{ia}+n_{e\rho}n_{ia}T_{ia})\right)\\ -n_d\left(\Upsilon(n_{ic\rho}\,\varepsilon_{ica}+n_{ica}\,\varepsilon_{ic\rho})\right)\end{array}\right]$$
$$-\frac{3}{2}k_B\delta_{in}t_0[(n_{i\rho}\nu_{ina}+n_{ia}\nu_{in\rho})(T_{ia}-T_0)+n_{ia}\nu_{ina}T_{i\rho}]\,, \qquad (4.10b)$$
$$-\frac{3}{2}k_B\delta_{ei}t_0[(n_{e\rho}\nu_{eia}+n_{ea}\nu_{ei\rho})(T_{ea}-T_{ia})+n_{ea}\nu_{eia}(T_{e\rho}-T_{i\rho})]$$

The simultaneous solution of Eqs. (4.5) - (4.10) for the stationary state (i.e., at $\tau\to\infty$) collectively provide the variation of different dusty plasma components along axis and radius, respectively, for both Gaussian and Sine time irradiance.

J. Modified dielectric permittivity:

Since pressure gradient of electrons and ionic gas is observed on account of non-uniform distribution of electrons and ionic temperature due to non-uniform irradiance of electromagnetic beam. Therefore, these gradients are balanced by space charge field in steady state. Thus, one can obtain

$$\frac{n_e}{n_{e0}} = \left(\frac{2T_{e0}}{T_e + T_{e0}} \right) \tag{4.16}$$

The modified dielectric permittivity in dust accompanying plasma may be given by [38-40]

$$\varepsilon_{ef} = \left(\frac{\omega_0^2}{\omega_d^2} \right) \frac{\omega_d^2}{(\nu_{ef}^2 + \omega_d^2)} \left(\frac{n_e}{n_{e0}} \right) = \varepsilon_a - (\rho^2 / \rho_0^2) \varepsilon_\rho \tag{4.16a}$$

$$\varepsilon_{ef} = \left(\frac{\omega_0^2}{\omega_d^2} \right) \frac{\omega_d^2}{(\nu_{ef}^2 + \omega_d^2)} \left(\frac{2T_{e0}}{T_e + T_{e0}} \right) = \varepsilon_a - (\rho^2 / \rho_0^2) \varepsilon_\rho . \tag{4.16b}$$

Substituting T_e and ν_{ef} corresponding to the Eq. (4.15) and comparing the coefficient of ρ^0 and ρ^2 / ρ_0^2 terms, one obtain,

$$\varepsilon_a = 1 - \left(\frac{\omega_0^2}{\omega_d^2} \right) \left(1 - \frac{\nu_{efa}^2}{\omega_d^2} \right) \left(\frac{2T_{e0}}{T_{ea} + T_{e0}} \right), \tag{4.16c}$$

and

$$\varepsilon_\rho = \left(\frac{\omega_0^2}{\omega_d^2 + \nu_{efa}^2} \right) \left(\frac{2T_{e0}}{T_{ea} + T_{e0}} \right) \left(\frac{\nu_{efa} \nu_{ef\rho}}{\omega_d^2 + \nu_{efa}^2} - \frac{T_{e\rho}}{T_{ea} + T_{e0}} \right), \tag{4.16d}$$

where $\varepsilon_a, \varepsilon_\rho, \nu_{efa}, \nu_{ef\rho}$ and $T_{ea}, T_{e\rho}$ are the modified dielectric permittivities, collision frequencies, and temperatures along axis and radius, respectively, under the influence of dust grains. Plasma frequencies represented by the term ω_0 in the absence of dust grains whereas ω_d represents the vice versa. On introducing, $\nu_{efa}, \nu_{ef\rho}, T_{ea}, and\ T_{e\rho}$ obtained by the coupled solution of Eqs.(4.5) - (4.10), we get the ε_a ,and ε_ρ as a function of $\beta_0 U_{00}^2$.

4.4 Propagation of Electromagnetic Beam with Time Irradiance In Dusty Plasma:

The irradiance of the Gaussian EM-beam in space and time is given by

$$\vec{U} = \hat{j}\ U_0(\rho, z, t) e^{i\omega_d t}, \tag{4.17}$$

where z is the direction of propagation and y is the direction of polarization represented by $\hat{j}$. The analogous equation corresponds to Eq. (4.13),

$$\nabla^2 \vec{U} - \nabla(\nabla \cdot \vec{U}) + \frac{\varepsilon_{ef}}{c^2} \frac{\partial^2 \vec{U}}{\partial t^2} = 0. \tag{4.18}$$

As the transverse component of a beam has zero divergence, hence the Eq. (4.18) reduces to

$$\nabla^2 U + (\omega_d^2 / c^2) \varepsilon_{ef} U = 0. \tag{4.19}$$

Eq. (4.19) can be represented in the following manner because of cylindrically symmetric nature of beam

$$\frac{\partial^2 U}{\partial z^2} + \frac{1}{\rho}\frac{\partial U}{\partial \rho} + \frac{\partial^2 U}{\partial \rho^2} = -\frac{\omega_d^2 \varepsilon_{ef}}{c^2} U. \tag{4.20}$$

The solution of Eq. (4.20) by Akhmanov *et al.* [38] can be described as

$$U(\rho, z, t) = A_0(\rho, z, t) e^{i(\omega_d t - kz)}, \tag{4.21}$$

$$A_0(\rho,z,t) = A_{00}(\rho,z,t)e^{-ik\mathbb{S}(\rho,z,t)}, \tag{4.22}$$

where $k = (\omega_d/c)\,\varepsilon_a^{1/2}$, A_{00} and $\mathbb{S}$ are real quantities, where $\mathbb{S}$ is called eikonal represent the wave phase.

Measuring the real and imaginary parts of the resulting equations, obtained from putting the values of U and A_0, respectively from Eqs. (4.21) and (4.22) in Eq. (4.20) and pursuing the Sodha *et al.* [39], we get

$$2\frac{\partial \mathbb{S}}{\partial z} + \left(\frac{\partial \mathbb{S}}{\partial \rho}\right)^2 + \frac{2}{V_g}\frac{\partial \mathbb{S}}{\partial t} = \frac{1}{\varepsilon_a}\Phi(t) + \frac{1}{k^2 A_{00}}\left\{\frac{\partial^2 A_{00}}{\partial \rho^2} + \frac{1}{\rho}\frac{\partial A_{00}}{\partial \rho}\right\}, \tag{4.23}$$

and

$$\frac{\partial A_{00}^2}{\partial z} + \frac{\partial \mathbb{S}}{\partial \rho}\frac{\partial A_{00}^2}{\partial \rho} + A_{00}^2\left(\frac{\partial^2 \mathbb{S}}{\partial \rho^2} + \frac{1}{\rho}\frac{\partial \mathbb{S}}{\partial \rho}\right) + \frac{1}{V_g}\frac{\partial A_{00}^2}{\partial t} = 0, \tag{4.24}$$

where $V_g = c\varepsilon_a^{1/2}\Big/(\varepsilon_a + \omega_d/2(\partial\varepsilon_a/\partial\omega_d))$ (4.24a)

is the group velocity of electromagnetic beam in dusty plasma,

and

$$\Phi(t) = \frac{\varepsilon_\rho e^{-t/\tau'}}{\tau'}\int_{-\infty}^{t} e^{t/\tau'} AA^* dt\,. \tag{4.24b}$$

On transforming the variable as $z' = z$ and $t' = t - z/V_g$, Eqs. (4.23) and (4.24) reduces to the form

$$2\frac{\partial \mathbb{S}}{\partial z'} + \left(\frac{\partial \mathbb{S}}{\partial \rho}\right)^2 = \frac{1}{\varepsilon_a}\Phi(t') + \frac{1}{k^2 A_{00}}\left\{\frac{\partial^2 A_{00}}{\partial \rho^2} + \frac{1}{\rho}\frac{\partial A_{00}}{\partial \rho}\right\}, \tag{4.25}$$

$$\frac{\partial A_{00}^2}{\partial z'}+\frac{\partial \mathbb{S}}{\partial \rho}\frac{\partial A_{00}^2}{\partial \rho}+A_{00}^2\left(\frac{\partial^2 \mathbb{S}}{\partial \rho^2}+\frac{1}{\rho}\frac{\partial \mathbb{S}}{\partial \rho}\right)=0. \tag{4.26}$$

Supporting the earlier observations [38, 40-41], the solution of Eqs. (4.25) and (4.26) can be expressed as

$$A_{00}^2 = \frac{U_{00}^2(t')}{f^2(z',t')}e^{\left(-\rho^2/\rho_0^2 f^2\right)}F(t'/t_0), \tag{4.27}$$

Substituting the expression of $\Phi(t')$ and A_{00}^2 from Eq. (4.24b) and Eq. (4.27), respectively in Eq. (4.25), we obtain

$$2\frac{\partial \mathbb{S}}{\partial z'}+\left(\frac{\partial \mathbb{S}}{\partial \rho}\right)^2=\frac{1}{2}\frac{\Phi(t')}{\varepsilon_a}-\frac{2}{k^2\rho_0^2 f^2}+\frac{\rho^2}{k^2\rho_0^4 f^4}. \tag{4.28}$$

The eikonal function $\mathbb{S}(\rho,z',t')$ in paraxial ray approximation approach, may be expressed as

$$\mathbb{S}(\rho,z',t')=\frac{\rho^2}{2}\mathrm{B}(z',t')+\Psi(z',t'), \tag{4.29}$$

where $\Psi(z',t')$ is any function of z' and t'

and $\mathrm{B}(z',t') = \frac{1}{f(z',t')}\frac{\partial f(z',t')}{\partial z'}$.

When beam propagates through dusty plasma, the solution of A_{00}^2 preserve the power and shape of the beam. Employing the expression for B in Eq. (4.29) and substituting $\mathbb{S}$ from Eq.(4.29) in Eq.(4.28) and equating the co-efficient of ρ^2/ρ_0^2 of the resulting equation (using the paraxial ray approximation), variation of beam waist parameter with the dimensionless length of transmission can be represented by the equation for both the profiles as

$$\frac{1}{f}\frac{\partial^2 f}{\partial z'^2} = \frac{1}{R_d^2}\frac{1}{f^4} - \frac{1}{2\rho_0^2}\frac{\varepsilon_\rho e^{-t'/\tau'}}{\varepsilon_a}\int_{-\infty}^{t'}\frac{U_{00}^2(t')e^{t'/\tau'}}{f^4}F'(t'/t_0)dt'. \quad (4.30)$$

Integral sign may be eliminated in the Eq. (4.30), if variation of $F'(t'/t_0)$ is of the order of relaxation time τ, which causes small non-linearity. Then the Eq. (4.30) can be simplified to

$$\frac{d^2 f}{dz'^2} = \frac{1}{R_d^2}\frac{1}{f^3} - \frac{1}{2\rho_0^2}\frac{\varepsilon_\rho}{\varepsilon_a}\frac{U_{00}^2(t')}{f^3}F'(t'/t_0) \quad (4.31)$$

or

$$\frac{d^2 f}{d\zeta^2} = -\frac{1}{R_{sl}^2}\frac{1}{f^3} + \frac{1}{f^3}, \quad (4.32)$$

where $R_{sl}\left(=\frac{2\varepsilon_a\rho_0^2}{\varepsilon_\rho U_{00}^2 F'(t'/t_0)}\right)^{1/2}$ is characterized by self-focusing length, $\zeta = \frac{z'}{R_d}$ and $R_d = k\rho_0^2$. On the right –hand side of Eq. (4.32), the initial term corresponds to the nonlinear self-focusing of the beam whereas the succeeding term indicates the divergence phenomenon.

4.5 Results and Discussion

In this analytical model, we present the comparative analysis of both Gaussian and Sine time irradiance of the beam propagating in plasma under the influence of dust grains in collisional plasma. Neutral ionization, recombination of electrons and ions with neutrals, elastic and charging collisions, charging flux via adsorption and photoemission, and ohmic heating due to electromagnetic beam propagating in dusty plasma are the basic energy exchange methods considered in this analysis. Numerical calculations have been carried out in accordance to the metallic dust cloud of stainless steel having high work function of 7.8 eV within close range of space where the photoemission is the dominant mechanism corresponds to Lyman alpha radiations with the spectrum of 1215.7 Å. The simultaneous solution of the coupled Eqs. (4.5) - (4.10) for both the Gaussian and Sine character of electromagnetic beam gives the dependence of modified electron temperature and collision frequency on time for distinguishable dust densities

using MATLAB and MATHEMATICA softwares. Employing the relevent parameter to get ε_a and ε_ρ. Also, at the boundary condition f=1, $\frac{df}{d\zeta} = 0$ at $\zeta = 0$, we obtain dependence of beam waist parameter upon dimensionless length of transmission, $\zeta\ (= z'/R_d)$ by substituting ε_a and ε_ρ, for different values of time width, dust densities, and collision frequency for both Gaussian and Sine time irradiance. The set of variables used in this analysis is listed below: $n_{e0} = n_{i0} = 10^6 cm^{-3}$, $n_0 = n_{00} = 2.5\times10^9 cm^{-3}$, $n_d = 10^3 cm^{-3}$, $k_B = 1.38\times10^{-16}$ ergsk^{-1}, $T_{e0} = 1700K$, $m_e = 9.1\times10^{-28}g$, $T_{i0} = 1300K$, $m_i = 16\times1.6\times10^{-24}g$, $\rho_0 = 5.5\times10^{-2}$cm, $\omega_d = 1.1\times10^8$ rads^{-1}, e = 4.8×10^{-10}statcoloumb, T_d = 275K, r_d=5x10^{-4}cm, σ_0=1.5×10^{-16}cm^2, $U_{00} = 10^6$ stat volt cm^{-1}.

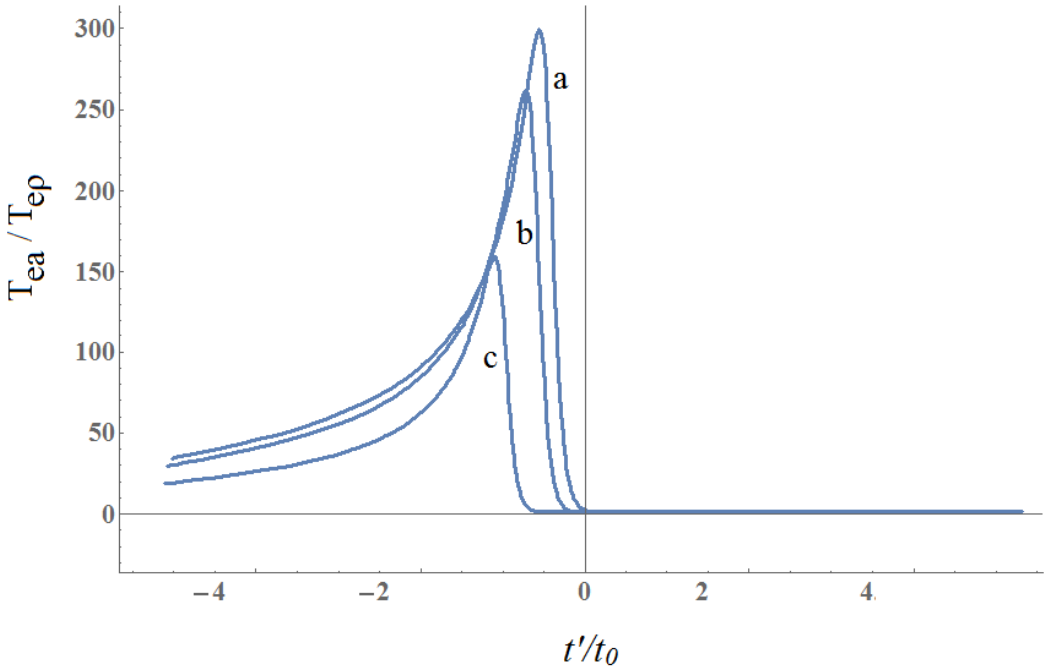

Fig. 4.2

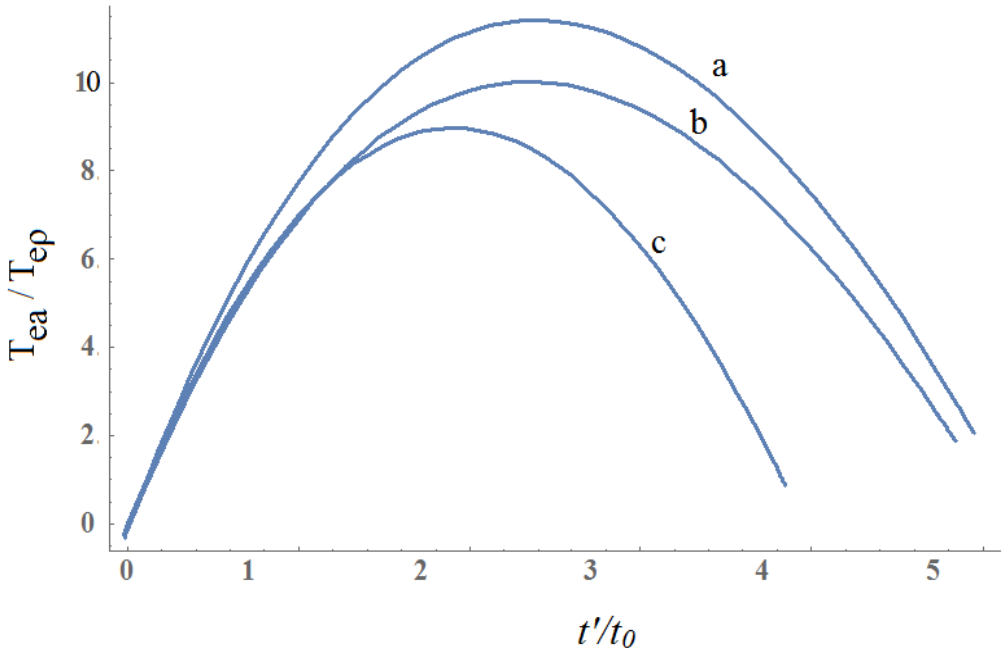

Fig. 4.3

Figs. 4.2 and 4.3 Dependence of dimensionless electron temperature T_{ea}/T_{ep} on dimensionless time width t'/t_0 for distinguishable dust densities for both Gaussian and Sine profile, respectively. The dust densities10, 10^2, 10^3 are labelled by a, b and c in cm^{-3}, respectively.

The time sensitivity of dimensionless electron temperature has been shown in figures 4.2 and 4.3 for variant dust densities for both Gaussian and Sine time characteristics respectively. Peak of temperature corresponding to extremum irradiance at t'/t_0 = (-0.5) for Gaussian pulse and 0.8π for Sine pulse is observed. A shift is observed from the dust free environment where the maxima is obtained at t'/t_0 =0(red shift) for Gaussian pulse and t'/t_0 =0.5π (blue shift) for Sine pulse [34] on account of increase in collision frequency due to the presence of dust. Also the maximal temperature decreases with increase in dust density on account of faster electron energy decay due to increase in collisions with the density of dust grains as shown in figures 4.4 and 4.5 which represent the variation of dimensionless modified collision frequency with time width for both the Gaussian and Sine time profiles for different dust densities, respectively.

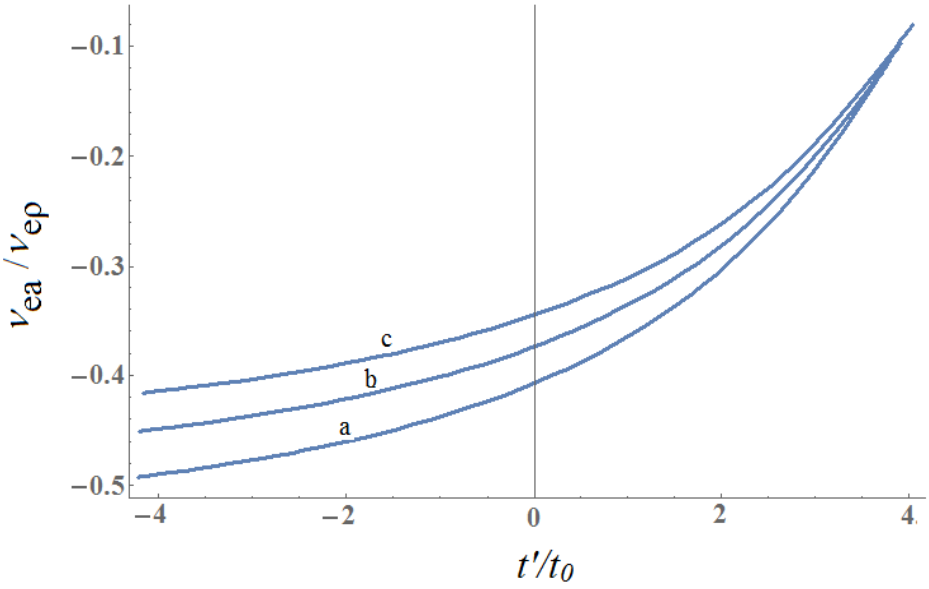

Fig. 4.4

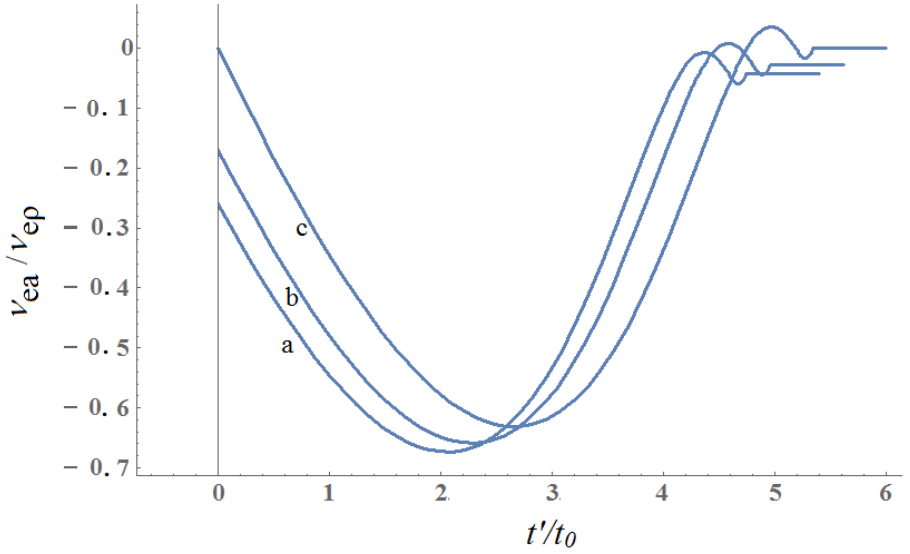

Fig. 4.5.

Figs. 4.4 and 4.5 Dependence of dimensionless electron frequency v_{ea}/v_{ep} *on dimensionless time width* t'/t_0 *for distinguishable dust densities for Gaussian and Sine time profile, respectively. The dust densities,* $n_d = 10, 10^2$, *and* 10^3, *in* cm^{-3} *are labelled by a, b and c, respectively.*

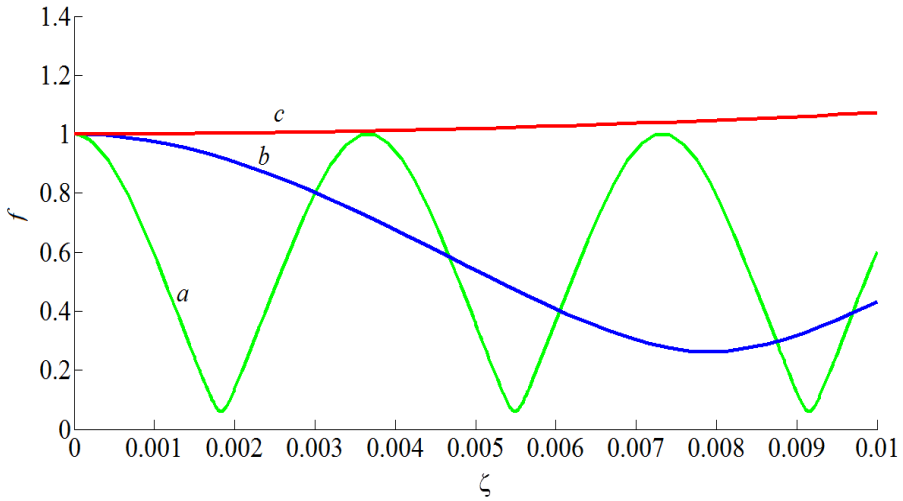

Fig. 4.6

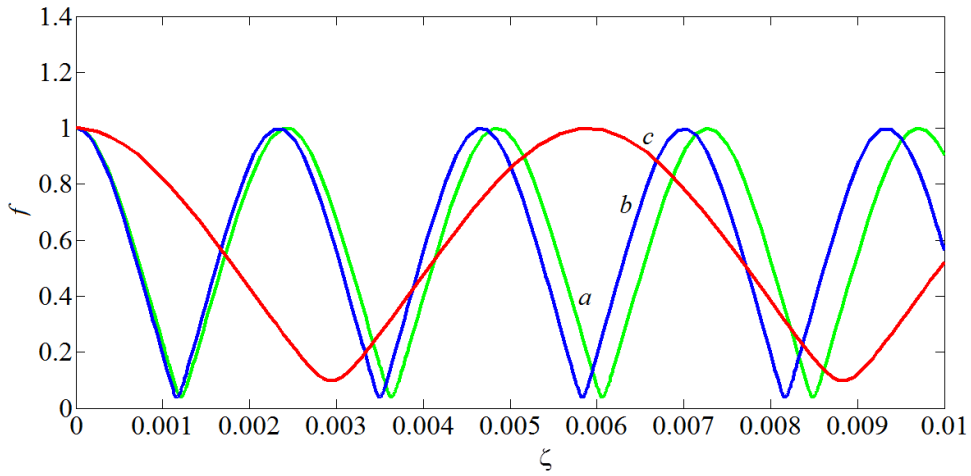

Fig. 4.7

Figs 4.6 and 4.7 Relying beam waist parameter f with the dimensionless length of transmission $\zeta(= z'/R_d)$ *for the Gaussian and Sine beam for different time width* t'/t_0. *The labels a, b and c indicate the dimensionless time width* t'/t_0 *= 1, 2, and 3, respectively.*

Figures 4.6 and 4.7 show the comparative analysis of propagation of beam waist parameter with the dimensionless length at the same time width for both the Gaussian and Sine time irradiance of the beam. Self-focusing enhances with lesser time width for both the profiles but beam get

self-focused faster in sinusoidal irradiance due to boost rate of nonlinearity under the influence of dust grains.

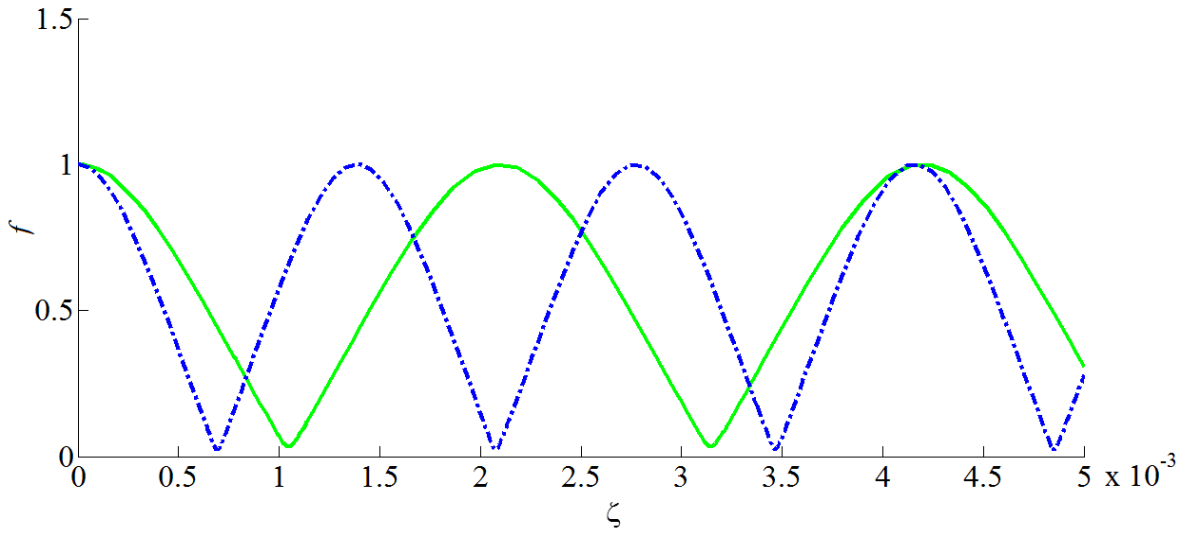

Fig. 4.8 Relying beam waist parameter f on the dimensionless length of transmission $\zeta (= z'/R_d)$ *for the Gaussian (solid) and Sine (dotted) beam as a function of maximal irradiance at time width* $t'/t_0 = -0.5$, *for Gaussian and* $t'/t_0 = 0.8\pi$ *for Sine beam .*

Figure 4.8 show the reliance of beam waist parameter with the dimensionless length of transmission at the same modified collision frequency and at the point of time width of maximal irradiance under the influence of dust grains shown by the solid (Gaussian) and dotted (Sine) lines. Both the exponential and Sine profiles how the oscillatory convergence but the frequency of Sine profile is greater than the Gaussian one on account of different rate of nonlinearity for both the profiles under the influence of dust grains. Even the waist of the beam becomes narrower as compared to the dust free environment [34].

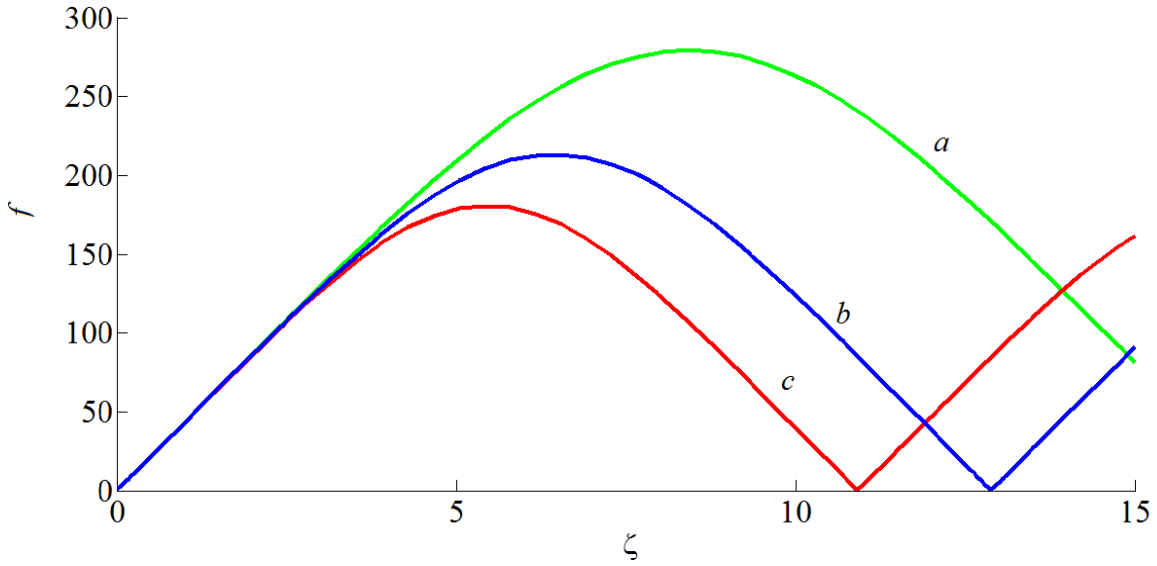

Fig. 4.9

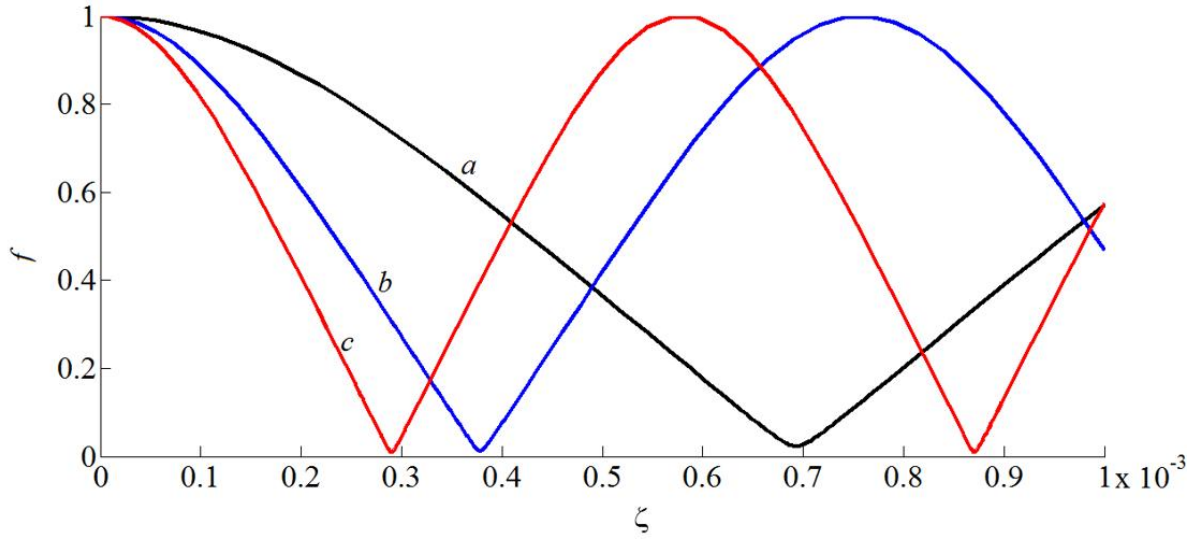

Fig. 4.10

Figs. 4.9 and 4.10 relying beam waist parameters f on the dimensionless length of transmission $\zeta(=z'/R_d)$ *for the Gaussian and Sine beam for distinguishable dust densities. The dust densities,* n_d=10, 100,1000 *in* cm^{-3}*, are labelled by a, b, and c, respectively.*

Figures 4.9 and 4.10 describe reliance of beam waist parameter on the dimensionless length of transmission for distinguishable dust densities. Since the collision frequency increases with dust density which further enhances the nonlinearity of the beam causing the enhanced self-focusing for both the profiles of the beam with the dust density but the Sine profile self-focused at faster rate than Gaussian profile.

4.6 Conclusions

This analytical model investigates the dust grains impact on self-focusing of both the Gaussian and Sine time irradiance of the beam transmitting through dusty plasma. A comparative analysis of growth of plasma parameters like temperature and collision frequencies modified under the influence of dust grains have been studied numerically to calculate the modified dielectric permittivity for both the profiles of the beam considering the paraxial ray approximation, neutrality of charge, ionization of neutrals, recombination of electrons with ions, charging flux via adsorption and photoemission of electrons and diffusion. Also, the comparative growth of beam waist parameter along the dimensionless transmission length as a function of time width, point of maximal irradiance, and dust densities have been analyzed for both the profiles in the impact of dust grains and compared with the dust free environment. The consequences of this model are beneficial for the domain of dust particles like astrophysics, manufacturing, fabrication, plasma processing etc.

REFRENCES

[1] A. V. Gurevich, *Nonlinear Phenomena in the Ionosphere* (Springer, New York, 1978).

[2] A. Gahlot, R. Walia, S. C. Sharma, and R. P. Sharma, J. Plasma Phys. **78**, 33(2012).

[3] M. S. Sodha, A. Dixit, and S. Srivastava, Appl. Phys. Lett. **94**, 251501 (2009).

[4] M. S. Sodha and A. Dixit, Appl. Phys. Lett. **95**, 101502(2009).

[5] M.S.Sodha, S. Misra, and S. K. Mishra, Phys Plasmas **16**, 123705 (2009).

[6] J. Goree, Plasma Sources Sci. Technol. **03**, 400 (1994).

[7] M. Mikikian, L. Boufendi, A. Bouchoule, H. M. Thomas, G. E. Morfill, A. P. Nefedov, V. E. Fortov,and the PKE–Nefedov team,New J. Phys. **5**, 19(2003).

[8] I. Denysenko, J. Berndt, E. Kovacevic, I. Stefanovic, V. Selenin, and J. Winter, Phys. Plasmas **13**, 073507(2006).

[9] D. Samsonov and J. Goree, Phys. Rev. E **59**, 1047(1999).

[10] P. K. Shukla and V. P. Silin, Phys. Scr. **45**, 508 (1992).

[11] R. L. Merlino, A. Barkan, C. Thompson, and N. D'Angelo, Phys. Plasmas **5**, 1607(1998)

[12] M Bonitz, C Henning and D Block, *Reports on Progress in Physics* **73**, 6(2010).

[13] S. V. Vladimirov, K. Ostrikov, and A. A. Samarian, *Physics and applications of complex plasmas* (Imperial College Press, London, 2005).

[14] V. N. Tsytovich, G. E. Morfill, S. V. Vladimirov, and H. M. Thomas, *Elementary Physics of Complex Plasmas* (Springer, Berlin, 2008).

[15] O. Ishihara, Journal of Physics D: Applied Physics **40**, 8(2007).

[16] H. Kersten, G. Thieme, M. Fröhlich, D. Bojic, D. H. Tung, M. Quaas, H. Wulff, and R. Hippler, Pure Appl. Chem.**77**, 415(2005).

[17] F. Verheest, Plasma Physics and Controlled Fusion **41**, 3A(1999)

[18] R. L. Merlino, "Dusty plasmas and applications in space and industry," Transworld Research Network 37/661(2), Fort P.O., Trivendrum 695023, Kerala, India, 2006.

[19] S. C. Sharma, A. Gahlot, and R. P. Sharma, Phys. Plasmas **15**, 043701(2008).

[20] M. S. Sodha, S. K. Mishra, and S. Misra, Phys. Plasmas **16**, 123701(2009).

[21] M. S. Sodha, *Kinetics of Complex Plasmas* (Springer, India, 2014).

[22] G. Sambandan, V. K. Tripathi, J. Parashar, and R. Bharuthram, Phys.Plasmas **6**, 762(1999).

[23] M. S. Sodha, S. K. Mishra, and S.Misra, Phys. Plasmas **18**, 023701(2011).

[24] F. Verheest, and P. Meuris, Phys. Lett. A **210**, 198(1996).

[25] J. Jia, C. Yuan, R. Gao, Y. Wang, Y. Liu, J. Gao, Z. Zhou, X. Sun, J. Wu, H. Li, and S. Pu,J. Phys. D: Appl. Phys.**48**, 465201(2015).

[26] S. K. Mishra, and S.Misra, Phys. Plasmas **26**, 023702 (2019).

[27] Ruchi Sharma and S. C. Sharma, Contrib. Plasma Phys.**59**, 211(2019).

[28] J. Jia, C. Yuan, S. Liu, F. Yue, R. Gao, Y. Wang, Z.-X. Zhou, J. Wu, H. Li, Phys. Plasmas **23**, 043302(2016).

[29] S. K. Mishra, S. Misra, and M. S. Sodha, Phys. Plasmas **18**, 043702 (2011).

[30] Hai-bo Wang, Yun-yun Chen, and Chung Huang, Optik-International Journal for Light and Electron optics **196**, 163148(2019).

[31] M. S. Sodha, S. K. Mishra, S. Misra, and S. Srivastava, Phys. Plasmas **17**, 073705(2010).

[32] M. Faisal, L.Bhasin, and M.S.Sodha, J. Geophys Res.**114**, A01305 (2009)

[33] M. Sodha and A.Sharma, J. Plasma Phys.**74**, 473(2009).

[34] M. Faisal, M. P. Verma, and M. S. Sodha, Phys Plasmas **15**, 102301 (2008).

[35] R. Fowler, *Statistical Mechanics*, (Cambridge University Press, Cambridge (1936)).

[36] M.S.Sodha, and A. Dixit, Appl. Phys. Lett. **95**, 101502(2009).

[37] J.D.Huba, *NRL physics Formularly* (Naval Research laboratory Washington, (D.C.)1998).

[38] S. A. Akhamanov, A. P. Sukhorukov, and R. V. Khokhlov, Sov. Phys. Usp **10**, 619(1968).

[39] M.S.Sodha, R.S. Mittal, S.Kumar, and V.K.Tripathi, Opto-electronics (London) **6**, 167(1974).

[40] M. S. Sodha, A. K. Ghatak, and V. K. Tripathi, *Self-filamentation of Laser Beams in Dielectrics, Semiconductors and Plasmas* (Tata-McGrawHills, Delhi, 1974).

[41] M.S.Sodha, A.K.Ghatak, and V.K.Tripathi, Prog.Opt.**13**, 169(1976).

Chapter 5

THEORETICAL MODEL FOR NONLINEAR PROPAGATION OF ELECTROMAGNETIC WAVE IN NON-THERMAL EXOSPHERIC DUSTY PLASMAS

5.1 Brief outline of the chapter

The physical significance of our present work is that how the presence of dust modifies the plasma parameters and nonlinear propagation of electromagnetic wave on account of ohmic heating with collisions in the upper atmospheric plasma conditions for mid-day time at an altitude of 1000 km as the temperature of electrons and ions increases with the day of time. This analysis is helpful in solving the applications of satellite communication system and rocky planet atmosphere. In this chapter, we have tried to show the modification in plasma parameters in the presence of dust components and field at an exospheric altitude of 1000 km on account of ohmic heating with collisions and how the presence of dust influence the nonlinear propagation of electromagnetic wave along the distance of propagation at an exospheric altitude.

For this purpose, we have used data of exosphere used in the book Gurevich and dust grains of CeO_2 of work function 5.34eV at an altitude of 1000 km in mid-day time atmosphere. For photoemission from dust grains, solar radiation flux in the range 10eV to 124eV has been considered in upper exosphere for X-rays and far UV radiations. Photo-ionization, electron-ion recombination and charge exchange mechanism are the basic mechanism through which molecules escape from exobase to upper atmosphere and provide translationally energetic atoms for energy exchange with exospheric plasma constituents in the presence of dust. Equations (5.1)-(5.6) represent the mechanism through which plasma parameters like dust charge , electron-ion number densities, electron-ion temperature are modified in the presence of dust on account of ohmic non-linearity with collisions due to propagation of electromagnetic beam in the upper exosphere at an altitude of 1000 km. Equations (5.7)-(5.9) represent the formulation for modified dielectric permittivity, refractive index, and absorption coefficient of the medium for the propagation of electromagnetic wave. Eqn (5.10) shows the formulation for solving

irradiance of electromagnetic wave along the dimensionless distance of propagation numerically in the exospheric environment.

5.2 Introduction

Nonlinear propagation of electromagnetic wave in upper atmospheric dusty plasma is a fascinated research world for millenary because of its enormous applications in earth-satellite communication system, and atmosphere of rocky planets etc.[1-11] The presence of dust influences the conductivity of plasma environment and facilitates the self-focusing of electromagnetic wave propagating through it. In this chapter, we consider exospheric plasma environment in which air is very thin and is mainly consist of hydrogen, helium and traces of other gases such as O atom and CO_2.[12] Exosphere in the vicinity of exobase is dominated with non-thermal escape mechanism of ions (mainly H). They gain their energy from ambipolar diffusion, where the interaction of ions, electrons and dust in plasma causes them to diffuse at the same rate. There are many non-thermal escape processes such as photo-dissociation, e^--ion recombination process, charge exchange mechanism, sputtering and solar wind pick-up.[13-14] Due to lesser gravity effect, the lighter particles like hydrogen, electrons escape into the upper atmosphere via diffusion limited escape process.[15] The diffusion limited flux (Φ_l) in upper atmospheric dusty plasma is given by $D_i n_i/H_a$, where D_i is a binary diffusion parameter, n_i is density of diffusing species, H_a is atmospheric scale height.

The dust particles floating in plasma act as source and sink of plasma constituents, acquire the negative/positive potential thereby modifying the electron density and hence the conductivity of plasma. Moreover, an electromagnetic beam passing through dusty plasma heats up the electron non-linearly. It enhances the electron temperature and consequently changes electron density and the charge on dust particles. The nonlinear change in electron density causes a depleted density channel and facilitates the beam to self-focus through it. [16, 17]

In this chapter, we have considered the process of ionization of neutral atoms, radiative and dissociative recombination of electrons and ions, mechanism of charge exchange, adsorption of electrons and photoemission from dust particles, diffusion limited escape flux, and ohmic heating by the electric vector in the exospheric environment. The motive is to study the variation of

plasma parameters with the electric vector of the wave in the presence of dust. For the sake of analysis, we have considered the region of exospheric altitude of 1000 km where hydrogen atoms are found abundantly. We have used mid day time data (Table I) specified by Gurevich [18]as temperature of electrons and ions increases very strongly with the day of time. We have also analyzed modification in electric vectors of electromagnetic waves with the normalized propagation distance at distinct exospheric plasma parameters in the presence of dust. Although, previously it was assumed that the upper atmosphere is collisionless fully ionized but presently it has been discovered that it is almost collisionless with infrequent collisions of escaping species with plasma constituents. In the present study, we have considered the charge exchange and collisions between plasma constituents in upper atmosphere. The section 5.3 of the theoretical model consists of sets of basic equations of non-thermal escape mechanism, dust-charge kinetics and propagation of electromagnetic wave in dusty plasma. The section 5.4 is comprised of exospheric data and computational scheme. Numerical results and their analysis are included in section 5.5. The present model is concluded under the section 5.6.

5.3 Basic Equations

As the atmospheric density decreases with increasing height, so does the collision frequency and at a height above which mean free path of molecules becomes equal to the scale height, the molecules have energies greater than gravitational binding energies so these can escape to space with outward radial velocities. The region of atmosphere at this height is called exosphere and the lower boundary for this region is called exobase at an atmospheric scale height, H_a. There are number of ways through which molecules can escape into the upper atmosphere or the exosphere.

A. Escape Mechanisms

The exospheric plasma mainly consists of electrons, ions, and neutrals, where X-rays and far UV radiations mainly cause ionization. The principal non-thermal collisional processes between exospheric constituents with charged species to produce atoms that are translationally energetic and incompletely thermalized are photoionization, electron-ion recombination and charge exchanges which are described as:

Photo-ionization

Photo ionization escape occurs due to the interaction of solar photons and photoelectrons with thermospheric molecules and lead to generation of more energetic particles.

$$H + h\nu \rightarrow H^+ + e^-$$

$$O + h\nu \rightarrow O^+ + e^-$$

$$He + h\nu \rightarrow He^+ + e^-$$

Electron-ion recombination

The escaping ions recombine with the electrons of exospheric plasma [19]and form the neutral molecules. The chemical equations involved are shown below.

$$H^+ + e^- \rightarrow H \qquad \alpha_H = 4\times10^{-13}(T_e/300)^{-0.7}\, cm^3 s^{-1},$$

$$He^+ + e^- \rightarrow He \qquad \alpha_{He} = 4\times10^{-7}(T_e/300)^{-0.5}\, cm^3 s^{-1},$$

$$O^+ + e^- \rightarrow O + \varepsilon_{rad} \qquad \alpha_O = 7.8\times10^{-8}(T_e/300)^{-0.5}\, cm^3 s^{-1},$$

where α_i is the coefficients of recombination for different ions, where i stands for H, He, and O ions. T_e represents the temperature of electrons in exospheric environment as shown in table I.

Charge Exchange mechanism

The main mechanism of non-thermal escape is production of translationally energetic species via elastic or reactive collisions.[20] The charge transfer between escaping ions and exospheric neutrals are given by

$$H^+ + H \rightarrow H + H^+ \qquad k_1 = 2.8\times10^{-7}\, cm^3 s^{-1},$$

$$H^+ + O \rightarrow O^+ + H \qquad k_2 = 4\times10^{-10}\, cm^3 s^{-1},$$

$$He^+ + O \rightarrow O^+ + He \qquad k_3 = 10^{-9}\, cm^3 s^{-1},$$

$$He^+ + H \rightarrow He + H^+ \qquad k_4 = 10^{-9}\, cm^3 s^{-1},$$

where k_i is the rate of charge transfer between different species, here i stands for 1,2,3,4.

B. Kinetics of exospheric plasma components in the presence of dust

Considering the above mechanism, we investigate the influence of the dust grains on kinetics of exospheric plasma components. The existence of dust grains enhances the rate of adsorption and photoemission of plasma species from the surface of dust grains. The temperature of neutrals and dust grains are considered to be constant because of their large thermal capacity. Following earlier analysis [21] on kinetics of dust particles in plasma, the sets of equations can be written as

1. *Charge balance of dust grains*

The balancing equation of charged dust grains on account of electronic and ionic flux over its surface is shown as

$$dZ/dt = (n_{H^+c} + n_{O^+c} + n_{He^+c}) - n_{ec} + n_{ph}, \tag{5.1}$$

where n_{ic} is ionic current adsorbing the dust surface and i stands for ions of H^+, He^+ ,and O^+, n_{ec} is the current of adsorption of electrons on dust grain surface and n_{ph} is the current of photoemission of electrons from dust grain surface.

2. *Number balance of electrons and ions*

The balancing equation of numbers of electrons and ions due to their formation and deformation on account of various processes can be written as

Number balance of electrons

$$dn_e/dt = [(q_{iH^+} + q_{iO^+} + q_{iHe^+}) - (\alpha_H n_{H^+} + \alpha_{He} n_{He^+} + \alpha_o n_{o^+}) n_e + D_a n_e / H_a] - n_d (n_{ec} - n_{ph}) . \quad (5.2)$$

Number balance of ions

$$dn_{H^+}/dt = [(q_{iH^+} - \alpha_H n_{H^+} n_e) + (k_1 n_{H^+} n_H + k_4 n_{He^+} n_H - k_2 n_{H^+} n_o) + D_a n_{H^+}/H_a] - n_d n_{H^+c} \quad (5.3a)$$

$$dn_{O^+}/dt = [(q_{iO^+} - \alpha_O n_{O^+} n_e) + (k_2 n_{H^+} n_o + k_3 n_{He^+} n_O) + D_a n_{O^+}/H_a] - n_d n_{O^+c} , \quad (5.3b)$$

$$dn_{He^+}/dt = [(q_{iHe^+} - \alpha_{He} n_{He^+} n_e) - (k_2 n_{H^+} n_o + k_3 n_{He^+} n_O) + D_a n_{He^+}/H_a] - n_d n_{He^+c} , \quad (5.3c)$$

where n_e is the electron density, n_d is the dust density and q_i is the rate of ionization. The first term on the right hand side of the Eqs. (5.2) and (5.3) specifies the gain in electron and ion densities due to neutral atom ionization, the second term refers to the electrons and ions recombination, and the third term represent the diffusion of electrons and ions. The last term corresponds to loss in electron and ion densities due to net flow of electrons and ions towards the dust grain surface. The number balance of electrons and ions with the charge balance of dust grains constitute the quasi neutrality condition which is given by

$$n_{H^+} + n_{He^+} + n_{O^+} - n_e = Z n_d , \quad (5.4)$$

where Z is dust charge state.

3. *Energy balance of electrons and ions*

The energy balance of electrons and ions via energy exchange between different plasma constituents due to various processes is given by

$$\frac{d}{dt}\left(\frac{3}{2}n_e k_B T_e\right)=[(q_{iH^+}+q_{iO^+}+q_{iHe^+})\varepsilon_e-\left(\frac{3}{2}k_B T_e\right)(\alpha_H n_{H^+}+\alpha_{He} n_{He^+}+\alpha_o n_{o^+})n_e]+$$
$$\left(\frac{3}{2}k_B T_e\right)(D_a n_e / H_a)-n_d(n_{ec}\varepsilon_{ec}-n_{ph}\varepsilon_{ph})$$
$$-\left(\frac{3}{2}k_B\right)\left(\sum_i n_e \nu_{ei}\delta_{ei}(T_e-T_i)+\sum_j n_e \nu_{ej}\delta_{ej}(T_e-T_j)\right)+\frac{\sigma_r E_0^2}{2}, \quad (5.5)$$

$$\frac{d}{dt}\left(\frac{3}{2}k_B T_i\sum_i n_i\right)=(q_{iH^+}+q_{iO^+}+q_{iHe^+})\varepsilon_i-\left(\frac{3}{2}k_B T_i\right)(\alpha_H n_{H^+}+\alpha_{He} n_{He^+}+\alpha_o n_{o^+})n_e+$$
$$\left(\frac{3}{2}k_B T_i\right)(D_a / H_a)\sum_i n_i - n_d(\sum_i n_{ic})\varepsilon_{ic}$$
$$-\left(\frac{3}{2}k_B\right)\left(\sum_{i,j} n_i \nu_{ij}\delta_{ij}(T_i-T_j)+\sum_i n_e \nu_{ei}\delta_{ei}(T_e-T_i)\right), \quad (5.6)$$

where k_B is Boltzmann's constant, i and j stands for H^+, He^+, and O^+ ions and H, He, and O atoms, T_e and T_i and T_j are the temperatures of electrons and ions and neutrals, ε_e and ε_i are the mean free energies of electrons and ions, ε_{ec}, ε_{ic} and ε_{ph} are the mean energies associated with adsorption of electrons and ions and photoemission of electrons from dust grain surface. ν_{ei}, ν_{ej}, and ν_{ij} are the collisional frequencies and δ_{ei}, δ_{ej}, and δ_{ij} are the fractions of energy loss associated with collisions of electrons-ions, electrons-neutrals, and ions-neutrals, respectively. σ_r is the complex conductivity of dusty plasma and E_0 is the amplitude of the irradiance of electromagnetic wave passing through it. The first two terms in Eqs. (5.5) and (5.6) represent the rate of gain of power per unit volume via neutral ionization and recombination of electrons and ions. The third term corresponds to the energy associated with diffusion of particles through the dusty plasma. The fourth and fifth terms signify the net power loss on the account of electronic and ionic flux and collisions between the exospheric dusty plasma constituents. The last term in Eq. (5.5) refers to rate of gain of power per unit volume due to ohmic heating.

The simultaneous numerical solution of the Eqs. (5.1)-(5.6) in the steady state determines the influence of dust grains on the exospheric plasma parameters when an electromagnetic wave is propagating through it and the solution assists the calculation of effective dielectric constant in the presence of dust.

C. Electromagnetics

1. Effective dielectric constants in dusty plasma

The effective dielectric constant in dusty plasma is given by [22]

$$\varepsilon = \varepsilon_r - i\varepsilon_i = 1 - \frac{4\pi n_e e^2 (\nu_{eff} - i\omega_d)}{m_e \omega_d (\nu_{eff}^2 + \omega_d^2)}, \tag{5.7}$$

where ε_r and ε_i are the real and imaginary part of dielectric constant in the presence of dust grains. Hence,

$$\varepsilon_r = 1 - \left(\frac{\omega_p^2}{\omega_d^2}\right)\left(\frac{n_e}{n_{e0}}\right)\left(\frac{\omega_d^2}{\nu_{eff}^2 + \omega_d^2}\right), \tag{5.7a}$$

$$\text{and } \varepsilon_i = 1 - \left(\frac{\omega_p^2}{\omega_d^2}\right)\left(\frac{n_e}{n_{e0}}\right)\left(\frac{\nu_{eff}\omega_d}{\nu_{eff}^2 + \omega_d^2}\right), \tag{5.7b}$$

where ω_d and $\omega_p = \left(\frac{4\pi n_{e0} e^2}{m_e}\right)^{1/2}$ are the electron plasma frequencies in the presence and absence of dust and field, respectively. ν_{eff} is the effective electron collision frequency in the presence of dust grains.

The complex conductivity of plasma is given by

$$\sigma = \left(\frac{n_e e^2}{m_e}\right)\left(\frac{\nu_{eff}}{\nu_{eff} + i\omega_d}\right), \tag{5.8}$$

where σ_r and σ_i are the real and imaginary parts of dielectric constant.

$$\sigma_r = \left(\frac{n_e e^2}{m_e}\right)\left(\frac{\nu_{eff}}{\nu_{eff}^2 + \omega_d^2}\right). \tag{5.9}$$

The absorption coefficient k and refractive index n are expressed as

$$k = [\{(\varepsilon_r^2 + \varepsilon_i^2)^{1/2} - \varepsilon_r\}/2]^{1/2} \tag{5.9a}$$

and

$$n = [\{(\varepsilon_r^2 + \varepsilon_i^2)^{1/2} + \varepsilon_r\}/2]^{1/2}, \text{ respectively.} \tag{5.9b}$$

Using the Eqs. (5.9a) and (5.9b), the complex refractive index is expressed as $(n - ik)$ .The dependence of absorption coefficients and refractive index may be obtained as a function of irradiance of electromagnetic wave corresponding to specific altitude dependence on electron temperature and plasma density.

5.4 Nonlinear propagation of electromagnetic wave in dusty plasma

Using JWKB approximation, Sodha et al. [23] have proposed that the amplitude and phase of electromagnetic wave $E = E_0 \exp\{i(\omega t + \psi - kx)\}$, propagating in a nonlinear dusty plasma medium is given by

$$E_0^{-1}[dE_0/d\xi] = -k - (2\mu_0^{-1})(d\mu_0/d\xi), \tag{5.10}$$

$$\text{or } (E_0^2)^{-1}[dE_0^2/d\xi] = -2k - (\mu_0^{-1})(d\mu_0/d\xi) \tag{5.10a}$$

$$\text{and } [d\psi/d\xi] = -n + (0.5)(d\theta/d\xi), \tag{5.10b}$$

where $\xi(=(\omega_d/c)x)$ is normalized propagation distance along x-axis,

$\mu = \mu_0 \exp(-i\theta) = (n - ik)$ is the complex refractive index and

$tan\theta(\xi) = k(\xi)/n(\xi)$.

By knowing the n, k, μ and θ, the relationship of E_0^2 and phase ψ with ξ can be established numerically.

5.5 Admissible Data and Expressions

A. *Exospheric data*

Our computational methodology is based on data obtained from the book written by Gurevich.[18] The number densities and temperatures of electrons, ions and neutrals in the unperturbed atmosphere for the range 700km-1000km for mid-day time are shown in table I.

TABLE I. Exospheric mid-latitude day time data for height in km, number densities in cm^{-3}, and temperature in K. n_{H^+}, n_{He^+}, *and* n_{O^+}, are the number densities of ions and $T_{e0}, T_{i0}, and\ T_{00}$ are the temperatures of electrons, ions, and neutrals, and n_{H^+}/n_{e0}, n_{He^+}/n_{e0}, *and* n_{O^+}/n_{e0} are the relative ionizations.

Height	n_{e0}	T_{e0}	T_{i0}	T_{00}	n_{H^+}/n_{e0}	n_{He^+}/n_{e0}	n_{O^+}/n_{e0}
700	$2x10^5$	2800	2200	1400	0.11	0.04	0.75
800	10^5	2870	2300	1400	0.21	0.06	0.61
900	$7x10^4$	2940	2400	1400	0.4	0.09	0.41
1000	$5x10^4$	3000	2500	1400	0.51	0.14	0.28

TABLE II n_{H+}, n_{He+}, *and* n_{O+}, are the number densities of neutrals and ω_p is the electron plasma frequency at an altitude of 1000 km.

Height	n_H	n_{He}	n_O	n_{00}	ω_p
700	$6.6x10^3$	$8.0x10^5$	$5.2x10^6$	$6.0x10^6$	$2.5x10^7$
800	$6.2x10^3$	$6.1x10^5$	$1.8x10^6$	$2.4x10^6$	$1.8x10^7$
900	$5.8x10^3$	$4.7x10^5$	$6.2x10^5$	$1.1x10^6$	$1.5x10^7$
1000	$5.4x10^3$	$3.7x10^5$	$2.2x10^5$	$6.0x10^5$	$1.3x10^7$

Expressions

Effective collision frequency

Since the exospheric dusty plasma is also associated with minor elastic and charging collisions between different dusty plasma components. The effective collision frequency of electrons in the presence of dust grains is given by

$$\nu_{eff} = \nu_{ei} + \nu_{ed} + \nu_{en} + \nu_{re} + \nu_{ac},$$

where $\nu_{ei} = \sum_i \nu_{ei0} (n_i/n_{e0}) \left(T_e/T_{e0}\right)^{-3/2}$ represents the electron-ion elastic collisions,[18]

where i stands for H^+, He^+, and O^+ ions and $\nu_{ei0} = \left(5.5 n_{e0}/T_{e0}^{3/2}\right) \ln\left(220 T_{e0}/n_{e0}^{1/3}\right)$.

$\nu_{ed} = \nu_{ed0} \left(T_e/T_{e0}\right)^{-3/2} Z_d^2$ represent the electron-dust elastic collisions,[22] where

$\nu_{ed0} = \left(2.9\times10^{-6}\right) n_d T_{e0}^{-3/2} \ln\Lambda_e$ [$\ln\Lambda_e$ (coulomb logarithm) = 10-13].

$\nu_{en} = \sum_{n0} \nu_{en0} \left(n_0/n_{00}\right) \left(T_e/T_{e0}\right)^{1/2}$ is the electron-neutral elastic collisions,[18] where

$\sum_n \nu_{en0} = \nu_{eH} + \nu_{eHe} + \nu_{eO} = (4.5\times10^{-10} n_H T_e^{1/2} + 4.6\times10^{-10} n_{He} T_e^{1/2} + 2.8\times10^{-10} n_O T_e^{1/2})$

$\nu_{in} = \sum_{n0,i} \nu_{in0} \left(n_0/n_{00}\right) \left(T_i + T_d/T_{i0} + T_d\right)^{1/2}$ is the ion-neutral collision frequency, where

$\nu_{in0} = \beta_{in0} (T_{i0} + T_{00})^{1/2} n_{00}$ and β_{in0} is the charge-exchange coefficient for various ion-neutral interactions shown in charge-exchange mechanism. The data is based on the coefficient mentioned by Gurevich.[18]

$\nu_{re} (= \sum_i \alpha_i n_i)$,[24] where α_i is the coefficient of recombination of electrons and ions reactions shown in section 5.3.

$\nu_{ac} = n_d (n_{ec}/n_e)$ is the rate of adsorption of electrons on dust grain surface.

1. Fractional loss of energy in collisions

δ_{ei}, δ_{ej}, and δ_{ij} are the fractions of energy loss associated with collisions of electrons-ions, electrons-neutrals, and ions-neutrals, respectively. Here,

$\delta_{ei} = 2m_e / m_i$, $\delta_{ej} = 2m_e / m_j$, $and \delta_{ij} = 2m_i / m_j$,

where i and j stands for H^+, He^+, and O^+ ions and H, He, and O atoms, respectively and m_i and m_e represent the masses of ions and electrons, respectively.

2. Adsorption current of electrons and ions and their mean energy

The adsorption current for electrons and ions over dust grain surface according to orbital motion limited theory and their mean energy are expressed as

For Z <0,

$$n_{ec} = \pi r_d^2 (8k_B T_e / \pi m_e)^{1/2} n_e \exp[Z\alpha_e],$$

$$n_{ijc} = \sum_{ij} \pi r_d^2 (8k_B T_{ij} / \pi m_{ij})^{1/2} n_{ij} \left[1 - Z\alpha_{ij}\right],$$

and $\alpha_e = (e^2 / r_d k_B T_e)$, $\alpha_{ij} = \sum_{ij} (e^2 / r_d k_B T_{ij})$,

$\varepsilon_{ec} (= 2k_B T_e - Z(e^2 / r_d))$, and

$\varepsilon_{ic} (= (2 - Z\alpha_i) / (1 - Z\alpha_i) k_B T_i)$,

where r_d is the dust grain radius and

j stands for H^+, He^+, and O^+ ions.

3. Photoemission current and mean energy

The day time exosphere is continuously illuminated by X-rays and far UV radiations causing the photoemission from dust grain surface. The photoemission current based on Fowler's theory [25] is expressed by

$$n_{ph}(Z-1) = \pi r_d^2 \int_{\varepsilon_{\nu 00}}^{\varepsilon_{\nu m}} \chi(\varepsilon_\nu) dn_{inc}, \quad \text{for (Z < 0),}$$

where $\varepsilon_{\nu m}$ is maximum limit of spectrum of solar radiation, $\varepsilon_{\nu 00}$ is the threshold photon energy of incident radiations depending upon work function ϕ of dust component, $\chi(\varepsilon_\nu)$ is the photoelectric yield of dust component.

$$dn_{inc} = (a_s / a_d)^2 (4\pi\varepsilon_\nu^2 / c^2)(eh/300)^3 [\exp(\varepsilon_\nu / kT_s) - 1]^{-1} d\varepsilon_\nu,$$

where dn_{inc} is the rate of incident photons per unit area lying in frequency range ε_ν and $(\varepsilon_\nu + d\nu)$. a_s is the radius of radiating surface of sun given by a_s(=6.9x10^{10}cm) and a_d (=1.45x10^{13}cm) is the mean distance between sun and gas dust ensemble. For $Z \le 0$

$$\frac{\varepsilon_{ph}(Z-1)}{kT_d} = \left[\frac{\pi r_d^2}{n_{ph}} \int_{\varepsilon_{\nu 00}}^{\varepsilon_{\nu m}} \left(\frac{\chi(\varepsilon_\nu)}{\phi(\eta)} \int_0^x y^2 [1 + \exp(y - \eta)]^{-1} dy \right) dn_{inc} \right] + Z\alpha_d,$$

where $\eta = (h\nu - \phi)/kT_d$, $\alpha_d = (e^2 / akT_d)$ and for the analysis, Spitzer formulation [26] is considered for the photo-efficiency which may be represented by $\chi(\varepsilon_\nu) = (729\chi_m / 16)(\varepsilon_{\nu 00} / \varepsilon_\nu)^4 [1 - (\varepsilon_{\nu 00} / \varepsilon_\nu)]^2$, where χ_m is the maximal photo-efficiency. ε_ν is the solar radiation flux lying within the range 10eV to 124eV (for the wavelength range 122nm > λ >10nm) is assumed as the origin of electron photoemission from the dust grain surface.

B. *Computational Methodology*

For a numerical appreciation, mid-day time exospheric plasma at an altitude of 1000 km from the surface of earth has been processed into the computation; plasma components and their configuration, and other related parameters are selected from the book of Gurevich[18] and shown in Table I. The exospheric plasma is assumed to be composed of

electrons, ions and metallic dust grains. The simultaneous solution of Eqs. (5.1) to (5.6) gives the influence of dust grains on plasma components when an electromagnetic beam is propagating through it. Neutral ionization, electron-ion recombination, photoemission and collisions are considered here in. Using these mechanisms, the effect of dust $CeO_2$with work function 5.34 eV have been explored. The mean surface temperature (T_s) of the sun can be determined by equating solar radiations absorbed by the dust particles to the power loss via neutral cooling and thermal conduction. The following set of parameters on the basis of exospheric plasma environment has been used.

$$T_s = 5800\,K,\ T_d = 300\,K,\ r_d = 10nm,\ m_i = m_p = m_H = 1.67\times10^{-24}\,g,\ m_{o^+} = 16m_i$$

$$m_{He^+} = 4m_i$$

5.6 Results and Discussion

A theoretical model to analyse the influence of dust grains on nonlinear propagation of electromagnetic beam including the diffusion limited escape theory, kinetics of plasma constituents in mid-day time exospheric layer at an altitude of 1000km has been developed. Photo ionization, recombination of electrons-ions, and mechanism of charge exchange are the basic non-thermal escape mechanisms in exospheric layer between the dominant hydrogen and traces of helium, and oxygen. Also, the electronic and ionic current towards and photoemission from the dust grain surface have been taken into account. For photoemission from dust grains, solar radiation flux in the range 10 eV to 124 eV has been considered. To see the influence of dust grains on plasma parameters like dust charge, electron/ion density, electron/ion temperature with square of electric field vector, Eqs. (5.1) to (5.6) using MATHEMATICA and MATLAB software have been simultaneously solved numerically. Also the dependence of E_0^2 on propagation distance as a function of absorption co-efficient, dust density, plasma frequency and collision frequency corresponding to metallic dust particles CeO_2 with work function of 5.34 eV and n_d=10cm^{-3} at an altitude of 1000km. For computation, we have used dust cloud in upper atmosphere where photoemission is dominant condition corresponds to Lyman alpha radiations of wavelength of 121.5nm and 10.20 eV. Figs. 5.1 to 5.7 represent the numerical outputs for the

variation of exospheric dusty plasma parameters with the electric vector of the wave propagating through it. Fig. 5.1 shows that the dust charge Z increases with increasing amplitude E_0^2 of electric vector of electromagnetic wave passing through the exospheric environment. This is on account of increase in ohmic heating of electrons of dusty plasma on the passage of electromagnetic beam through it. As a result of which electronic adsorption current increases towards the dust grain surface and causes an increase in dust charge on its surface.

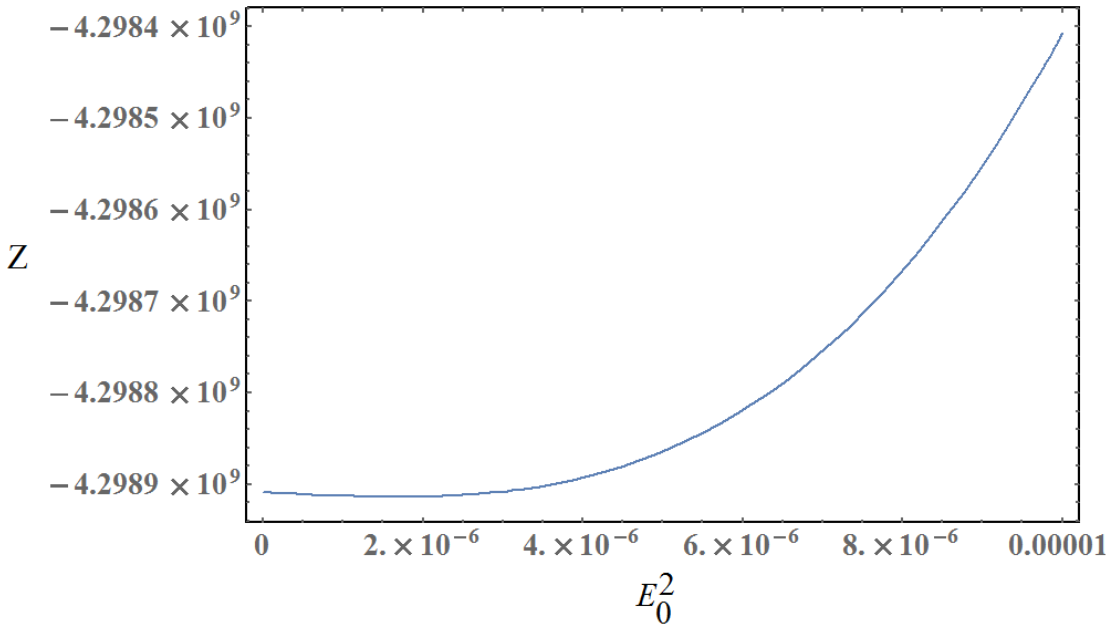

Fig. 5.1

Fig. 5.2 illustrates the enhanced rate of reduction in normalized electron density with E_0^2 in the presence of dust. This is on account of increase in recombination coefficient as well as electron adsorption current to the dust grain surface on passage of electromagnetic beam through dusty plasma whereas the behaviour of ion densities is a consequence of quasi neutrality as well as the charge neutrality condition as shown in figures 5.3, 5.4, and 5.5. It may be noted that the magnitude of hydrogen ion density increases sharply than the oxygen and helium ions which represent the abundance of hydrogen ions in exospheric dusty plasma.

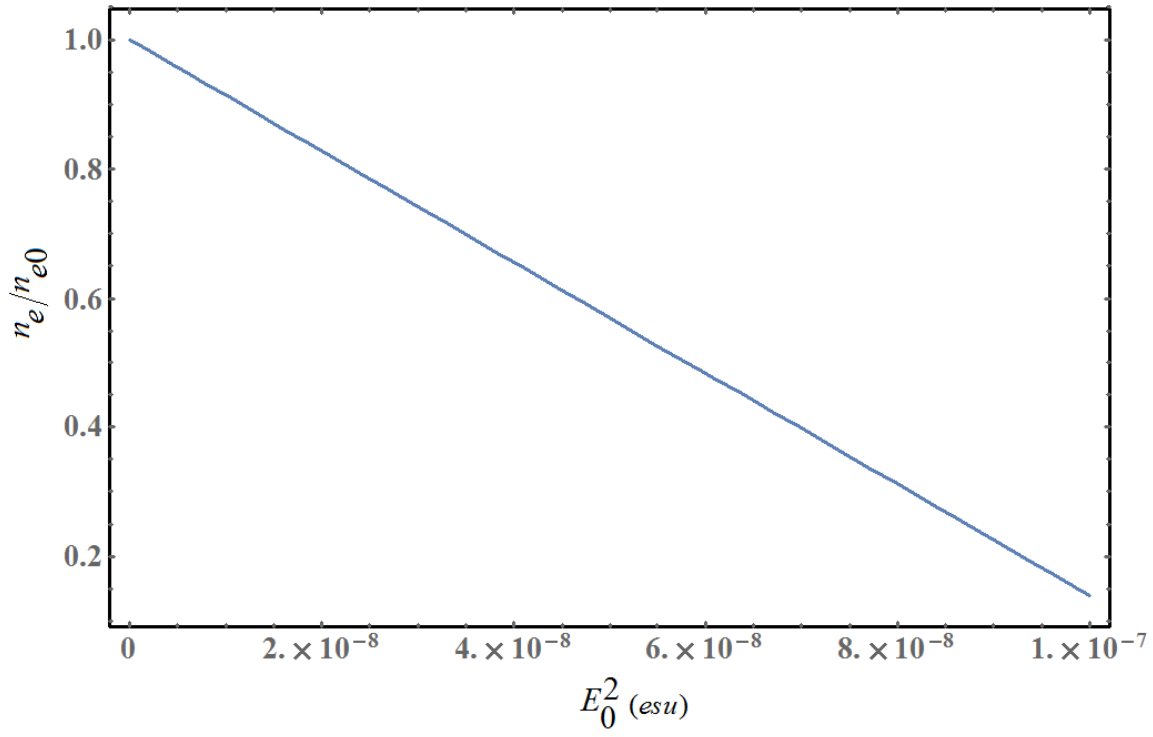
1.0
0.8
0.6
0.4
0.2
n_e/n_{e0}
0
$2.\times10^{-8}$
$4.\times10^{-8}$
$6.\times10^{-8}$
$8.\times10^{-8}$
$1.\times10^{-7}$
E_0^2 (esu)

Fig. 5.2

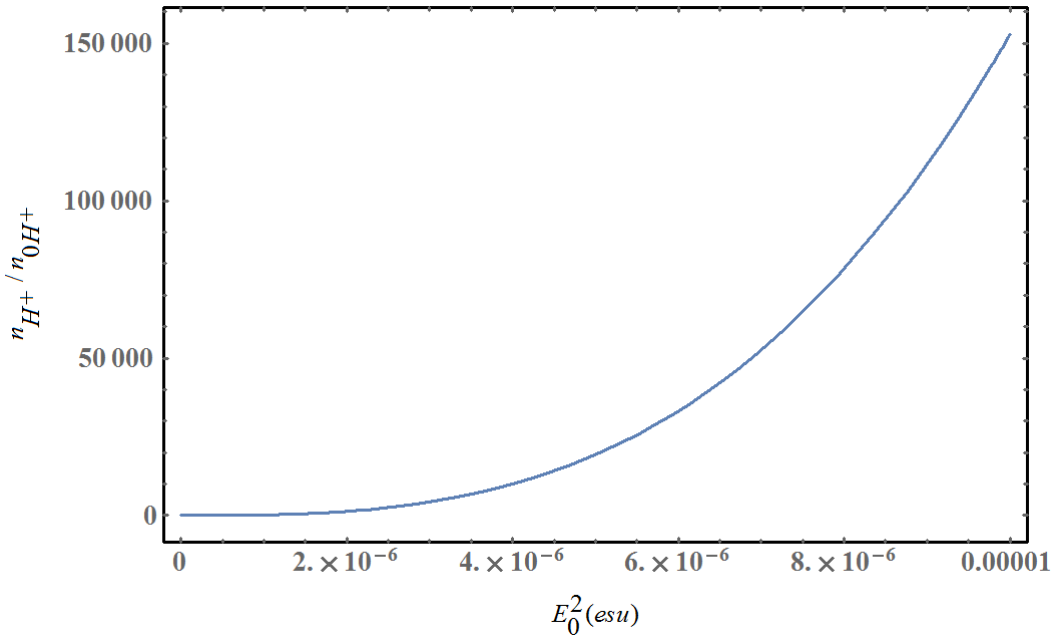
150 000
100 000
50 000
0
n_{H^+}/n_{0H^+}
0
$2.\times10^{-6}$
$4.\times10^{-6}$
$6.\times10^{-6}$
$8.\times10^{-6}$
0.00001
$E_0^2(esu)$

Fig. 5.3

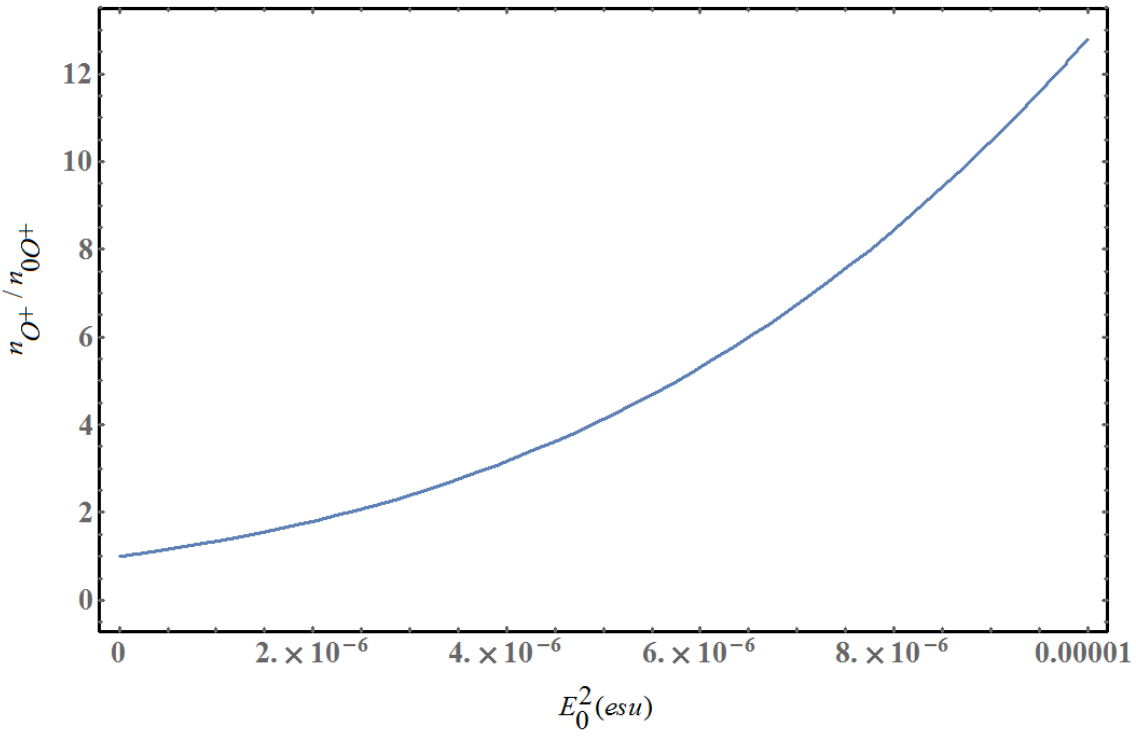
12
10
8
6
4
2
0
n_{O^+}/n_{0O^+}
0
$2.\times10^{-6}$
$4.\times10^{-6}$
$6.\times10^{-6}$
$8.\times10^{-6}$
0.00001
$E_0^2(esu)$

Fig. 5.4

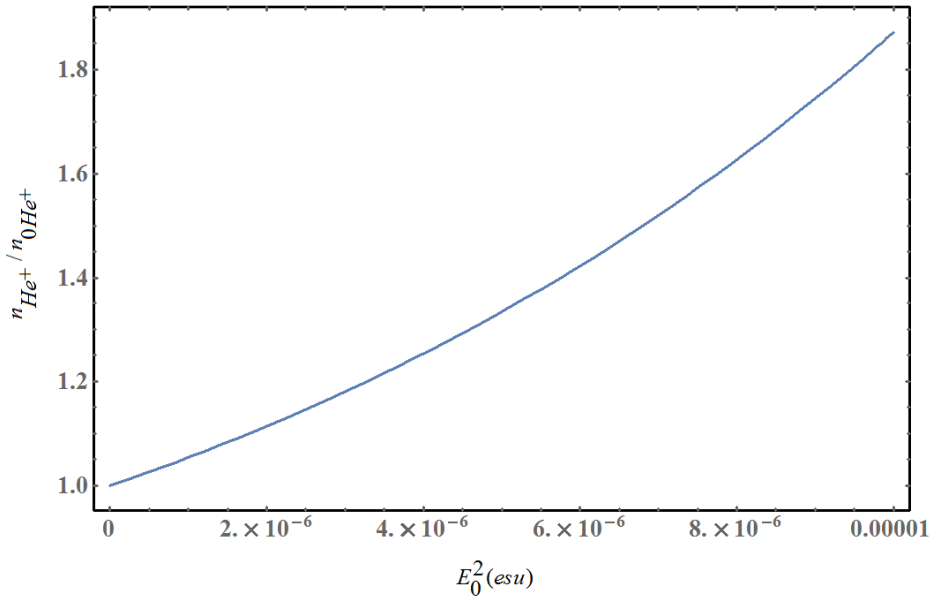
1.8
1.6
1.4
1.2
1.0
n_{He^+}/n_{0He^+}
0
$2.\times10^{-6}$
$4.\times10^{-6}$
$6.\times10^{-6}$
$8.\times10^{-6}$
0.00001
$E_0^2(esu)$

Fig. 5.5

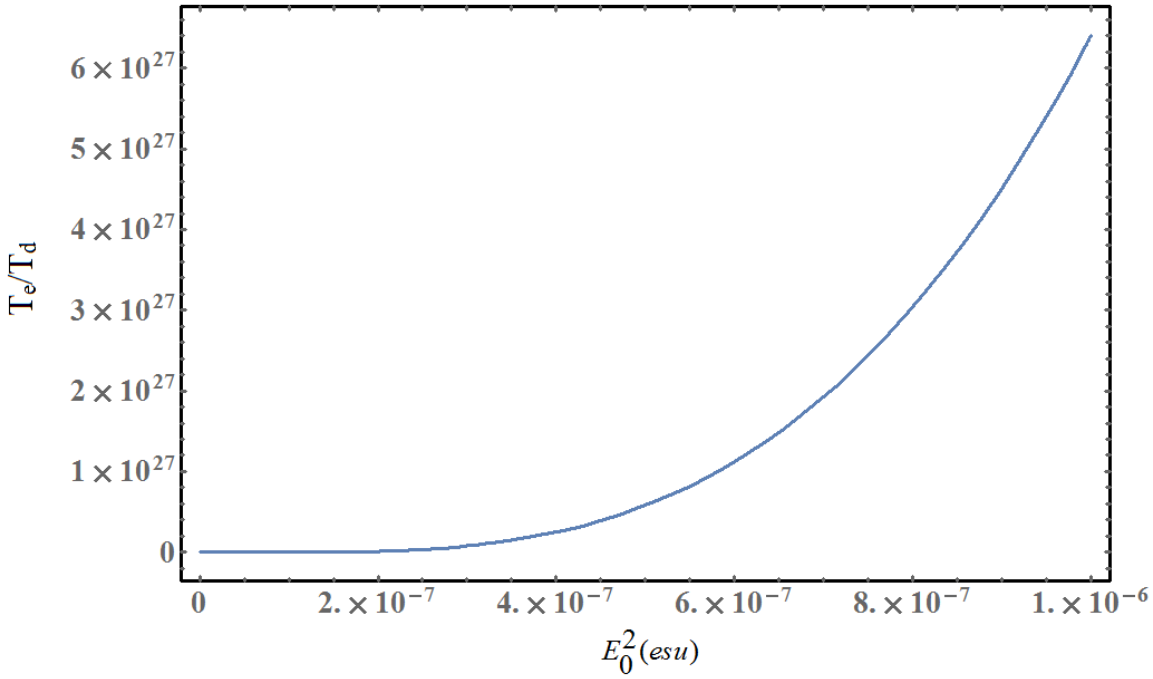
6×10^{27}
5×10^{27}
4×10^{27}
3×10^{27}
2×10^{27}
1×10^{27}
0
T_e/T_d
0
$2.\times10^{-7}$
$4.\times10^{-7}$
$6.\times10^{-7}$
$8.\times10^{-7}$
$1.\times10^{-6}$
$E_0^2(esu)$

Fig. 5.6

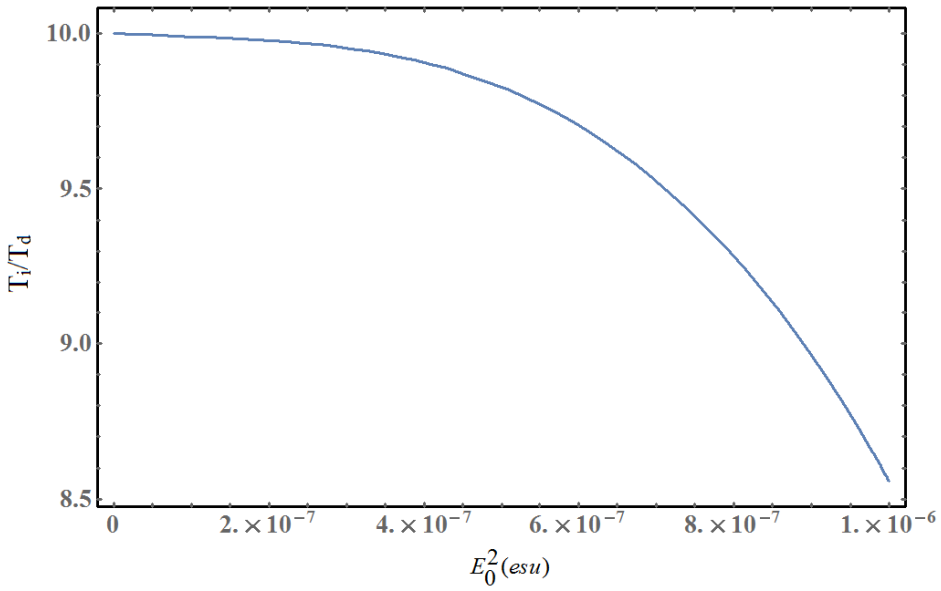
10.0
9.5
9.0
8.5
T_i/T_d
0
$2.\times10^{-7}$
$4.\times10^{-7}$
$6.\times10^{-7}$
$8.\times10^{-7}$
$1.\times10^{-6}$
$E_0^2(esu)$

Fig. 5.7

Figs. Dependence of (5.1) dust charge, (5.2) electron density, (5.3) hydrogen ion density,(5.4) oxygen ion density, (5.5) helium ion density, (5.6) electron temperature, and (5.7) ion temperature on E_0^2 *(in e.s.u.) at a height of 1000 km based on data mentioned in tables I and II.*

Fig.5.6 represents the electron temperature in the presence of dust increases more abruptly on passing the electromagnetic beam through it while the fig.5.7 represents a decrease in ionic temperature with E_0^2 in the presence of dust. This happens due to enhancement in effective collision frequency of electrons in the presence of dust on the account of increase in their ohmic heating on passing the electromagnetic beam through it while in case of ions; dissipation due to ohmic heating is lesser because of their heavier mass.

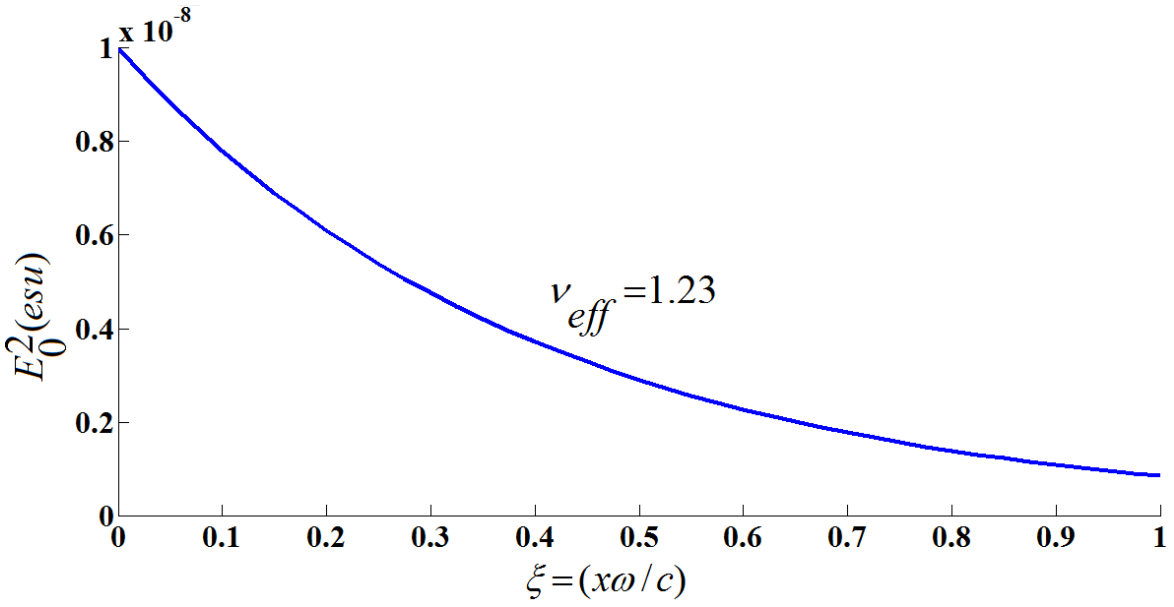

Fig. 5.8

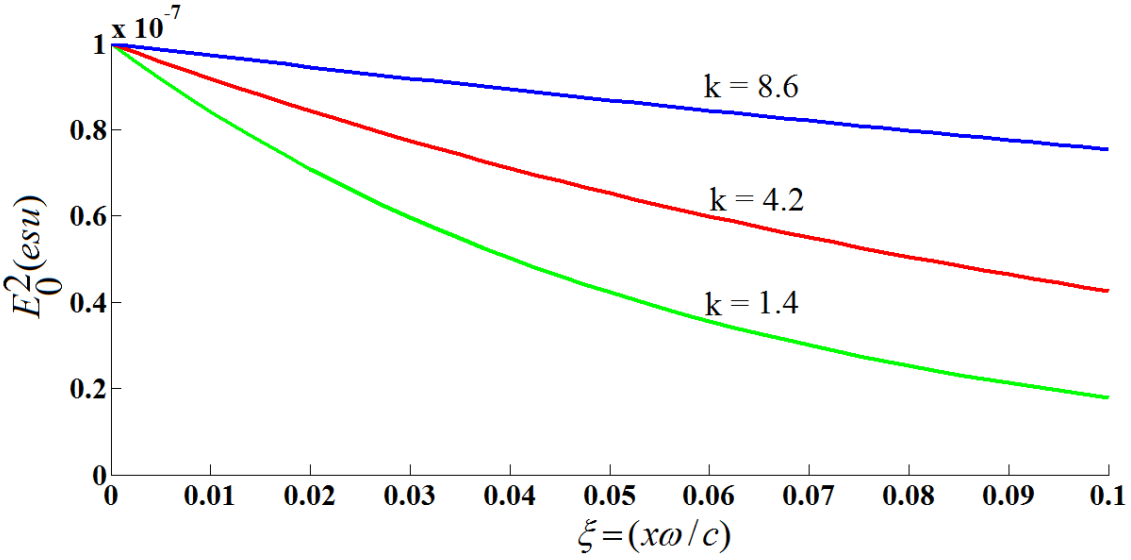

Fig. 5.9

Figures 5.8-5.11 indicate that the irradiance E_0^2 decreases asymptotically with the normalized propagation distance as a function of dusty plasma parameters like collision frequencies, absorption coefficients, dust densities, and plasma frequencies. This is due to the fact that the E_0^2 decreases to a value beyond which its behaviour is almost constant with exospheric dusty plasma parameters. Fig. 5.8 indicates that the irradiance decreases as a function of collision frequency with the propagation of beam in the presence of dust. Since in exospheric dusty plasma the magnitude of collision frequency is almost constant therefore a monotonic variation is obtained. The reduction in irradiance is obtained due to increase in ohmic loss with the collision frequency as evidenced by fig. 5.8. Fig. 5.9 shows the decrease in irradiance with the progress of wave in the presence of dust .The decay is faster with the increased value of absorption coefficients. This is attributed by decrease in electron density with the irradiance as evidenced by fig.5.2 and is a consequence of Eq. 5.9. Hence, wave gets less absorbed with lower value of absorption coefficient.

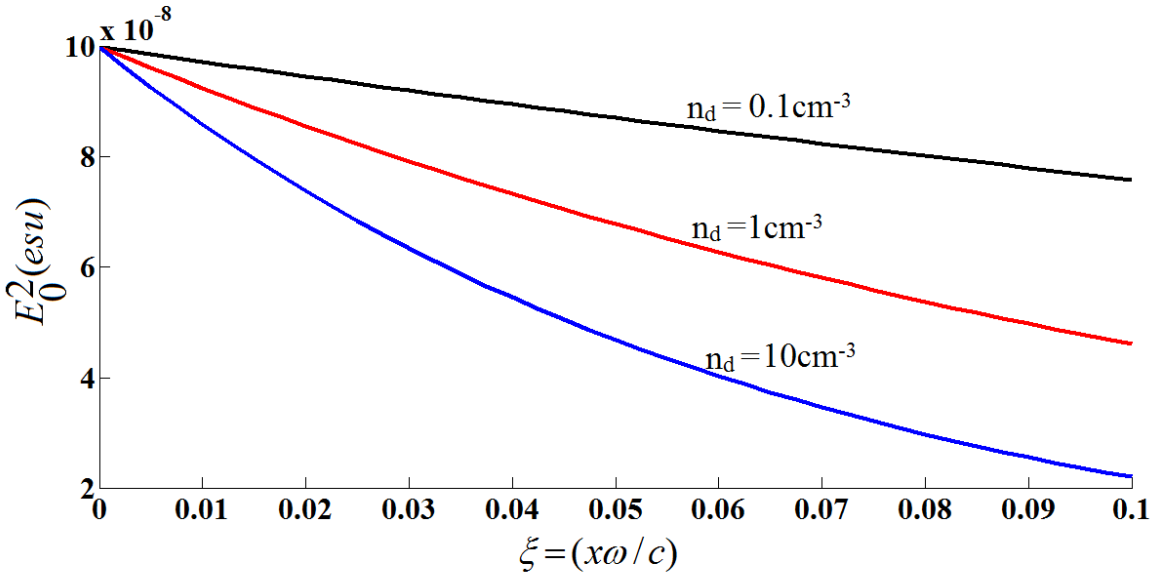

Fig. 5.10

The fig. 5.10 represents the decay in E_0^2 with the propagation of wave as a function of dust density. It is observed from the figure that the wave gets less absorbed with higher value of dust density. This is on account of the fact that the electron density decreases with the increase in dust density as well as with progress of wave as shown by fig. 5.2 and as a result of decrease in electron density absorbtion coefficient also decreases as a consequence of Eq. 5.9.

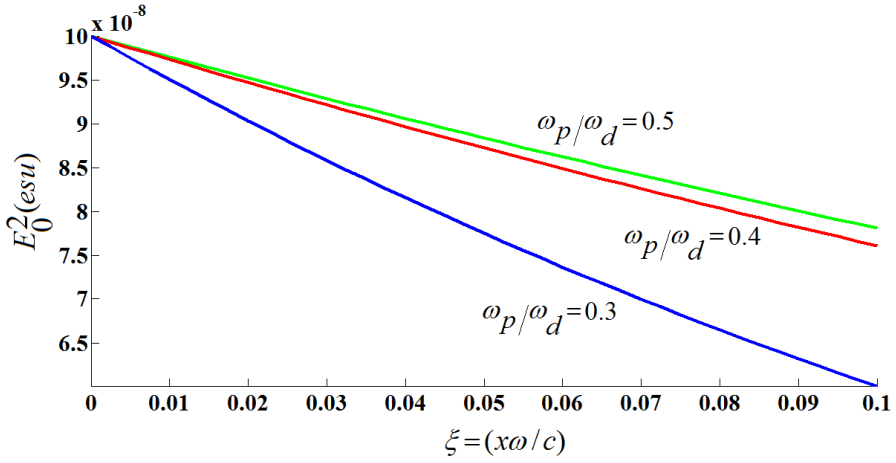

Fig. 5.11

Figs. Dependence of E_0^2 *(in e.s.u.) on the normalized propagation distance* $\xi = (x\omega / c)$ *as a function of (5.8) collision frequency, (5.9) absorption coefficient, (5.10) dust density, (5.11) plasma frequency at an exospheric altitude of 1000 km.*

From Fig. 5.11, it is seen that the E_0^2 decays faster with the progress of wave as a function of plasma frequencies in the presence of dust. It is seen that the wave get less absorbed for lower value of ω_p / ω_d .

5.7 Conclusions

Although, previously the upper atmosphere is considered as collisionless but in the present study, we have obtained a model to see the effect of dust grains on nonlinear propagation of electromagnetic wave considering the ohmic non-linearity with collisions in exospheric plasma at an altitude of 1000 km. In this model, we have included the diffusion limited escape theory, basic escape mechanisms, and kinetics of dusty plasma constituents. It is observed that the dielectric constant, consequently refractive index and absorption coefficients can be easily modified by introducing dust grains of appropriate work function in exospheric plasma environment. Considering the non-thermal escape processes, the variation of plasma parameters in the presence of dust grains with square of electric vector have been analysed for mid-day time for an exospheric height of 1000 km. Also, the effect of dust grains have been analysed numerically on the nonlinear progress of wave for different dusty plasma parameters like effective collision frequency, absorption coefficient, dust density, and plasma frequency in exospheric environment. Such modification in plasma parameters by considering collisions between different plasma constituents in the presence of dust in upper atmosphere provides the ease of propagation of signals in exospheric layer and facilitates the satellite communication. This theory is also helpful in solving the problems in atmosphere of rocky planets like Mars and Venus etc.

REFERENCES

[1] Ruchi Sharma and S. C. Sharma, Contrib. Plasma Phys.**59**, 211(2019).

[2] A. Gahlot, R. Walia, S. C. Sharma, and R. P. Sharma, J. Plasma Phys. **78**, 33(2012).

[3] M.S.Sodha, S. Misra, and S. K. Mishra, Phys Plasmas **16**, 123705 (2009).

[4] M.S.Sodha and S.K.Agarwal, Phys Plasmas **25**, 052903 (2018).

[5] J. Goree, Plasma Sources Sci. Technol. **03**, 400 (1994).

[6] I. Denysenko, J. Berndt, E. Kovacevic, I. Stefanovic, V. Selenin, and J. Winter, Phys. Plasmas **13**, 073507(2006).

[7] R. L. Merlino, A. Barkan, C. Thompson, and N. D'Angelo, Phys. Plasmas **5**, 1607(1998).

[8] R. L. Merlino, "Dusty plasmas and applications in space and industry," Transworld Research Network 37/661(2), Fort P.O., Trivendrum 695023, Kerala, India, 2006.

[9] M. S. Sodha, *Kinetics of Complex Plasmas* (Springer, India, 2014).

[10] G. Sambandan, V. K. Tripathi, J. Parashar, and R. Bharuthram, Phys.Plasmas **6**, 762(1999).

[11] S. C. Sharma, A. Gahlot, and R. P. Sharma, Phys. Plasmas **15**, 043701 (2008).

[12] S.C.Liu and T.M.Donahue, J. Atmos Sci.**31**, 1466(1974).

[13] Guido Visconti, J. Atmos. Sci. **34**, 193(1977).

[14] Bernie D. Shizgal and Gregory G. Arkos, Reviews of Geophysics **34**, 483(1996).

[15] David C. Catling and James F. Kasting, *"Escape of Atmospheres to space,"*(Cambridge University Press, (2017)).

[16] M.S.Sodha and S.K.Mishra, Phys Plasmas **24**, 043705 (2017).

[17] M.S.Sodha and R.K.Verma, Phys Plasmas **25**, 022302 (2018).

[18] A.V.Gurevich, *Nonlinear process in the ionosphere*, (Springer Verlag, New York, 1978).

[19] Manfred A. Biond, Canadian Journal of Chemistry **47**, 1711 (1969).

[20] S. J. Bauer, "Hydrogen and Helium ions", Goddard Space Flight Center, Greenbelt, Maryland (1965).

[21] S. Misra and S. K. Mishra, Phys. Plasmas **22**, 023706(2015).

[22] M.S.Sodha, S.K.Mishra, and Shikha Misra, Phys.Plasmas **18**, 023701(2011).

[23] M.S.Sodha, S.K.Mishra, and S. K. Agarwal, IEEE Trans. Plasma Sci. **37**, 375(2009).

[24] S. K. Mishra, and S.Misra, Phys. Plasmas **26**, 023702 (2019).

[25] R.H.Fowler, "*Statistical Mechanics*: *The Theory of Properties of Matter in Equilibrium" (*Cambridge University Press, London, 1955).

[26] L.Spitzer, Astrophys. J. **107**, 06(1948).

Chapter 6

THRESHOLD POWER OF AMLITUDE MODULATED LASER BEAM IN COMPLEX PLASMA

6.1 Brief outline of the chapter

A theoretical investigation describing the effect of dust on the threshold power of the amplitude modulated laser beam propagating in complex plasma has been done. In this analysis, momentum and energy balance equations have been solved simultaneously to govern the relation between the beam width parameter and normalizes length of progression of amplitude modified beam advancing in complex plasma. The dependence of beam width parameter on the progression length has been evaluated for different values of dust grain size and dust charge state. Moreover, the dependence of critical power of self-focusing on dust grain size and dust charge state has also been investigated. It is found that the critical power augments with the increase in dust grain size as well as with the increase of the dust charge state.

6.2 Introduction

Numerous articles have been come out with the self-trapping of an electromagnetic wave in complex plasma (consist of electrons, ions and positively or negatively charged dust grains) being supported by several reviews.[1,2] Sometime, these small charged dust grains are responsible for reducing the attainment of industrial devices.[3,4] whereas some mechanization preferred their presence.[5] In addition, the presence of dust grains strongly influence the discharge properties of plasma.[6-8] Dust grains become charged on account of accumulation of electrons on its surface, secondary electron emission, photoemission etc. and cause the variation in electron temperature and electron density. Generally, electron concentration decreases with increase in size of dust grain which leads to variation in critical power of self-focusing. For regulating the complex plasma properties, understanding of networking between complex plasma domains and dust grain parameters is essential. In this chapter, we describe the nonlinear self-focusing of beam in dusty plasma due to interaction between electrons and the dust grains by considering the nonlinear heating of electrons.

In general, curves have drawn to show the dependence of beam width parameter on the normalized length of progression for the distinct parameters of amplitude modified beam advancing in complex plasma and to analyse the change in critical power of self-focusing with the formation and charging of the dust grain.

6.3 Dynamics of complex plasma

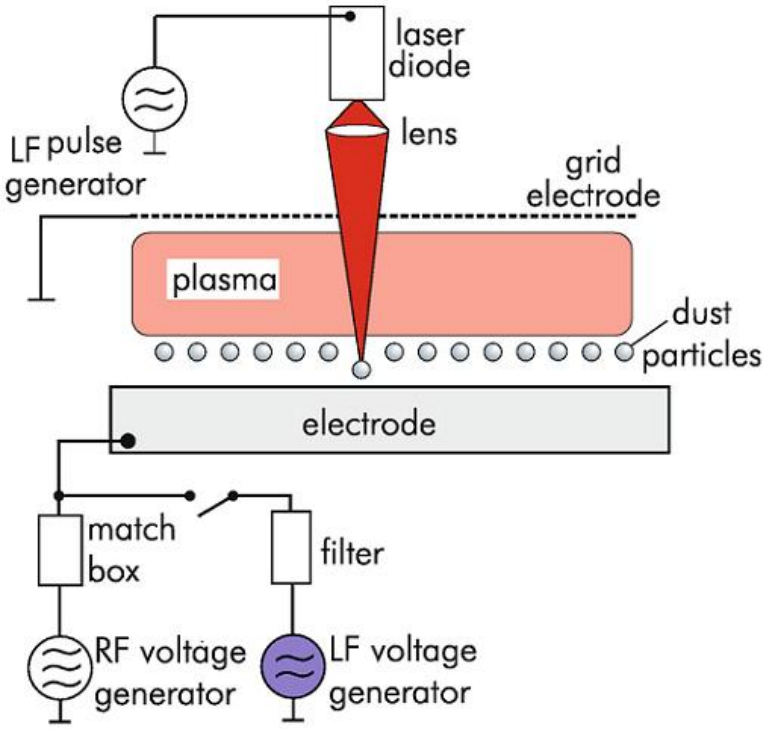

FIG.6.1 Schematic diagram of processing of dust particles in plasma [9]

Let n_{0i}, n_{0e}, and n_{0d} are the density of complex plasma constituents i.e., ions, electrons and negatively charged dust grains, respectively. In equilibrium, $Z_{0d}en_{0d}+en_{0e} = Z_{0i}en_{0i}$, where –e is charge on electron, $-Z_{0d}e$ is the charge on dust and $Z_{0i}e$ is the charge on ion. Let us assume a high power amplitude modified electromagnetic beam travelling along z-direction in a complex plasma with the electric vector given by

$$\vec{E}=A_0(r,z)(1+\mu_0\cos\omega t)\exp[-i(\omega_0 t-kz)], \tag{6.1}$$

where

$$A_0^2=A_{00}^2(1+\mu_0\cos\omega t)^2 e^{-r^2/r_0^2}, \tag{6.2}$$

k is the propagation constant, ω is modulation frequency, $\mu_0$is modulation index, A_{00} is amplitude of electric vector, r_0 is the initial width of the beam .

For z >0,

$$A_0^2=\frac{A_{00}^2}{f^2}(1+\mu_0\cos\omega t)^2 e^{-r^2/r_0^2f^2}, \tag{6.3}$$

where *f* represents the beam width parameter, r_0 is the beam spot size. The momentum and energy balance of the equation is given by

$$m_e\frac{d\vec{v_e}}{dt}+m_e\nu\vec{v_e}=-e\vec{E}, \tag{6.4}$$

and $$\frac{3}{2}K_b\frac{dT_e}{dt}+\frac{3}{2}K_b\delta_{dusty}\nu(T_e-T_0)=-\frac{1}{2}e\vec{E}.\vec{v}, \tag{6.5}$$

where m_e, T_e, and v_e are the mass, temperature and velocity of electrons, respectively. K_b is the Boltzmann's constant. δ_{dusty} is a part of energy transfer via charging collision of electrons with dust, elastic collisions of electron with dust and ions, represented as $\delta_{dusty}(=\nu_{chg}/\nu_{chg}+\nu_{ei}+\nu_{ed})$ and $\nu(=\nu_{chg}+\nu_{ei}+\nu_{ed})$ is the effective collision frequency, where $\nu_{chg},\nu_{ei},\nu_{ed}$ are the charging, electrons-ions and electrons-dust grains collision frequencies, respectively. The Eqs. (6.1) - (6.5) solved simultaneously to obtain dielectric constant in the existence of dust particles which is substituted in wave equation for electric field vector of propagating electromagnetic beam to obtain an equation to see the change in beam width parameter with the normalized length of progression, expressed as

$$\frac{d^2f}{d\xi^2}=-\frac{1}{R_n^2}\frac{1}{f^3}(1+\mu_0\cos\omega t)^2+\frac{1}{R_d^2f^3}, \tag{6.6}$$

where $R_d=\frac{\omega_0}{c}\varepsilon_0^{1/2}r_0^2$, $R_n^2\left(=r_0^2\varepsilon_0/\varepsilon_2A_{00}^2\right)$,$R_n$ is the typical length of self-focusing and $\varepsilon_2=\left(\omega_p^2/\omega_0^2\right)\left(e^2/6m_e\delta_{dusty}T_0\omega_0^2\right)$ is an effective dielectric constant in complex plasma. In

the right-hand side, the first part of Eq. (6.6) represents the nonlinear self-focusing term while the second diffraction divergence of the beam.

6.4 Critical power of self-focusing

From Eq. (6.6), the critical power of self-focusing (for which $d^2f/d\xi^2 = 0$, f = 1, for every values of ξ) can be written as $P_{cr} = \varepsilon_0^{1/2} c^3 / 8\omega_0^2 \varepsilon_2$.

6.5 Results and discussion

Fig. 6.2 and Fig. 6.3 represent the deviation of beam width parameter with the normalized length of progression, $\xi = (z/R_d)$ for different parameters of dust grain size and dust charge number and Fig.6.3 and Fig. 6.4 represent the rate of change of critical power of self-focusing with thedust grain size and dust charge number in the following domain: $\omega_p / \omega_0 = 31.167$, $\delta_{dusty} = 2.03 \times 10^{-4}$, $T_0 = 6.4$ eV, Z_d (dust charge state) = $- 2 \times 10^4$and a_d (dust grain size) = 10^{-4}cm, $A_{00} = 10^5$ stat volt cm^{-1}, $\varepsilon_0 = 0.97$,$\varepsilon_2 = 0.8\times10^{-10}$,e =4.8×10^{-10}esu. With these parameters, critical power comes out to be 0.947×10^{18}ergs/s.

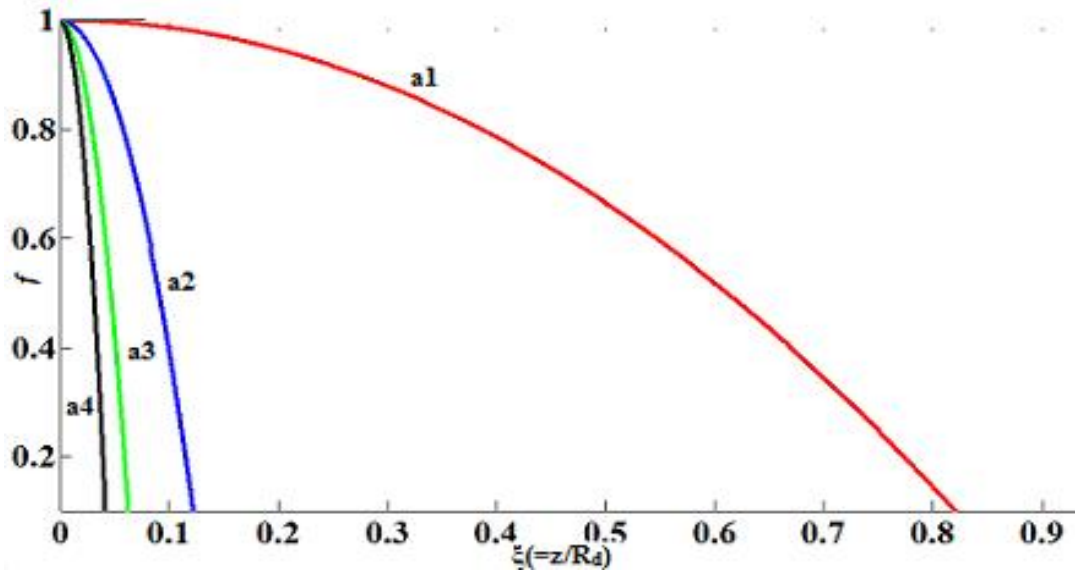

Fig. 6.2: Dependence of f on ξ, for different values of dust grain size labelled as a1, a2, a3 and a4 corresponds to r_d = 1μm, 5μm, 10μm and15μm, respectively.

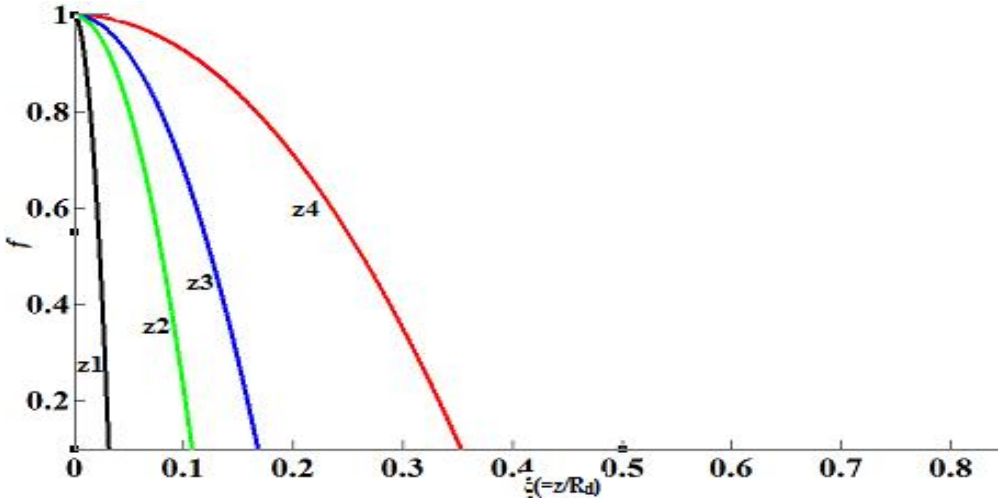

Fig. 6.3 Dependence of f on ξ, for different values of dust charge number labelled as z1, z2, z3 and z4 corresponds Z_d = -8×10^3, -6×10^3, -4×10^3, -2×10^3, *respectively.*

Fig.6.2 and Fig.6.3 show that the self- focusing of the amplitude modulated beam increases with the increases in dust grain size because of dominating self-focusing term whereas decreases with the enhanced dust charge number due to strengthening in diffraction divergence term.

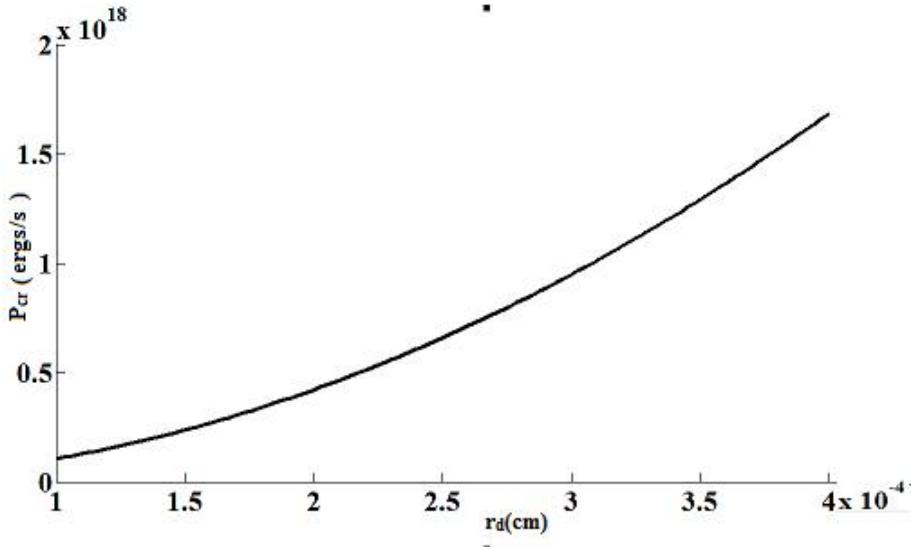

Fig.6.4 Variation of critical power P_{cr}*(in ergs/s)with dust grain radius* r_d.

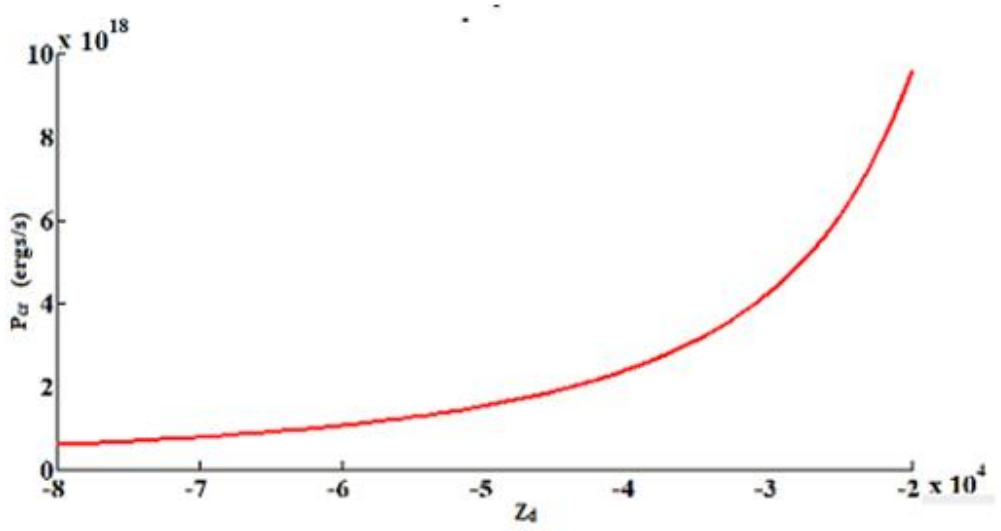

Fig.6.5 Variation of critical power P_{cr}(in ergs/s)with dust charge state Z_d.

Fig. 6.4 and Fig. 6.5 show that the critical power of self-focusing augmented with the increase in dust grain size as well as with the increase of the dust charge state. This is because with the increase of dust grain size and dust charge state, more and more accumulation of electrons takes place on its surface which results in decrease of electron density and increase of critical power of self-focusing.

REFRENCES

[1] A. Gahlot, RituWalia, Suresh C. Sharma, and R. P. Sharma, J. Plasma Physics **78**, 33(2012).

[2] M.S. Sodha, S. K. Mishra, and ShikhaMisra, Phys. Plasmas **16**,123701 (2009).

[3] F. Verheest and P. Meuris, Phys. Lett. A **210**, 198 (1996).

[4] G. S. Selwyn, Jpn. J. Appl. Phys., Part 1 **32**, 3068 (1993).

[5] E.Stoffels, W.W.Stoffels, D. vender, G.M.W.Kroesen, and F.J de Hoog, IEEE transaction on Plasma Science **22**, 2(1994).

[6] I. Denysenko, J. Berndt, E. Kovacevic, I.Stefanovic,V.Selenin, and J.Winter, Phys. Plasmas**13**, 074507(2006).

[7] I.Stefanovic, E. Kovacevic, J.Berndt, and J.Winter, New J. Phys. **5**, 39.1(2003).

[8] G. Sambandan, V. K. Tripathi, J. Parashar, and R. Bharuthram, Phys. Plasmas **6**, 762(1999).

[9] A.Melzer, *Physics of dusty plasmas*, 31-57(2019).

Chapter 7

THEORETICAL MODEL FOR SELF-TRAPPING OF GAUSSIAN ELECTROMAGNETIC BEAM IN DUSTY PLASMA

7.1 Brief outline of the chapter

A theoretical model for self-trapping of Gaussian electromagnetic beam has been developed in dusty plasma. This model comprises of balancing of charge, number density, and energy exchange between plasma components having charge neutrality. Ionization of neutrals, recombination, emission and sticking of electrons to the dust particles, and the collisions between the constituents are considered herein. For numerical appreciation, curves have been drawn for variation of electron density with time and beam waist parameter with the different values of dust densities and dust grain sizes. It is observed that the electron density decay with time due to their larger stickiness to the surface of dust grains with its embryonic growth. Self-trapping of the beam increases with increasing dust grain size but reverse in the case of number density. This is because of increase in non-linearity on account of predominant self-trapping term with the increasing dust grain size and decreasing number density. This formulation is helpful for explaining the results of dusty plasma in space and laboratories.

7.2 Introduction

Several investigations [1-7] on nonlinear propagation of Gaussian electromagnetic beam in dusty plasma have been published in last decades due to its numerous applications in space and industry [8-9]. In this chapter, nonlinear heating of electrons takes place because of non-uniform irradiance of electromagnetic beam in dusty plasma. This causes more and more electrons sticking to the surface of dust grains and generates a depleted density channel which leads to self-trapping of electromagnetic beam in dusty plasma. Ionization of neutrals, recombination, stickiness and electron emission by the dust grains, and the collisions between the constituents are considered in the present model. A wave equation has been evaluated using the perturbed density of electrons and modified permittivity to study the behaviour of Gaussian electromagnetic beam in dusty plasma due to nonlinear ohmic heating of electrons and curves have been drawn between beam waist parameter and dimensionless length of propagation for distinct values of number density and sizes of dust grains. The remaining chapter is framed as follows: Sec.7.3 is designed by the balancing equations of the charge, number density and energy exchange between dusty plasma components to give the dielectric constant of the plasma in the existence of dust grains and solving the wave equation to show the variation of beam waist parameter '*f*' with the dimensionless propagation length ζ on account of propagation of electromagnetic beam in dusty plasma and Sec. 7.6 is structured by results of the present analysis. Sec. 7.7 concludes the summary of our paper.

7.3 Theoretical Model

Assume a dusty plasma, formed by electrons, ions, neutrals and dust grains having charge Ze (where Z is the charge state of dust and e is the charge on an electron); is non-linearly irradiated by Gaussian electromagnetic beam.

Balancing Equations

Neutral atoms and ions conservations

$$n_i + n_0 = n_{i0} + n_{00}\,, \tag{7.1}$$

where n_i, n_0 and n_{i0}, n_{00} are the ions and neutrals number densities in the presence and absence of dust grains, respectively.

Charge neutrality

$$Zn_d + n_i - n_e = 0, \tag{7.2}$$

where n_d and n_e are the dust and electrons number densities.

Charge balance of dust grains

$$\frac{dZ}{d\tau} = n_{ic} + n_{ph} - n_{ec}, \tag{7.3}$$

where $n_{ic} = \pi r_d^2 (8k_B T_i/\pi m_i)^{1/2} n_i [1 - Z\alpha_i]$ is the sticky current of ions to the dust grain surface, $n_{ph} = \pi r_d^2 n_p$ is the photocurrent emitting from surface of negatively charged dust grains, and $n_{ec} = \pi r_d^2 (8k_B T_e/\pi m_e)^{1/2} n_e \exp[Z\alpha_e]$ is the sticky current of electrons to the dust grain surface, $\alpha_i = (e^2/r_d k_B T_i)$, $\alpha_e = (e^2/r_d k_B T_e)$, r_d is radius of dust grain, k_B is Boltzmann's constant, T_i and T_e are the ions and electrons temperature, m_i and m_e are the masses of ions and electrons, respectively. n_p represents the degree of photoelectric emission per unit time per unit area from a negatively charged or neutral surface of dust grain.

Number density balance of electrons and ions

$$\frac{dn_e}{d\tau} = \beta_i n_0 - \alpha_r n_e n_i - n_d (n_{ec} - n_{ph}) \tag{7.4}$$

and

$$\frac{dn_i}{d\tau} = \beta_i n_0 - \alpha_r n_e n_i - n_d n_{ic}, \tag{7.5}$$

where β_i indicates the co-efficient of ionization, $\alpha_r=(\alpha_{r0}(300/T_e)^k)$ cm^3/s represent the recombination coefficient, k and α_{r0} are the constants. The initial terms on RHS of (7.4) and (7.5) correlate with the rate of increase of densities due to ionization of neutral atoms. The succeeding two terms in both the equations refer to the rate of density decay due to their recombination, and net sticking to the surface of dust grains.

Energy balance of electrons and ions

$$\frac{d}{d\tau}\left(\frac{3}{2}n_e k_B T_e\right)=\beta_i n_0\varepsilon_e-\alpha_r n_e n_i\left(\frac{3}{2}k_B T_e\right)-n_d(n_{ec}\varepsilon_{ec}-n_{ph}\varepsilon_{ph})+\frac{n_e e^2\nu_{eff}U_0^2}{4m_e(\omega_d^2+\nu_{eff}^2)}$$
$$-\nu_{em}\delta_{em}\frac{3}{2}n_e k_B(T_e-T_0)+\nu_{ei}\delta_{ei}\frac{3}{2}n_e k_B(T_e-T_i) \qquad (7.6)$$

And

$$\frac{d}{d\tau}\left(\frac{3}{2}n_i k_B T_i\right)=\beta_i n_0\varepsilon_i-\alpha_r n_e n_i\left(\frac{3}{2}k_B T_i\right)-n_d n_{ic}\varepsilon_{ic}$$
$$-\nu_{im}\delta_{im}\frac{3}{2}n_i k_B(T_i-T_0)+\nu_{ei}\delta_{ei}\frac{3}{2}n_e k_B(T_e-T_i), \qquad (7.7)$$

where ε_e and ε_i are related to electrons and ions average energy because of ionization of neutral atom, ε_{ec} and ε_{ic} represent the mean value of sticking energy of electrons and ions to the surface of dust grains. ε_{ph} is the energy corresponding to photoemission, δ is the fractional energy loss, and $\nu_{eff}\,(=\nu_{ei}+\nu_{ed}+\nu_{em}+\nu_{sc})$ is the effective collision frequency as a result of collisions of electron with ions, dust, neutrals, and sticking collisions, and T_d is the temperature of dust assumed to be constant due to efficient thermal efficiency.

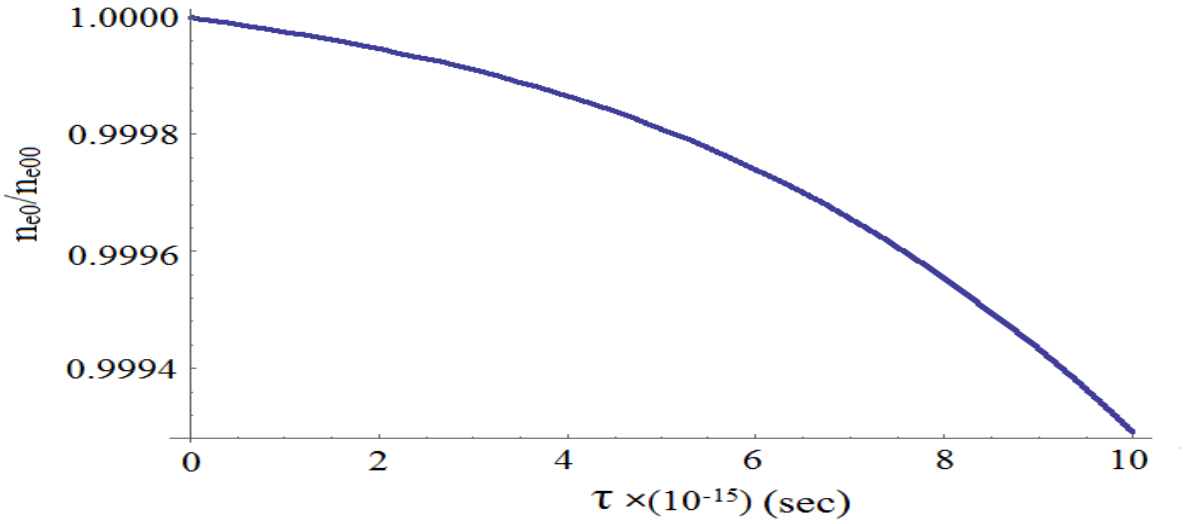

Fig. 7.1 Dependence of dimensionless electron density (n_{e0}/n_{e00}) on the parameter τ (sec).

By estimating ionization coefficient and mean energy of electrons and ions through imposing the initial conditions of dust free plasma, Eqs. (7.1)-(7.7) can be concurrently solved for $\tau \to \infty$ in stationary state and the variables n_e, T_e, n_i, T_i, and Z got evaluated numerically. The variation of normalized electron density with time is shown in Fig.7.1.

7.4 Modified Dielectric Permittivity

Using these parameters and paraxial approximations, modified dielectric permittivity is given by

$$\varepsilon_0 = 1-\left(\frac{\omega_0^2}{\omega_d^2}\right)\left(1-\frac{\nu_{eff0}^2}{\omega_d^2}\right)\left(\frac{n_{e0}}{n_{e2}}\right) \text{ and } \varepsilon_2 = \left(\frac{\omega_0^2}{\omega_d^2}\right)\left[\left(1-\frac{\nu_{eff0}^2}{\omega_d^2}\right)\left(\frac{n_{e2}}{n_{e00}}\right)-\left(\frac{n_{e0}}{n_{e00}}\right)\left(\frac{2\nu_{eff0}\nu_{eff2}}{\omega_d^2}\right)\right], \quad (7.8)$$

where ε_0 and ε_2 are the modified dielectric permittivity, ν_{eff0} and ν_{eff2} are the effective collision frequencies, n_{e0} and n_{e2} are the number densities in the presence of dust grains along axis and radius , respectively. n_{e00} is the electron density in the absence of pulse and dust, and ω_0 and ω_d refer to the electron plasma frequencies with and without dust grain Eqs. (7.1) - (7.7)

are accompanied by unison solution to use n_{e0}, n_{e2} ν_{eff0}, ν_{eff2} in (7.8), and to get ε_0 and ε_2, in term $\beta_0 U_{00}^2$.

7.5 Propagation of Gaussian Electromagnetic Beam in Dusty Plasma

Assume a y-axial uniformly polarized Gaussian electromagnetic beam propagating in dusty plasma along the z-axis; the cylindrical coordinate of its electric field vector U is defined as

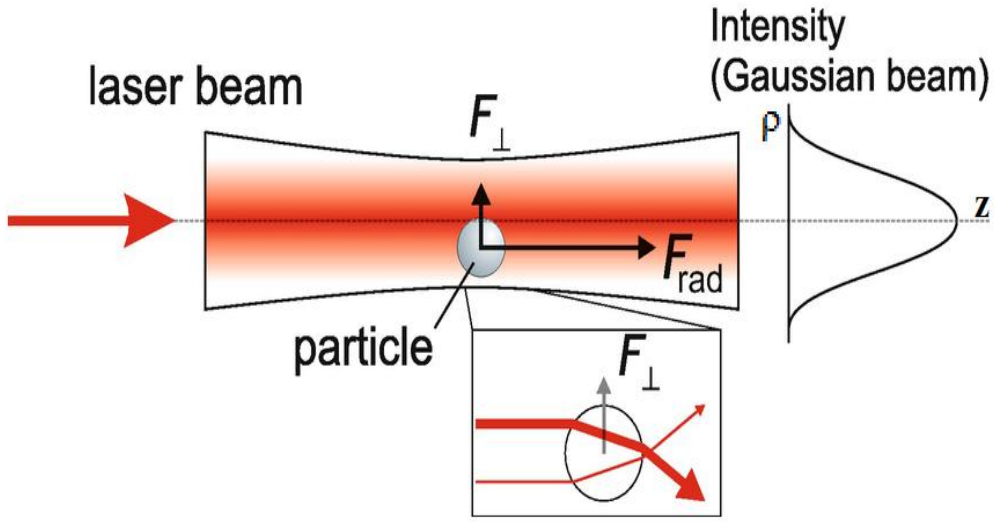

Fig.7.2 Schematic diagram of propagation of cylinderical Gaussian electromagnetic beam

$$U(z)=\hat{j}\, U_0(\rho,z)e^{i\omega_d t}, \tag{7.9}$$

where $(U_0)_{z=0} = U_{00}e^{\left(-\rho^2/\rho_0^2\right)}$, and $\hat{j}$ is the y-axial unit vector.

Concerned wave equations for the transverse and cylindrically symmetrical beam is given by

$$\frac{\partial^2 \overrightarrow{U_0}}{\partial z^2}+\frac{1}{\rho}\frac{\partial \overrightarrow{U_0}}{\partial \rho}+\frac{\partial^2 \overrightarrow{U_0}}{\partial \rho^2}=\frac{\omega_d^2 \varepsilon_{eff}(\rho,z)}{c^2}\vec{U}_0. \tag{7.10}$$

Following Akhmanov*et al.*[10] and Sodha *et al*. [11] solution of (7.10)can be represented as

$$U_0(\rho,z)=A_0(\rho,z)e^{-ikz}, \tag{7.11}$$

$$A_0(\rho,z)=A_{00}(\rho,z)e^{-iks(\rho,z)}, \tag{7.12}$$

where $k=(\omega_d/c)\varepsilon_0^{1/2}$. A_{00} and s are real. By employing Ansatz for Gaussian beam $A_{00}^2=\frac{U_{00}^2}{f^2}e^{-\frac{\rho^2}{\rho_0^2 f^2}}$ and solving in paraxial ray approximation using eikonal function $s(\rho,z)$ as $s=(\rho^2/2)b(z)+\Psi(z)$, where $\Psi(z)$ is an arbitrary function of z and $b(z)=\frac{1}{f}\frac{df}{dz}$, we get

$$\frac{d^2f}{d\zeta^2}=-\frac{1}{R_s^2}\frac{1}{f^3}+\frac{1}{f^3}, \tag{7.13}$$

where $R_s\left(=\frac{2\varepsilon_0\rho_0^2}{\varepsilon_2 U_{00}^2}\right)^{1/2}$ is the typical length of self-trapping, $\zeta=\frac{z}{R_d}$ and $R_d=k\rho_0^2$.The initial term on the right –hand side in (7.13) represent the nonlinear self-trapping term although later is the diffraction term

7.6 Results and Discussion

To study the characteristics of propagation of Gaussian electromagnetic beam in dusty plasma, curves have been drawn for variation in electron density with time and beam waist parameter with the dimensionless length of propagation for distinct number density and sizes of dust grains in the following domain : $\alpha_{r0}=5.5\times10^{-7}cm^3/s$, $n_{e0}=n_{i0}=2.45\times10^6cm^{-3}$, $n_0=n_{00}=0.9\times10^{12}cm^{-3}$, $k=1.1$, $n_d=10^2cm^{-3}$, $\rho_0=5.5\times10^{-2}cm$, $k_B=1.38\times10^{-16}ergsk^{-1}$, $T_{e0}=1001K$, $m_e=9.1\times10^{-28}g$, $m_i=29\times1.6\times10^{-24}g$, $m_d=39\times1.6\times10^{-24}g$, $\omega_d=1.1\times10^8 s^{-1}$, $e=4.8\times10^{-10}$statcoloumb, $T_d=300K$, $r_d=10^{-5}cm$, $U_{00}=10^5$statvolt cm^{-1} and 6×10^5 statvolt cm^{-1}.

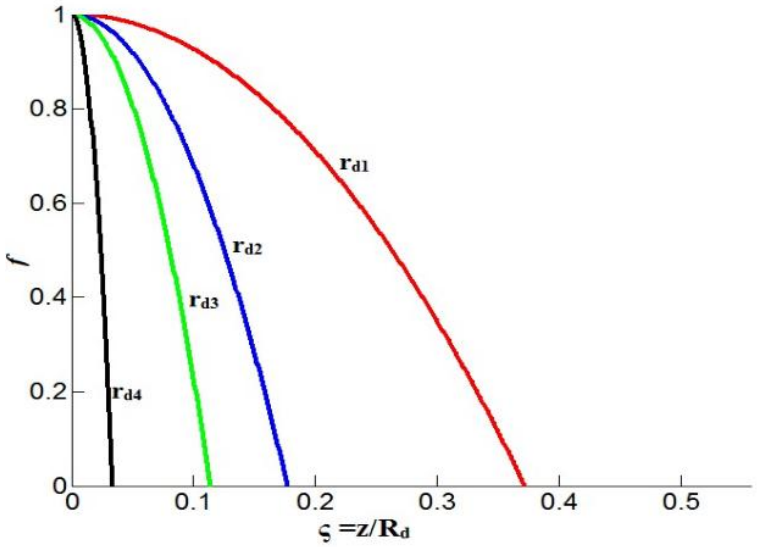

Fig.7.3. Deviation in beam waist parameter (f) with the dimensionless length of propagation $\zeta = z/R_d$ *for distinct values of dust grain sizes corresponds to* $r_{d1} = 4\times10^{-6}$*cm,* $r_{d2} = 6\times10^{-6}$*cm,* $r_{d3} = 8\times10^{-6}$*cm,* $r_{d4} = 10\times10^{-6}$*cm.*

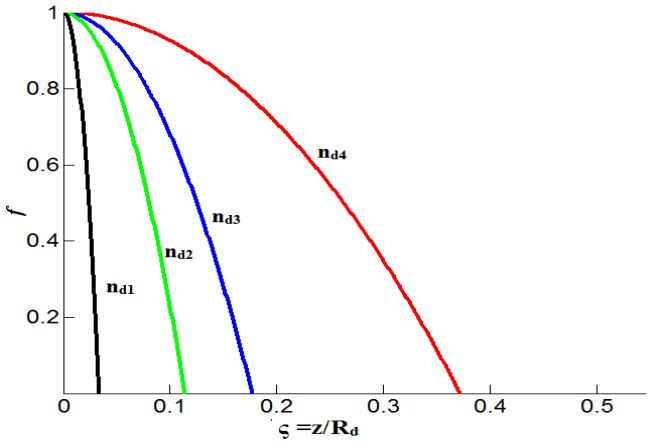

Fig.7.4. Deviation in beam waist parameter (f) with the dimensionless length of propagation $\zeta = z/R_d$ *for distinct values of number density of dust grains corresponds to* $n_{d1} = 10^3 cm^{-3}$, $n_{d2} = 10^4 cm^{-3}$, $n_{d3} = 10^5 cm^{-3}$, $n_{d4} = 10^6 cm^{-3}$.

Figure 7.2 indicates the electron density decay with time due to their larger stickiness to the surface of dust grains with its embryonic growth. Figure 7.3 shows the self-trapping of the beam increases with increasing dust grain size but reverse the case of number density of dist grains in fig. 7.4. This is because of increase in non-linearity on account of predominant self-trapping term with the increasing dust grain size and decreasing number density.

7.7 Conclusions

A theoretical model for self-trapping of Gaussian electromagnetic beam in dusty plasma has been developed. The variation in electron density with time in the presence of dust has been analyzed numerically by solving the coupled equations (7.1) to (7.7) using the MATLAB and MATHEMATICA software. The modification in dielectric permittivity has been formulated. Also, the beam width parameter of the Gaussian beam has been plotted with the normalized distance of propagation for different values of dust grain sizes and dust densities. The results of our analysis are useful in space and laboratory plasma.

REFERENCES

[1] M.S. Sodha, S. K. Mishra, and Shikha Misra, Phys. Plasmas **16**, 123701(2009).

[2] Ruchi Sharma and Suresh C. Sharma, Contrib. Plasma Phys. **59**, 211–225(2019).

[3] Y. Hong , C.Yuan , J. Jia , R. Gao , Y. Wang, Z. Zhou , X. Wang , H. Li , and J. Wu, Phys.Sci.Technol.**19**, 055301(2017).

[4] Jieshu Jia, Chengxun Yuan, Ruilin Gao, Ying Wang, Yaoze Liu, Junying Gao, Zhongxiang Zhou, Xiudong Sun, Jian Wu and Hui Li, and Shaozhi Pu, J. Phys. D: Appl.Phys.**48**, 46520 (2015).

[5] M. S. Sodha, A. Dixit, S. Srivastava, S. K Mishra, M. P. Verma, and L. Bhasin, Plasma Sources Sci. Technol. **19**,015006 (2010).

[6] Suresh C. Sharma, A.Gahlot, and R.P.Sharma, Phys. Plasmas **15**, 043701 (2008).

[7] S. K. Mishra, Shikha Misra, and M. S. Sodha, Phys. Plasmas**18**, 043702(2011).

[8] R.L. Merlino and J.A. Goree, Physics Today **57**, 32-38 (2004).

[9] A. Barkan, N. D'Angelo, and R.L. Merlino, Planet. Space Sci. **43**, 905-908(1995).

[10] S. A. Akhamanov, A. P. Sukhorukov, and R. V. Khokhlov, Sov. Phys. Usp. **10**, 619 (1968).

[11] M.S.Sodha, A.K.Ghatak, and V.K.Tripathi, Prog.Optics (North Holand and Co.)**13**,169 (1976).

Chapter 8

SUMMARY AND FUTURE ASPECTS

This thesis provides a broad perspective and opens up future development of the rapidly expanding field to interested researchers normally working in the area of dusty plasma. Dusty plasma is formed when dispersed particles are introduced into gas discharge or into high frequency plasma at low pressure. It is found in interplanetary space, planetary rings, circumsolar dusty rings, comet tails, interstellar molecular clouds, phosphorescing clouds in the article troposphere, mesosphere and pre thunderstorm clouds. This is attributed to collisions in gaseous phase and thermal electron emission from the surface of condensed particles.

The interest in plasma particle interaction in dusty plasma has been grown in respect to its application in material science, surface processing technology and plasma diagnostic [1]. But powder formation has also been a critical concern for microelectronics industry because the dust contamination severely reduces the yield and performance of fabricated devices. Since the dust particles deposited on the surface of processed wafers can obscure device regions cause voice and dislocation and reduce the adhesion of thin films. But now-a-days, dust particles are not anymore considered as unwanted pollutant. Some positive aspects of dusty plasma have plasma emerged and powder produced using plasma technology have interesting and potentially useful properties, for example, very small sizes, uniform size distribution and chemical activity, size structure and composition can be tailored to specific requirements depending upon desired applications.

In the light of applications of dusty plasma in material science research, two major trends can be followed. One is surface modification technology like coating, surface activation, etching, modification and separating of clustered grain into plasma, can be considered by treating the

surface of dust particles to improve its properties for specific purpose. In this type of technology, the particles are either grown in plasma or externally injected. A second important trend in applied dusty plasma research is the incorporation of dust particles in plasma enhanced chemical vapour deposition (PECVD).

The future scope of interaction of electromagnetic beam with dusty plasma is its linear and nonlinear effects. These effects include wave dissipation, modulation and filamentation instabilities, linear and nonlinear wave propagation, parametric instabilities and self-focusing etc. These effects are useful in study of transient's nature of spokes in Saturn's B ring that took into account electromagnetic effect on charged dust particles [2], the dust stream emanating from Jupiter based on gravitational and electromagnetic forces on charged dust in solar system, close to earth; noctilucent clouds (NLCs) and polar mesospheric summer echoes (PMSEs) are the atmospheric effects connected with charged ice particles in earth's mesosphere at about 85 km altitude. These echoes refer to strong radar backscattering are connected to electron density anamolies associated with charged ice particles.

REFERENCES:

[1] H. Kersten, H. Deutsch, E. Stoffel, W. W. Stoffel, G. M. W. Kroesen, "Plasma–powder interaction: trends in applications and diagnostics, International Journal of Mass Spectroscopy **223**, 313(2003).

[2] R. L. Merlino, "Dusty plasmas and applications in space and industry," Plasma Physics Applied, 73(2006).